Empirical Validation of Building Simulation Software

Modelling of Double Facades

Kalyanova, Olena; Heiselberg, Per

Publication date:
2007

Document Version
Publisher's PDF, also known as Version of record

International Energy Agency
Energy Conservation in Buildings and Community Systems Programme

Empirical Validation of Building Simulation Software: Modelling of Double Facades
1st Draft

Technical Report

IEA ECBCS Annex43 / SHC Task 34
Validation of Building Energy Simulation Tools

Subtask E

O. Kalyanova
P. Heiselberg

SOLAR HEATING & COOLING PROGRAMME
INTERNATIONAL ENERGY AGENCY

ISSN 1901-726X
DCE Technical Report No. 030

AALBORG UNIVERSITY
Department of Civil Engineering

Aalborg University
Department of Civil Engineering
Indoor Environmental Engineering Research Group

DCE Technical Report No. 030

Empirical Validation of Building Simulation Software: Modelling of Double Facades

by

O. Kalyanova
P. Heiselberg

January 2008

Scientific Publications at the Department of Civil Engineering

Technical Reports are published for timely dissemination of research results and scientific work carried out at the Department of Civil Engineering (DCE) at Aalborg University. This medium allows publication of more detailed explanations and results than typically allowed in scientific journals.

Technical Memoranda are produced to enable the preliminary dissemination of scientific work by the personnel of the DCE where such release is deemed to be appropriate. Documents of this kind may be incomplete or temporary versions of papers—or part of continuing work. This should be kept in mind when references are given to publications of this kind.

Contract Reports are produced to report scientific work carried out under contract. Publications of this kind contain confidential matter and are reserved for the sponsors and the DCE. Therefore, Contract Reports are generally not available for public circulation.

Lecture Notes contain material produced by the lecturers at the DCE for educational purposes. This may be scientific notes, lecture books, example problems or manuals for laboratory work, or computer programs developed at the DCE.

Theses are monograms or collections of papers published to report the scientific work carried out at the DCE to obtain a degree as either PhD or Doctor of Technology. The thesis is publicly available after the defence of the degree.

Latest News is published to enable rapid communication of information about scientific work carried out at the DCE. This includes the status of research projects, developments in the laboratories, information about collaborative work and recent research results.

Published 2008 by
Aalborg University
Department of Civil Engineering
Sohngaardsholmsvej 57,
DK-9000 Aalborg, Denmark

Printed in Denmark at Aalborg University

ISSN 1901-726X
DCE Technical Report No. 030

Acknowledgements

The work described in this report is the result of a collaborative effort of members of the International Energy Agency (IEA), Task 34/43: Testing and validation of building energy simulation tools experts group. The authors are especially grateful to all those who participated in this work by running their programs, for their teamwork and dedication:

Clemens Felsmann	Technical University of Dresden (TUD) Germany (program TRNSYS-TUD) felsmann@itg-dresden.de
Harris Poirazis Bengt Hellström	Division of Energy and Building Design Department of Architecture and Built Environment Lund Institute of Technology (LTH) Sweden (program IDA) harris.poirazis@ebd.lth.se bengt.hellstrom@ebd.lth.se
Paul Strachan	Energy Systems Research Unit (ESRU) Dept. of Mechanical Eng. University of Strathclyde Glasgow Scotland (program ESP-r) paul@esru.strath.ac.uk
Aad Wijsman	VABI Software BV Netherlands (program VA114) a.wijsman@vabi.nl

We are also indebted to all those who took the effort to review and comment on a multiple number of preliminary reports and to all of those that have reviewed and given the input to the final report as it is.

The authors would like to acknowledge all those who contributed to this work by sharing the ideas and insights, their experience, knowledge and technical expertise through the Annex meetings, break-out sessions, correspondence or benefiting discussions.

For assistance in testing the spectral properties of constructions in the test facility, we wish to thank Dr. Heinrich Manz, of EMPA: Matherials, Science & Technology.

Also, we appreciate the support and guidance of Ron Judkoff and Joel Neymark as operating agents for the task 34/43.

Finally, our gratitude to Torben Christiansen, Carl Erik Hyldgaard and Rasmus Lund Jensen, who spent a lot of their time and effort to found, establish and refine the test facility, for the enthusiastic technical and field support during the tests and experiments.

The authors are grateful to the participants of the Subtask E: Double Skin Façade (DSF) for completing their test cases and modeler reports that included in Appendix:

Clemens Felsmann	-	TRNSYS-TUD
Harris Poirazis Bengt Hellström	-	IDA
Paul Strachan	-	ESP-r
Aad Wijsman	-	VA114

Preface

This report is a product of a joint effort between International Energy Agency Solar Heating and Cooling (IEA SHC) Task 34 and Energy Conservation in Buildings and Community Systems (ECBCS) Annex 43. Ron Judkoff of the National Renewable Energy Laboratory (NREL) was the Operating Agent for IEA 34/43 on behalf of the United States Department of Energy.

International Energy Agency

The International Energy Agency (IEA) was established in 1974 within the framework of the Organisation for Economic Co-operation and Development (OECD) to implement an international energy programme. A basic aim of the IEA is to foster co-operation among the twenty-four IEA participating countries and to increase energy security through energy conservation, development of alternative energy sources and energy research, development and demonstration (RD&D).

Solar Heating and Cooling Programme

The Solar Heating and Cooling Programme was one of the first IEA Implementing Agreements to be established. Since 1977, its members have been collaborating to advance active solar, passive solar and photovoltaic technologies and their application in buildings and other areas, such as agriculture and industry. Current members are:

Australia	Finland	Portugal
Austria	France	Spain
Belgium	Italy	Sweden
Canada	Mexico	Switzerland
Denmark	Netherlands	United States
European Commission	New Zealand	
Germany	Norway	

A total of 37 Tasks have been initiated, 26 of which have been completed. Each Task is managed by an Operating Agent from one of the participating countries. Overall control of the program rests with an Executive Committee comprised of one representative from each contracting party to the Implementing Agreement. In addition to the Task work, a number of special activities—Memorandum of Understanding with solar thermal trade organizations, statistics collection and analysis, conferences and workshops—have been undertaken.

The Tasks of the IEA Solar Heating and Cooling Programme, both underway and completed are as follows:

1. Current Tasks:

Task 27	*Performance of Solar Facade Components*
Task 29	*Solar Crop Drying*
Task 31	*Daylighting Buildings in the 21st Century*
Task 32	*Advanced Storage Concepts for Solar and Low Energy Buildings*
Task 33	*Solar Heat for Industrial Processes*
Task 34	*Testing and Validation of Building Energy Simulation Tools*
Task 35	*PV/Thermal Solar Systems*
Task 36	*Solar Resource Knowledge Management*
Task 37	*Advanced Housing Renovation with Solar & Conservation*

Completed Tasks:

Task 1	*Investigation of the Performance of Solar Heating and Cooling Systems*
Task 2	*Coordination of Solar Heating and Cooling R&D*
Task 3	*Performance Testing of Solar Collectors*
Task 4	*Development of an Insolation Handbook and Instrument Package*
Task 5	*Use of Existing Meteorological Information for Solar Energy Application*

Task 6	*Performance of Solar Systems Using Evacuated Collectors*
Task 7	*Central Solar Heating Plants with Seasonal Storage*
Task 8	*Passive and Hybrid Solar Low Energy Buildings*
Task 9	*Solar Radiation and Pyranometry Studies*
Task 10	*Solar Materials R&D*
Task 11	*Passive and Hybrid Solar Commercial Buildings*
Task 12	*Building Energy Analysis and Design Tools for Solar Applications*
Task 13	*Advance Solar Low Energy Buildings*
Task 14	*Advance Active Solar Energy Systems*
Task 16	*Photovoltaics in Buildings*
Task 17	*Measuring and Modeling Spectral Radiation*
Task 18	*Advanced Glazing and Associated Materials for Solar and Building Applications*
Task 19	*Solar Air Systems*
Task 20	*Solar Energy in Building Renovation*
Task 21	*Daylight in Buildings*
Task 22	*Building Energy Analysis Tools*
Task 23	*Optimization of Solar Energy Use in Large Buildings*
Task 24	*Solar Procurement*
Task 25	*Solar Assisted Air Conditioning of Buildings*
Task 26	*Solar Combisystems*
Task 28	*olar Sustainable Housing*

Completed Working Groups:
CSHPSS, ISOLDE, Materials in Solar Thermal Collectors, and the Evaluation of Task 13 Houses

To find more IEA Solar Heating and Cooling Programme publications or learn about the Programme visit our Internet site at www.iea-shc.org or contact the SHC Executive Secretary, Pamela Murphy, e-mail: pmurphy@MorseAssociatesInc.com.

Energy Conservation in Buildings and Community Systems

The IEA sponsors research and development in a number of areas related to energy. The mission of one of those areas, the ECBCS - Energy Conservation for Building and Community Systems Programme, is to facilitate and accelerate the introduction of energy conservation, and environmentally sustainable technologies into healthy buildings and community systems, through innovation and research in decision-making, building assemblies and systems, and commercialisation. The objectives of collaborative work within the ECBCS R&D program are directly derived from the on-going energy and environmental challenges facing IEA countries in the area of construction, energy market and research. ECBCS addresses major challenges and takes advantage of opportunities in the following areas:

- exploitation of innovation and information technology;
- impact of energy measures on indoor health and usability;
- integration of building energy measures and tools to changes in lifestyles, work environment alternatives, and business environment.

The Executive Committee

Overall control of the program is maintained by an Executive Committee, which not only monitors existing projects but also identifies new areas where collaborative effort may be beneficial. To date the following projects have been initiated by the executive committee on Energy Conservation in Buildings and Community Systems (completed projects are identified by (*)):

Annex 1:	Load Energy Determination of Buildings (*)
Annex 2:	Ekistics and Advanced Community Energy Systems (*)
Annex 3:	Energy Conservation in Residential Buildings (*)
Annex 4:	Glasgow Commercial Building Monitoring (*)
Annex 5:	Air Infiltration and Ventilation Centre
Annex 6:	Energy Systems and Design of Communities (*)
Annex 7:	Local Government Energy Planning (*)
Annex 8:	Inhabitants Behaviour with Regard to Ventilation (*)

Annex 9: Minimum Ventilation Rates (*)
Annex 10: Building HVAC System Simulation (*)
Annex 11: Energy Auditing (*)
Annex 12: Windows and Fenestration (*)
Annex 13: Energy Management in Hospitals (*)
Annex 14: Condensation and Energy (*)
Annex 15: Energy Efficiency in Schools (*)
Annex 16: BEMS 1- User Interfaces and System Integration (*)
Annex 17: BEMS 2- Evaluation and Emulation Techniques (*)
Annex 18: Demand Controlled Ventilation Systems (*)
Annex 19: Low Slope Roof Systems (*)
Annex 20: Air Flow Patterns within Buildings (*)
Annex 21: Thermal Modelling (*)
Annex 22: Energy Efficient Communities (*)
Annex 23: Multi Zone Air Flow Modelling (COMIS) (*)
Annex 24: Heat, Air and Moisture Transfer in Envelopes (*)
Annex 25: Real time HEVAC Simulation (*)
Annex 26: Energy Efficient Ventilation of Large Enclosures (*)
Annex 27: Evaluation and Demonstration of Domestic Ventilation Systems (*)
Annex 28: Low Energy Cooling Systems (*)
Annex 29: Daylight in Buildings (*)
Annex 30: Bringing Simulation to Application (*)
Annex 31: Energy-Related Environmental Impact of Buildings (*)
Annex 32: Integral Building Envelope Performance Assessment (*)
Annex 33: Advanced Local Energy Planning (*)
Annex 34: Computer-Aided Evaluation of HVAC System Performance (*)
Annex 35: Design of Energy Efficient Hybrid Ventilation (HYBVENT) (*)
Annex 36: Retrofitting of Educational Buildings (*)
Annex 37: Low Exergy Systems for Heating and Cooling of Buildings (LowEx) (*)
Annex 38: Solar Sustainable Housing (*)
Annex 39: High Performance Insulation Systems (*)
Annex 40: Building Commissioning to Improve Energy Performance (*)
Annex 41: Whole Building Heat, Air and Moisture Response (MOIST-ENG)
Annex 42: The Simulation of Building-Integrated Fuel Cell and Other Cogeneration Systems (FC+COGEN-SIM)
Annex 43: Testing and Validation of Building Energy Simulation Tools
Annex 44: Integrating Environmentally Responsive Elements in Buildings
Annex 45: Energy Efficient Electric Lighting for Buildings
Annex 46: Holistic Assessment Tool-kit on Energy Efficient Retrofit Measures for Government Buildings (EnERGo)
Annex 47: Cost-Effective Commissioning for Existing and Low Energy Buildings
Annex 48: Heat Pumping and Reversible Air Conditioning
Annex 49: Low Exergy Systems for High Performance Built Environments and Communities
Annex 50: Prefabricated Systems for Low Energy / High Comfort Building Renewal

Working Group - Energy Efficiency in Educational Buildings (*)
Working Group - Indicators of Energy Efficiency in Cold Climate Buildings (*)
Working Group - Annex 36 Extension: The Energy Concept Adviser (*)
(*) – Completed

Participating countries in ECBCS:
Australia, Belgium, CEC, Canada, Czech Republic, Denmark, Finland, France, Germany, Greece, Israel, Italy, Japan, the Netherlands, New Zealand, Norway, Poland, Portugal, Sweden, Switzerland, Turkey, United Kingdom and the United States of America.

SHC Task 34 / ECBCS Annex 43: Testing and Validation of Building Energy Simulation Tools

Goal and Objectives

The goal of this Task/Annex is to undertake pre-normative research to develop a comprehensive and integrated suite of building energy analysis tool tests involving analytical, comparative, and empirical methods. These methods will provide for quality assurance of software, and some of the methods will be enacted by codes and standards bodies to certify software used for showing compliance to building energy standards. This goal will be pursued by accomplishing the following objectives:

- Create and make widely available a comprehensive and integrated suite of IEA Building Energy Simulation Test (BESTEST) cases for evaluating, diagnosing, and correcting building energy simulation software. Tests will address modeling of the building thermal fabric and building mechanical equipment systems in the context of innovative low energy buildings.
- Maintain and expand as appropriate analytical solutions for building energy analysis tool evaluation.
- Create and make widely available high quality empirical validation data sets, including detailed and unambiguous documentation of the input data required for validating software, for a selected number of representative design conditions.

Scope

This Task/Annex investigates the availability and accuracy of building energy analysis tools and engineering models to evaluate the performance of innovative low-energy buildings. Innovative low-energy buildings attempt to be highly energy efficient through use of advanced energy-efficiency technologies or a combination of energy efficiency and solar energy technologies. To be useful in a practical sense such tools must also be capable of modeling conventional buildings. The scope of the Task is limited to building energy simulation tools, including emerging modular type tools, and to widely used innovative low-energy design concepts. Activities will include development of analytical, comparative and empirical methods for evaluating, diagnosing, and correcting errors in building energy simulation software.

The audience for the results of the Task/Annex is building energy simulation tool developers, and codes and standards (normes) organizations that need methods for certifying software. However, tool users, such as architects, engineers, energy consultants, product manufacturers, and building owners and managers, are the ultimate beneficiaries of the research, and will be informed through targeted reports and articles.

Means

The objectives are to be achieved by the Participants in the following Projects.

Comparative and Analytical Verification Tests:
Project A: Ground-Coupled Heat Transfer with respect to Floor Slab and Basement Constructions
Project B: Multi-Zone Buildings and Air Flow
Empirical Validation and Comparative Tests:
Project C: Shading/Daylighting/Load Interaction
Project D: Mechanical Equipment and Controls
Project E: Buildings with Double-Skin Facades
Other:
Project G: Web Site for Consolidation of Tool Evaluation Tests

Participants

The participants in the task are Australia, Belgium, Canada, Czech Republic, Denmark, France, Germany, Japan, the Netherlands, Spain, Sweden, Switzerland, the United Kingdom, and the United States. The United States served as the Operating Agent for this Task, with Ron Judkoff of the National Renewable Energy Laboratory providing Operating Agent services on behalf of the U.S. Department of Energy.

This report documents work carried out under Project E: Buildings with Double-Skin Facades.

TABLE OF CONTENTS

1. INTRODUCTION

1.1 Foreword

The main objective of the Subtask E is for buildings with Double Skin Facades (DSF) to assess suitability and awareness of building energy analysis tools for predicting energy consumption, heat transfer, ventilation flow rates, cavity air and surface temperatures and solar protection effect and interaction with building services systems.

The starting point of this subtask was to develop a set of empirical test cases for the experimental validation of building simulation software tools. From the literature review [1], it is clear that an identification of a double skin facade with a typical performance is not easy, as every double skin facade building is almost unique. Thus, considering the empirical validation of the double skin facade modeling, a number of questions appeared:

- What is the DSF construction to choose for the empirical validation (positioning of openings, type of glazing, dimension of the DSF cavity, application of shading device, partitioning of the cavity etc.)
- What is the operational principle for the DSF to choose for the empirical validation (naturally/mechanically ventilated, flow direction and origin of air flow)

In order to answer some of the questions, first, a set of comparative test cases was defined, simulated and analyzed in the period of construction of the experimental test facility. Completion of the comparative test cases helped to point out the areas of modeling difficulties, the necessary empirical test cases for completing the subtask assignment and the important parameters to measure during the empirical test cases. Moreover useful feedback was obtained from the participants with comments on the test case specification, measurements and the review of the comparative/experimental results. Finally, the close collaboration made the authors familiar with the tools and approaches used in the software tools participating in the subtask exercises.

Completed comparative exercises demonstrate some severe disagreements between the simulation tools when predicting the air flow rate in a naturally ventilated cavity, and thus demonstrate the necessity for the empirical exercises to complete the validation procedure. Only a limited number of comparative test cases were defined, but these were sufficient to inform the experimental design and to appreciate the magnitude of differences between different simulation programs. As a result the main emphasis of Subtask E was on the empirical tests to provide the reference against which modeling predictions could be compared.

The set of empirical test cases includes a case with the naturally induced flow in the DSF cavity when the outer openings open to the outside (external air curtain mode) and a case with all windows closed (thermal insulation mode). The third empirical case with the mechanically driven flow in the cavity was prepared, but not included into the subtask activity.

1.2 Facts about the empirical test case specification

1.2.1 Empirical test case specification. General

The empirical test case specification [2] was prepared for the outdoor test facility at Aalborg University, the 'Cube'. The geometry and the definition of the constructions, their properties in the specification are given according to the actual geometry and properties in the 'Cube'. Major part of the output parameters requested in the specification have a reference value among the empirical data. In the empirical specification, such parameters as air tightness, optical properties of the constructions etc. are defined according to the results of additional sets of measurements (see in [3])

As a result of discussion and evaluation of the results after each round of modeling, the empirical test case specification was changed a number of times by including additional output parameters, information, clarification and improvements to the defined test cases.

1.2.2 Test cases in the empirical test case specification

Case DSF100. All the openings are closed. There is no exchange of the zone air with the external or internal environment. The zone air temperature results from the conduction, convection and radiation heat exchange. The movement of the air in the DSF appears due to convective flows in the DSF. The test case is focused on assessment of the resulting cavity temperature in DSF and solar radiation transmitted through the DSF into adjacent zone.

Case DSF200. Openings are open to the outside. The DSF function is to remove the surplus solar heat gains by means of natural cooling. Temperature conditions and air flow conditions in the DSF are to be examined together with the magnitude of natural driving forces.

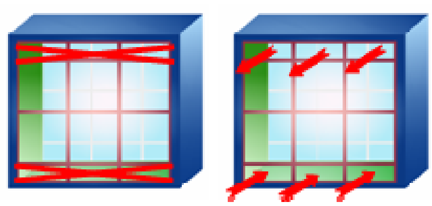

DSF 100 **DSF200**

Figure **1**. Empirical test cases.

Test case	Solar shading	Driving force			Boundary conditions		Control of opening	Corresponding comparative test case
		Buoyancy	Wind	Mechanical	Internal	External		
DSF100_e	No	-	-	-	constant	variable	-	DSF100_2
DSF200_e	No	YES	YES	-	constant	variable	-	DSF200_4
DSF400_e	No	-	-	YES*	constant	variable	-	DSF400_3

* The test case DSF400_e is defined, but not included into the subtask E activity

Table **1**. Empirical test cases.

1.2.3 Weather data

For each empirical test case the weather data is provided in the xls-file format. There are two types of data for each test case: one with the 10-minutes averaged values and another one with 1hour-averaged values.

Parameters given in the weather data files as following:

- External air temperature, °C
- Global solar irradiation on horizontal surface, W/m^2
- Diffuse solar irradiation on horizontal surface W/m^2
- The wind direction, deg
- Wind speed, m/s, measured at 10 m above the ground
- Air relative humidity, %
- Atmospheric pressure, Pa

Period of the climate data is provided as following:

DSF100_e	19.10.2006 - 06.11.2006 (both days are included)
DSF200_e	01.10.2006 – 15.10.2006 (both days are included)

Besides the climate data, the ground temperature below the foundation in the experiment room is given as a boundary condition, together with the air temperature in neighboring zones (instrument room and engine room).

1.2.4 Test case objective

Since the full-scale measurements are very difficult and time consuming, only two empirical test cases were defined to begin with (test case DSF100_e and DSF200_e). The experimental data is also available for the case with the mechanically induced flow (test case DSF400_e) although it was not included into the subtask E activity.

From the complexity point of view, the test case DSF100_e is twofold. In truth, the convective flows in the DSF cavity with the all openings closed can become very complex and very difficult to model. However, the building simulation tools aren't always able to model the intricate convective flows. In many occasions the convective models are simplified and the test case becomes relatively easy to model. An application of the advanced convection modeling for this case may involve coupling of building simulation tool with CFD or involve superior models for evaluation of flow regime and convective heat transfer coefficients and, in that case, the modeling become more complex and time consuming.

Regarding the results of the comparative validation exercises [4], the differences between the air temperature in the DSF cavity calculated by different building simulation tools appeared to be significant, as well as the energy load in the zone 2. It is obvious, that there are different parameters that can cause these large deviations between the models. The convective heat transfer is one of the parameters that is likely to be significant, but, at the same time, it is not the task to perform the direct validation of the convective heat transfer, while the indirect validation is performed via global parameters, such as the air temperature, energy load, etc.

Availability of the experimental data for this and other test cases simplifies the level of assumption when assessing the model or its components such as flow element, convective heat transfer etc.

Looking upon the comparative test case DSF200_3 and DSF200_4, the comparative results have demonstrated a great degree of deviations between the programs also when calculating the air flow rate and the air temperature in the DSF cavity. As a result, the differences in predictions of energy load to the experiment room appear reasonable. The fact that these are the test cases, which involve the phenomena of the natural air flow doesn't allow any further conclusions, as the naturally induced air flow has a complex nature and no model is experimentally validated for the application with the DSF. Therefore, the empirical test cases had to include the extensive measurements of the air flow rate in the DSF cavity in order to be able to rely on the results of the empirical validation in the corresponding empirical test case DSF200_e. Finally, the objective of the empirical validation is to complete the validation procedure of the building simulation software for modeling buildings with DSF upon the experimental reference values.

1.2.5 Definition of zones

There are two main zones defined in the empirical test cases. Experts were asked to model a double skin facade as a separate zone – zone 1. The zone adjacent to the double skin facade is defined as zone 2, the experiment room. The heating and cooling system in zone 2 keeps the air temperature in the zone constant at apx. 22°C. The ability of building simulation tools to simulate the necessary energy consumption in zone 2, and the air temperature and airflow in zone 1 are the main quantitative measures of the building simulation tool performance and its validation.

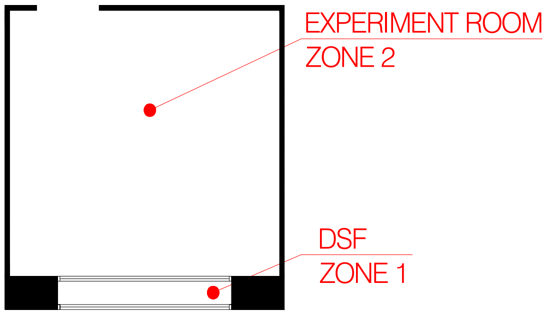

Figure 2. Definition of zones in the empirical test case specification.

1.2.6 Modeling requirements

Various building simulation software includes different approaches and applications for modeling of the physical processes involved. Initially, it was desired that all case-models involve the same applications for the same parameters in every model and use the most detailed level of modeling allowed by simulation program being tested.

Cases specified for the modeling involve interaction of various processes; thus modeling may require different combinations of software applications and their options. For this reason the building and its systems were specified in detail, but the way in which they were modeled was not prescribed. The design of the model had to be completed depending on the capability of the simulating software and the user's decision, but as close as possible to the specification.

In addition, it was requested that participants perform consistent modeling of the test cases. Modelers were asked to include in the modeling report detailed documentation of any discrepancy between the test case specification and the model.

Finally, the participants were asked to perform a consistent modeling of the empirical test case in relation to the comparative once.

1.2.7 Output parameters

The output parameters are defined in the specification. The following are the output parameters shared for all test cases:

N	Output	Unit	Description
1	Direct solar irradiation on the window surface	W/m^2	Mean hourly value
2	Diffuse solar irradiation on the window surface	W/m^2	Mean hourly value
3	Total solar irradiation on the window surface	W/m^2	Mean hourly value
4	Total solar radiation received on the external window glass surface	kW	Mean hourly value
5	Solar radiation transmitted from the outside into zone1	kW	Mean hourly value
6	Solar radiation transmitted from zone 1 into zone2 (first order of solar transmission)	kW	Mean hourly value
7	Energy used for cooling/heating in the zone 2	kW	Mean hourly value (with the '+'sign for heating and '-'sign for cooling)
8	Hour averaged surface temperature of external window surface facing external	°C	Mean hourly value
9	Hour averaged surface temperature of external window surface facing zone1	°C	Mean hourly value
10	Hour averaged surface temperature of internal window surface facing zone1,	°C	Mean hourly value
11	Hour averaged surface temperature of internal window surface facing zone2	°C	Mean hourly value
12	Hour averaged floor surface temperature in the zone 1	°C	Mean hourly value
13	Hour averaged ceiling surface temperature in the zone 1	°C	Mean hourly value
14	Hour averaged floor surface temperature in the zone 2	°C	Mean hourly value
15	Hour averaged ceiling surface temperature in the zone 2	°C	Mean hourly value
16	Hour averaged air temperature in the zone 1	°C	Mean hourly value

Table 2. Output parameters shared for the all test cases.

In the test cases DSF100_e the solar altitude is included as a separate output parameter.
In the test case DSF200_e the air flow rate is included as a separate output parameter.

1.3 Participants in the empirical validation

Results of the empirical exercise are compared between several building energy simulation programs and experiments. The following is the list of organizations who participated in the exercises and the simulation programs they used to perform the simulations.

Organization		Program
VABI	VABI Software BV Netherlands	VA114
ESRU	Dept. of Mechanical Eng. University of Strathclyde Glasgow Scotland	ESP-r
TUD	Technical University of Dresden (TUD) Germany	TRNSYS-TUD
LTH	Division of Energy and Building Design Department of Architecture and Built Environment Lund Institute of Technology (LTH) Sweden	IDA
AAU	Dept. of Civil Engineering Aalborg University Denmark	BSim

Table **3**. Organizations that performed the simulations and the simulation programs used.

2. THE DOUBLE SKIN FAÇADE THEORY AND MODELING OF THE EMPIRICAL TEST CASES

2.1 Modeling of the double skin façade

This chapter of the report is aimed to summarize the main issues when modeling DSF performance. The complexity of the DSF modeling is well known and there are no doubts about the necessity for the comparative and empirical exercises completed during the IEA Annex 34/43 activity. On the contrary, a general concern is expressed in the literature about the lack of the experimental data and validated software tools for the DSF buildings [1]. Moreover, there is a literature available with the clarification *why* it is difficult to perform the modeling of the DSF performance. Looking upon these arguments it is easy to understand why there is still an active hunt for a better model for the DSF modeling.

From another point of view, there are number of well developed building simulation tools, able to perform calculations necessary for the DSF modeling. Then appear a question:

- Does the claim that none of the simulation tools are able to perform an accurate modeling of a building with the DSF express a general fear for DSF modeling?
- Or does this call for a new DSF model appear due to the lack of experience and knowledge about the DSF physics, when applying already existing building simulation tools or lack of knowledge about the suitable tool to use?
- Or is this just a call for a model that would simplify the modeling of the DSF?

In the literature review [1] the details about difficulties in DSF modeling are summarized. There is also made a classification of the main elements in the DSF physics, these are the optical, heat transfer and air flow element. Earlier, the participants of the comparative and empirical exercises have agreed that the optics and heat transfer elements are the common issues for the whole field of building simulations, then this report and whole activity of the subtask is focused on the investigations of the air flow element in modeling of the DSF performance, as it's assessment is crucial for the indoor climate and evaluation of the performance of the double skin façade.

However, the convective flows in the DSF cavity can be very strong and can have a serious impact on a final result of simulation. At the same time the different building simulation software uses different models in calculation of surface heat transfer coefficients. In order to help reader in evaluation of performance of different simulation tools, this chapter includes a section with a short summary over the surface heat transfer coefficients used in different models, while even more details can be found in the modeler reports, which are included in appendix.

2.2 Surface heat transfer coefficients. Convection

All of the models in the empirical validation exercises make a split between the convective and radiative surface heat transfer coefficients. As it can be seen from the table below, all of the models use longwave radiation exchange with the sky and the ground, the details about it can be found in the modeler reports. When looking upon the level of detail in modeling of external longwave radiation exchange all of the models include almost the same level of detail and therefore this will not be discussed further. However, it is not possible to do the same conclusion on the subject of convection heat transfer, as it is demonstrated in the table below. But first, the role of convective heat transfer in the specified empirical test cases is discussed.

The operational mode of the DSF can vary according to its function in one or another building, but the design of the DSF cavity is more or less the same: two layers of fenestration, separated with the air gap, which, in most of the cases, includes shading device. No matter the operational strategy of the DSF, the air temperature in the gap is the result of the solar radiation absorbed by glazing and/or shading device. As a result, the air temperature in the DSF cavity is mainly the result of the convective heat transfer between the heated surfaces of glass and air. The floor or ceiling and side walls of the DSF rarely have any importance, as the weight of their areas is very small compared to the area of fenestration and shading.

The convective heat transfer is relatively easier to estimate for the mechanically induced flow motion compared to the naturally driven flow, where the convection heat transfer depends on size, shape, orientation, flow regime, temperature etc. At the same time the results of simulations can be very sensitive to the convective heat transfer coefficient in the models and the differences between the convection heat transfer coefficients in the models are important. Below is the table of summary of the convection heat transfer coefficients used in models in the empirical exercises.

Software	BSim	VA114	ESP-r	TRNSYS-TUD	IDA
External heat transfer coefficient					
Convection, function of	if $v_{wind} \leq 5\ m/s$ $h = 5.82 + 3.96\, v_{wind}$ else $h = \frac{7.68 \cdot v_{wind}}{\sqrt{v_{wind}}}$	18 W/(m^2°C)	Wind direction and wind velocity, same as for IDA: $h = 5.678 \cdot \left(a + b \cdot \left(\frac{V_{loc}}{0.3048} \right)^n \right)$ Paul, is this correct? Clarke [5], p.198	25 W/(m^2°C)	$V_{loc}^{windward} = \max(0.25\, v_{wind}; 0.5)$ $V_{loc}^{leeward} = 0.3 + 0.05\, v_{wind}$ $h = 5.678 \cdot \left(a + b \cdot \left(\frac{V_{loc}}{0.3048} \right)^n \right)$ if $v_{wind} \leq 4.88$ $a=1.09,\ b=0.23,\ n=1$ else $a=0,\ b=0.53,\ n=0.78$
Radiation components)	sky, ground	sky, ground	sky, ground	sky, ground	sky, ground
Internal heat transfer coefficient					
Convection, function of	for vertical surfaces: $if\ \Delta T \leq 9.5/L^3$ $h = 1.42 \left(\frac{\Delta T}{L} \right)^{0.25}$ $if\ \Delta T > 9.5/L^3$ $h = 1.31 (\Delta T)^{0.33}$	3 W/(m^2°C)	Buoyancy correlations of Alamdari and Hammond (1983) from [5] $h_c = \left\{ \left(a \cdot \left(\frac{\Delta\theta}{d} \right)^p \right)^m + \left(b (\Delta\theta)^q \right)^m \right\}^{\frac{1}{m}}$	4.4W/(m^2°C), except 3W/(m^2°C) for ceiling and floor	Min 1956 Brown 1963 Δ t, surface inclination include functions
Radiation	Linearized coefficients based on surface emissivity and view factors	Linearized coefficients based on surface emissivity and view factors	Linearized coefficients based on surface emissivity and view factors	Nonlinear treatment of radiation heat exchange	Linearized coefficients based on surface emissivity and view factors

2.3 Air (mass) flow models

This section deals with the models for calculation of the air flow rate in a naturally ventilated DSF cavity applied in the empirical validation exercise. The air flow in naturally ventilated spaces is induced by the pressure differences, which evoke from the wind pressure, wind fluctuations and buoyancy forces (the mechanical force is not discussed in this section). The determination of the buoyancy force is straight forward, while the main difficulties in the theory of the natural ventilation exist due to highly transient wind phenomenon.

There is a number of approaches used for calculations of air flow in a naturally ventilated (multizone) buildings, however, all of them have most of the following issues in common:

- Challenge to represent the wind speed reduction from the meteorological data to the local microclimate near the building
- Challenge in determination of the wind pressure coefficients
- Challenge to decide on appropriate discharge coefficients and pressure loss coefficients in general
- Challenge to agree on an appropriate relation between pressure loss and air flow rate through the opening (determination of coefficients in the relationships), etc.

Depending on external conditions and the double skin façade running mode the air flow rate in a ventilated cavity can have significant variation in order of magnitude and in occurrence of a reverse flow. Contradictory, in a traditionally ventilated domain the minimum air change rate is specified in requirements for the indoor air quality, while maximum is normally restricted by the energy savings considerations. In view of that, the great variations in the magnitude of the airflow rate are identified as the distinctive element of the cavity flow. The variation of the flow magnitude may result in variation of the flow regimes and will further intricate the situation.

The commonly used models for calculation of the natural air flow rates are:

- The network pressure model – is based on continuity equations to determine pressures in different zones of the network and then the air flow rates are determined on the basis of different relationships (orifice, power-law etc.)
- The loop pressure equation model – is method where the pressure loop equations are written for the whole air path loop, and the air flow rate is determined on the basis of those equations.
- The experimental method is using empirical relationships for the determination of the air flow rates depending on temperature, wind speed, pressure difference coefficients and the discharge coefficient.

The pressure network and the pressure loop method are very similar. Moreover, both of these methods can apply the orifice and the power-law relationships for determination of the air flow rate on the basis of pressure difference. However, an application of one or another relationship is a sensitive matter, as the classic orifice equation is more suitable for the large openings and fully developed turbulent flow. Meanwhile the power-law equation is more flexible and can be adjusted to different conditions and opening sizes via the exponent n and coefficient C.

Equation 2-1

$$\Delta P = \frac{\rho \dot{V}^2}{2 \cdot C_D \cdot A^2}$$ Orifice equation

Equation 2-2

$$\Delta P = \left(\frac{\dot{V}}{C} \right)^{\frac{1}{n}}$$ Power-law equation

ΔP	- pressure difference across the opening
ρ	- air density
$\dot{V}$	- volume flow
C_D	- discharge coefficient
A	- opening area
n, C	- exponent and flow coefficient

The experimental method is the simplified one, where the transient character of the wind is simplified and a relationship as shown below used for the calculation of air flow rates.

Equation 2-3

$$\dot{V} = \left| \frac{c_v}{|c_v|} \cdot (c_v \cdot V_{10})^2 + \frac{\Delta T}{|\Delta T|} \cdot (c_t \cdot |\Delta T|)^2 \right|^{1/2}$$

Equation 2-4

$$c_t = \sum_{j=1}^{n} c_{D,j} \cdot A_j \cdot \left(\frac{2 \cdot (H_o - H_j) \cdot g}{T_i} \right)^{1/2}$$

Equation 2-5

$$c_v = 0.03 \cdot A$$

$\dot{V}$	- volume flow
c_v, c_t	- coefficient for the wind force and buoyancy correspondingly
V_{10}	- the reference wind velocity at the height 10m
ΔT	- temperature difference between two environments
n	- number of openings
j	- opening number
C_D	- the discharge coefficient
A_j	- area of the opening 'j'
H_o	- height of the neutral plan
H_j	- height of the opening 'j'
g	- gravity force

The summary of the model used for the empirical exercises is done in the table below:

Software		BSim	VA114	ESP-r	TRNSYS-TUD	IDA
Influencing parameters in the flow model	wind force	x	x	x	x	x
	wind fluctuations	-	x	-	-	-
	buoyancy	x	x	x	x	x
Air flow model*		experimental	network	network	network	network
Pressure-Airflow relationship used			power-law	orifice	???	orifice
Coefficients in the power-law equation	exponent *n*		1.5		?	
Discharge coefficient		0.65	0.61	as in spec. 0.65/0.72	0.65	as in spec 0.65/0.72
Pressure difference coefficients		different from spec, ΔCp=0, but wind impact is included by application of C_v-coefficient	different from spec, ΔCp=0	as in spec	as in spec	interpolated from spec.?
Model for wind fluctuations		-	[9], [10]	-	-	-

* None uses the loop equations

Openings in the empirical exercises were specified, all of them have the same orientation and therefore the wind pressure component can become less influencing or equal zero (in VA114). In such situation the wind turbulence can generate a substantial flow rate. However, only VA114 consider the wind fluctuations.

In the empirical specification the size of the openings isn't the same as in the comparative one, besides the opening size is different for the top and the bottom openings. Consequently, in the empirical validation the friction losses and contraction of the jet are different for the top and the bottom openings and also different from the comparative test cases. This is specified via the discharge coefficients C_d for the openings on the basis of experiments; however only ESP-r and IDA models have used this data.

The pressure coefficients given in the empirical test case specification are given for the wind velocity at the building height (6m), however the wind velocity in the climate data file is given for the wind velocity at the 10m height. Besides the parameters included into the table above the reduction of the wind speed to the local terrain next to the building can have some degree of influence on the calculations of the wind pressure magnitude and influence of the wind turbulence for the air flow calculations. Below is given the comparison of the wind speed reduction relationships used in different models and it demonstrates that the models use almost the same wind reduction relationship in the simulations.

Software:	BSim	VA114	ESP-r	TRNSYS-TUD	IDA
Reduction factor to the reference wind velocity at the height of 10m:	0.922	0.922	0.922	0.84	ASHRAE?

n the comparative exercises the infiltration parameters were set to negligible minimum, while in the empirical exercises this were specified, however not for the zone 1. According to the measurements the experimental test facility has superior air tightness; therefore the assumption of negligible infiltration in the empirical models is also satisfactory.

3. RESULTS FROM THE EMPIRICAL TEST CASES

3.1 Foreword

Results of the empirical validation are reliant with the quality and accuracy in the experimental data, besides it was highly essential to obtain the experimental data for the global parameters, such as cooling/heating load to the experiment room, air flow and volume averaged air temperature in the double skin façade cavity.

The detailed description of the experimental test facility and the measurement procedure can be found in [3].

Similar to the comparative validation the evaluation of the results from the empirical test cases will be performed in the following sections, separated for each test case, with application of three types of visualization:

1. Profiles with the results from the whole period of simulation
2. Profiles for a day with the high and low solar irradiation
3. Figure of the average, min and max values over the whole period of simulation

The first method of evaluation is very easy and visual: it gives an overview of the whole situation, and allows the identification of conditions when the model experiences difficulties etc. More details can be seen in the plots made for a day with the high and day low solar radiation. The final evaluation is supported with some statistical data and bar-plots for min, average and max values.

This time the results of simulations are plotted together with the empirical results, when the experimental data is available. Moreover, some statistical analysis is performed for the results of simulations in relation to the experiments.

Minimum	MIN	$Xmin=Min(X_t)$
Maximum	MAX	$Xmax=Max(X_t)$
Average	MEAN	$\overline{X} = \sum_{t=1}^{n} \frac{X_t}{n}$
Difference	DT	$D_t=X_t - M_t$
Difference 5%	DT95	*5%percentile* (D_t)
Difference 95%	DT5	*95%percentile* (D_t)
Average Difference	MEANDT	$\overline{D} = \sum_{t=1}^{n} \frac{D_t}{n}$
Absolute Average Difference	ABMEANDT	$\left\|\overline{D}\right\| = \sum_{t=1}^{n} \left\|\frac{D_t}{n}\right\|$
Root Mean Square Difference	RSQMEANDT	$\sqrt{D^2} = \sqrt{\sum_{t=1}^{n} \frac{D_t^{\,2}}{n}}$
Standard Error	STDERR	$\sigma = \sqrt{\frac{1}{n} \sum_{t=1}^{n} (D_t - \overline{D})}$

Where

X_t - predicted value at hour t

M - measured value at hour t

n - total hours in period of comparison.

3.2 Investigation of boundary conditions

In order to be able to compare results from the empirical test cases, first, it is necessary to look at the boundary conditions which are *calculated* by various programs on the basis of defined weather conditions. These are the solar altitude, solar irradiation on the double skin facade surface (direct, diffuse and total), solar radiation transmitted into the DSF and into the adjacent experiment room, air temperature in the neighboring zones, etc. In the test case DSF100_e the experts were asked to include the solar altitude as an output parameter and there were three programs able to give an access to this data. The comparison plots are included in the following chapters, separately for each test case. Here, the main principles of calculations in the models are discussed and summarized.

Modelers completed their simulations with the Perez model (1990 or 1987) and the circum solar radiation treated as diffuse. The choice of the Perez model was partly made on the basis of previous experience from the comparative validation exercises.

Calculation of the solar irradiation on a surface mainly depends on the solar model used in calculations. The differences between models are often expressed in different treatment of circum solar radiation and in calculations of the diffuse solar radiation, in general. The transmission of solar radiation depends on such factors in the model as:

- Calculation of solar path and path of solar radiation through the building (calculation of sunlit surfaces and surfaces in the shadow)
- Various treatment of diffuse and direct solar radiation (when calculating transmission of solar radiation)
- Level of detail in the window model
- Model for calculation of ground reflected solar radiation
- Incidence angle dependency
- etc.

3.2.1 Transmission of solar radiation

This section is focused on investigation of the window model used in different software. The reason for that is the variety of involved parameters and software limitations. Although the experimental data to characterize the optical properties of the glazing is provided in the specification, it is seldom the building simulation software is integrated with the routine for the advanced calculations of optical properties, such as incidence angle dependency of solar transmission, reflection and absorption. Still, some of the tools include only the intermediate complexity level of window model, using the fixed function of incidence in the program upon provided in the specification glazing properties for normal angle of incidence. However, a number of programs allow manual definition of function of angle of incidence. In the latter case the modelers have translated the spectral data into the transmission and absorption property as a function of angle of incidence using external software or manual calculations, i.e. in ESP-r model these were calculated using WIS software upon the spectral data provided in the specification (essential agreement was obtained with the values for normal angle of incidence in specification). TRNSYS – same for empirical and comparative (according modeler report)? The variety of the methods when calculating the transmission of solar radiation is the explanation for the necessary comparison between the glazing properties and window models in different models.

TRANSMITTANCE OF THE DIRECT SOLAR RADIATION

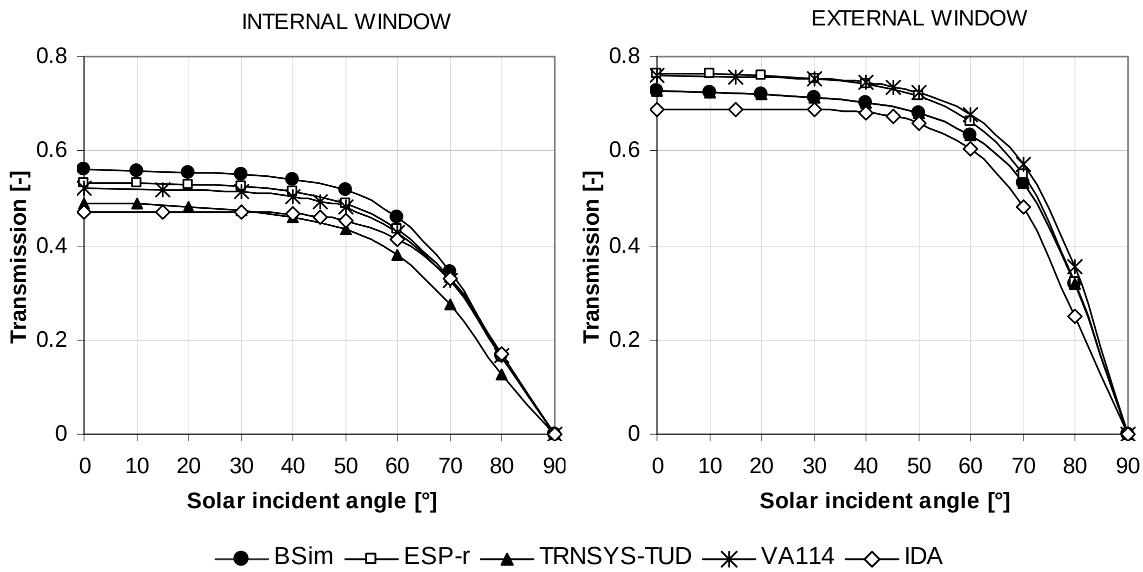

The transmission and reflection of solar radiation is provided as user defined function of solar incidence in TRNSYS-TUD, ESP-r and BSim. The above figure shows some degree of deviation between the models, especially when compare the internal window transmittance property. Functions for the external window represent three groups: a group with the low values of solar transmission (IDA), maximum values for ESP-r and VA114, and the intermediate values for (TRNSYS-TUD and BSim). However, the ESP-r function is only the one that is established on the basis of the detailed optical calculations.

Regarding VA114 and IDA, the default function for calculation of solar heat gain coefficient used (g-value), in this case the g-value for the normal angle of incidence used as the main input. The default incidence angle function in VA-114 follows the one from ESP-r.

Another important issue in calculations of transmitted solar radiation is the form that the solar energy takes when passes the first bounce with the glass (direct or diffuse). This is not a physical question, as the form of solar energy in a software tool, direct or diffuse, depends purely on the assumptions in the mathematical model of simulation tool. However, various software tools treat the diffuse and direct solar radiation separately, when calculating the transmission or distribution of solar radiation. Different calculation procedures are used depending whether the solar radiation is diffuse or direct. Therefore the final error in predictions of transmitted or distributed solar radiation will depend on the level of detail in each of these calculations.

The following table is prepared in order to make a clear picture of solar calculations by different building simulation tools:

Property	BSim	VA114	ESP-r	TRNSYS-TUD	IDA
Transmittance of the direct solar radiation into the zone 1	f(α)	f(α), fixed	f(α)	f(α)	f(α), fixed
Transmittance of the direct solar radiation into the zone 2	f(α)	f(45°)	f(α)	f(α)	f(α), fixed
Transmittance of the diffuse solar radiation into the zone 1	f(60°)	f(58°)	f(51°)	f(const)	~f(45 °)
Form of the direct solar radiation after the 1st bounce	direct	direct	diffuse	direct (change comparative report !)	direct

α- an incidence angle

The spectral data to evaluate the optical properties of the ground and internal constructions were in provided in the empirical specification, however, due to the limitations in the programs, different values from the specification have been used. Comparison of the ground reflectivity used in different models is given in the table:

Property	BSim	VA114	ESP-r	TRNSYS-TUD	IDA
Ground reflectivity	0.1	0.1	0.1	0.08	0.08
Shortwave reflectance of constructions in zone 1	0*	0.66	0.66	0.78	0.67
Shortwave reflectance of constructions in zone 2	0*	0.66	0.66	0.76	0.67
Longwave emissivity of the internal surfaces	0.88	0.88	0.88	?	0.88

* All solar radiation striking the surface is fully absorbed

Comparison of the input parameters in the empirical models demonstrates that the ground reflectivity and longwave emissivity is almost identical for all of the models. Serious limitation is demonstrated for BSim, as all of solar radiation striking the surface is fully absorbed, this will lead to overestimation of solar gains in the zones and finally to overestimation of energy consumption for cooling. In TRNSYS-TUD, the shortwave reflectance of the constructions is slightly higher than in VA114, ESP-r and IDA, and can have an impact on calculation of energy consumption.

DSF100_e

3.3 Test case DSF100_e

This test case is different from the any other case because it doesn't include air flow through the double skin façade cavity. In this case, a complex convective flow field can develop in the DSF cavity, which can be significant for the final result. The complexity of such a cavity flow can be solved by an advanced convection model: model with the dynamic calculation of the convection heat transfer surface coefficients, more than one temperature node calculations and even the mass balance for the convective flows. The maximum level of detail can be obtained by CFD.

Since, the participants in this empirical exercise haven't used the CFD-calculations, their flow models aren't able to count on the mass flow rate in the convective boundary layer and the calculation of the convective surface heat transfer coefficient is reasonably simplified, then this test case become relatively easy to model compared to the test cases DSF200_e. In the simple model DSF100_e the double skin façade actions as a conventional window and the heat transfer processes are relatively straight forward. So, the question is: how good the model performance can be achieved with the described above limitations? It was not possible to answer that question during the comparative validation procedure, since the models have demonstrated a great deal of disagreement.

3.3.1 Solar altitude

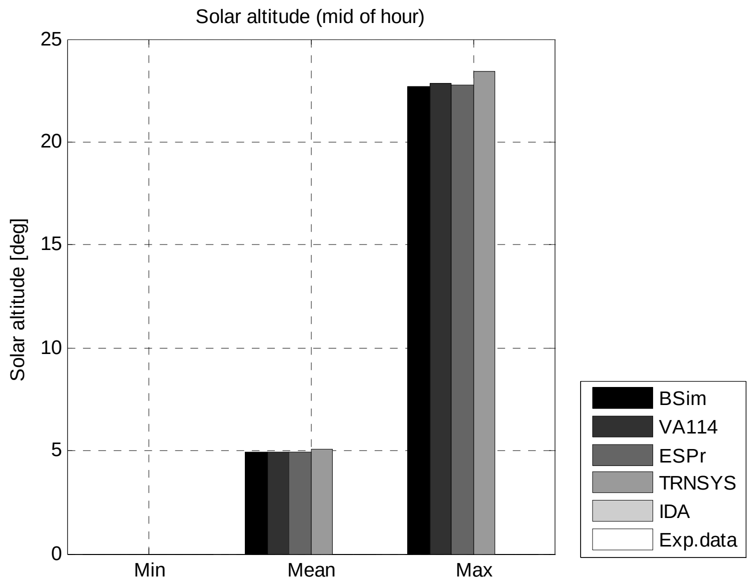

Solar altitude	BSim	VA114	ESP-r	TRNSYS-TUD	IDA
MIN, deg	-	0	0	0	-
MAX, deg	-	22.8	22.8	23.4	-
MEAN, deg	-	4.9	4.9	5.1	-

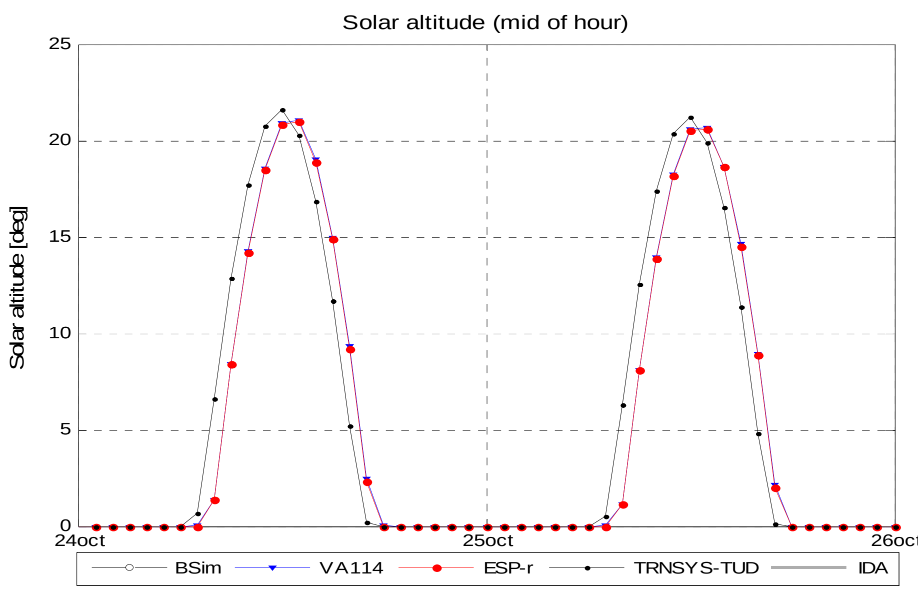

The solar height is available only for three programs: VA114, TRNSYS-TUD and ESP-r. From the above plots and the table, it is noticeable that there is a difference in calculation of the solar height, TRNSYS-TUD seems to be 1 hour ahead of ESP-r and VA114 when calculating the sunrise, but still the sunset is calculated at the same time.

3.3.2 Direct solar irradiation

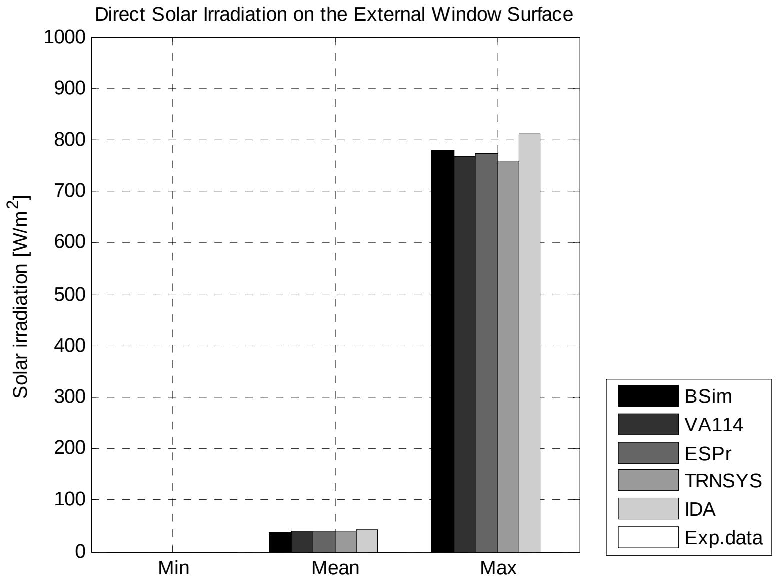

Direct solar rad. on ext window surface	BSim	VA114	ESP-r	TRNSYS-TUD	IDA
MIN, W/m^2	0	0	0	0	0
MAX, W/m^2	779	767	775	757	813
MEAN, W/m^2	37	39	40	39	43

Maximum values are calculated by IDA (813W/m^2), while the differences between the other models are in the range of 10W/m^2. Good correspondence of the results can be seen for the average values and especially for the days with the low solar intensity (see figure below).

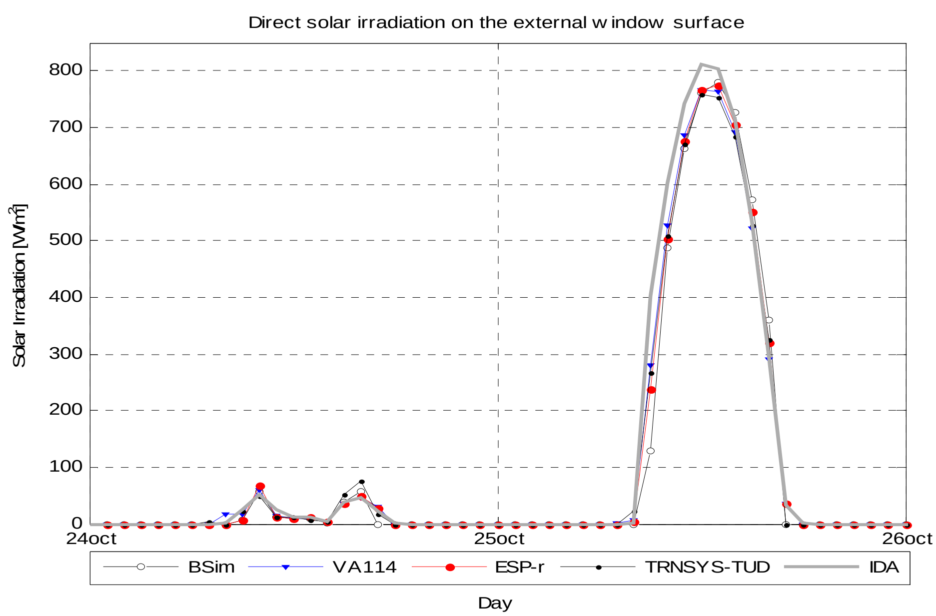

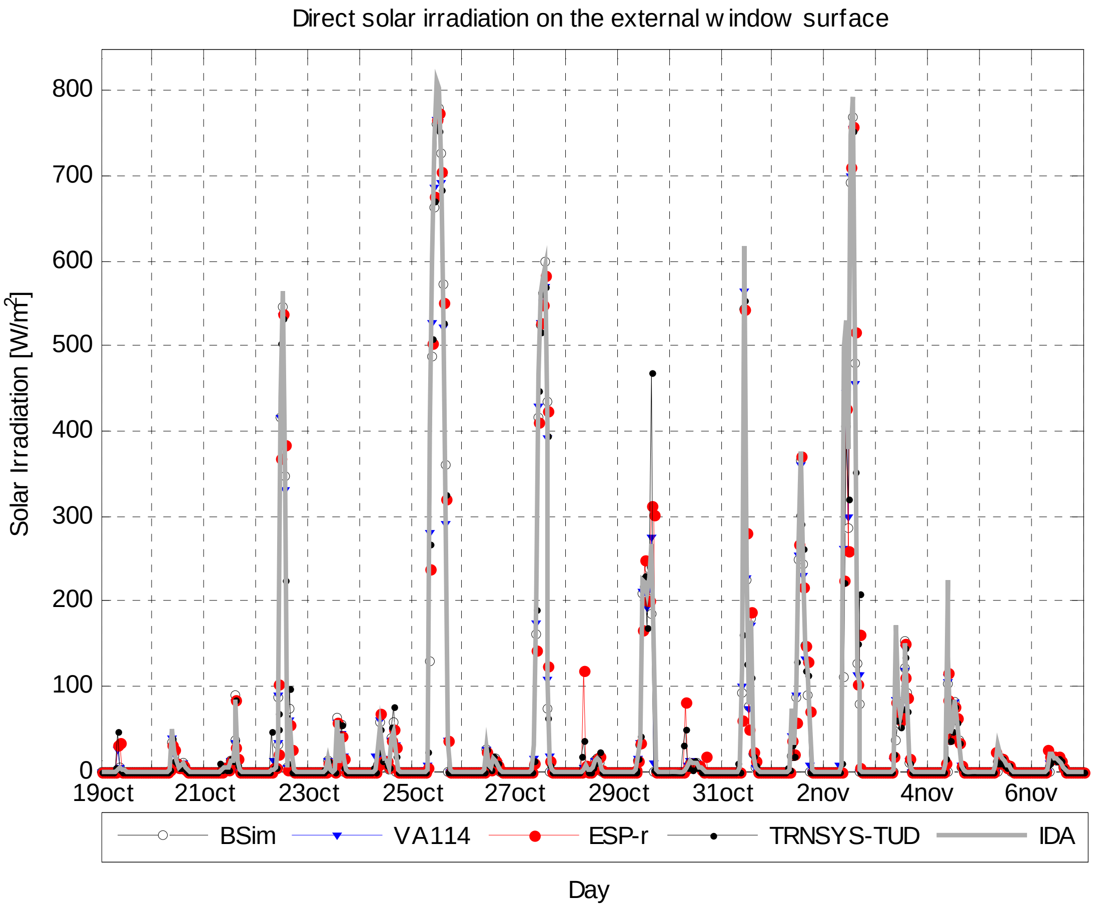

3.3.3 Diffuse solar irradiation

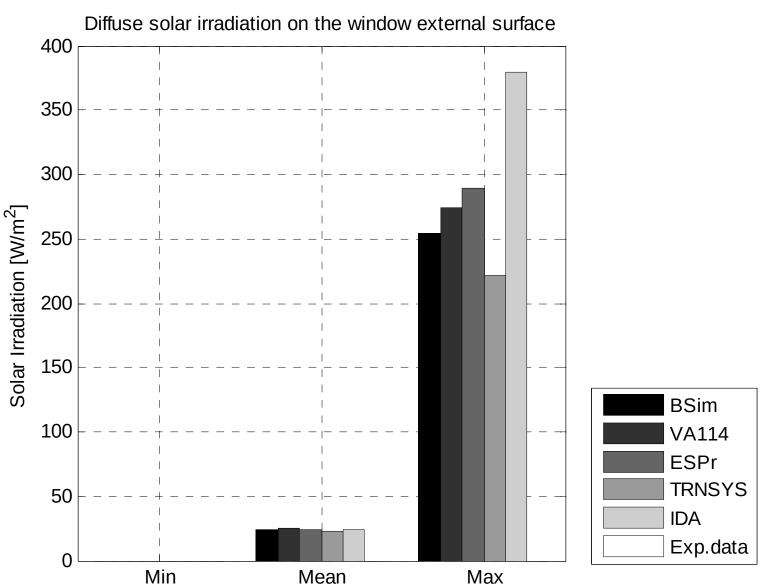

Diffuse solar rad. on the window ext. surface	BSim	VA114	ESP-r	TRNSYS-TUD	IDA
MIN, W/m²	0	0	0	0	0
MAX, W/m²	254	274	290	222	379
MEAN, W/m²	24	25	24	22	24

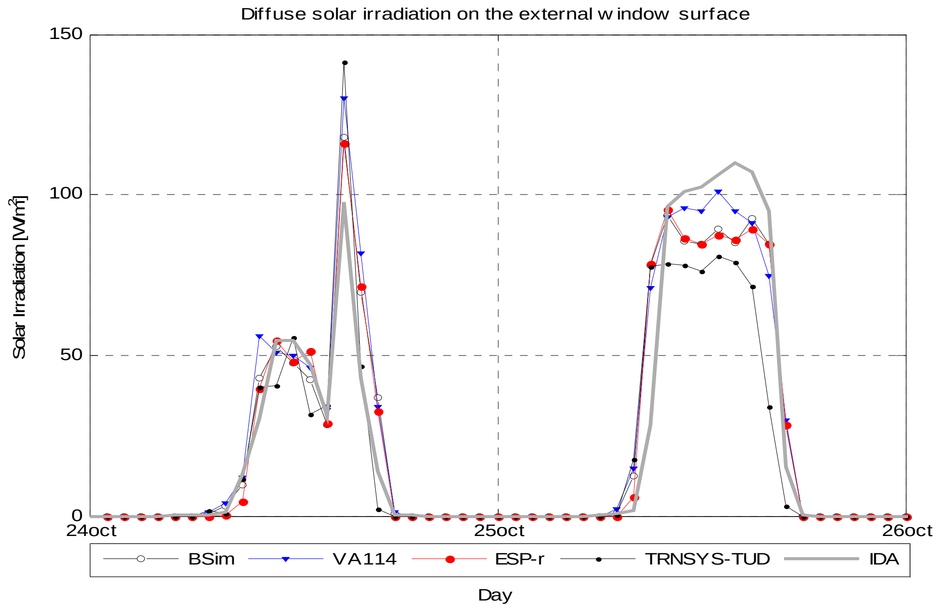

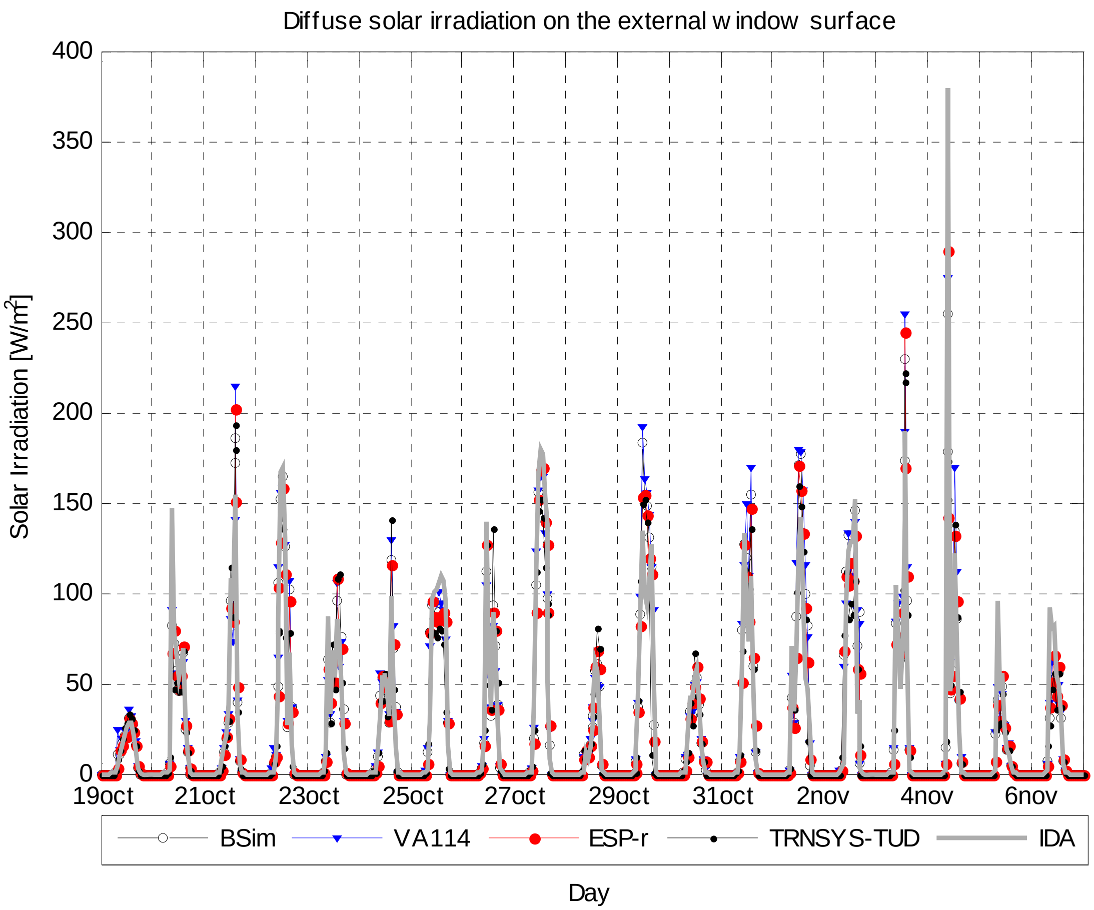

Prediction of the diffuse solar radiation shows relatively good correspondence between the mean values, while the maximal differ: significantly higher values obtained by IDA and noticeably low values obtained by TRNSYS-TUD. Looking upon the plot with the whole period of measurement, one can notice highly varying cloud distribution and actually none of the model continuously underestimates or overestimates the diffuse solar irradiation.

3.3.4 Total solar irradiation

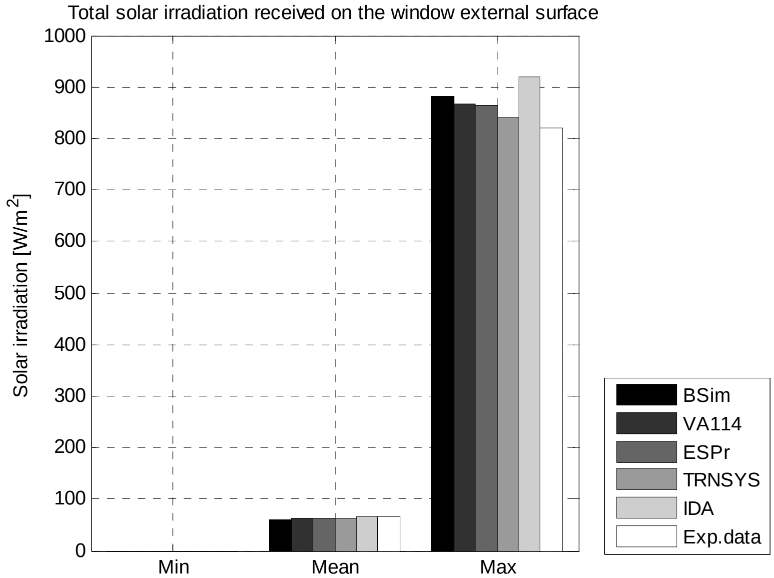

Total solar rad. on ext window surface	BSim	VA114	ESP-r	TRNSYS-TUD	IDA	Exp.
MIN, W/m^2	0	0	0	0	0	0
MAX, W/m^2	882	866	864	841	921	821
MEAN, W/m^2	61	64	63	62	67	65
DT95, W/m^2	-4	0	-7	-19	-4	
DT5, W/m^2	44	45	44	52	69	
MEANDT, W/m^2	5	7	6	5	9	
ABMEANDT, W/m^2	8	9	9	11	11	
RSQMEANDT, W/m^2	21	19	21	25	28	
STDERR, W/m^2	20	18	20	25	27	

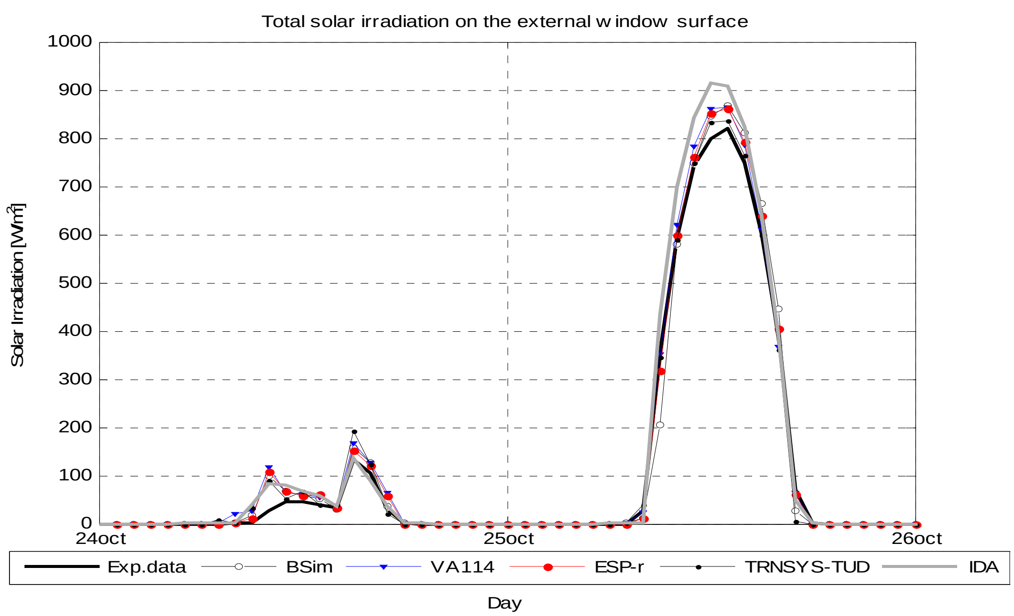

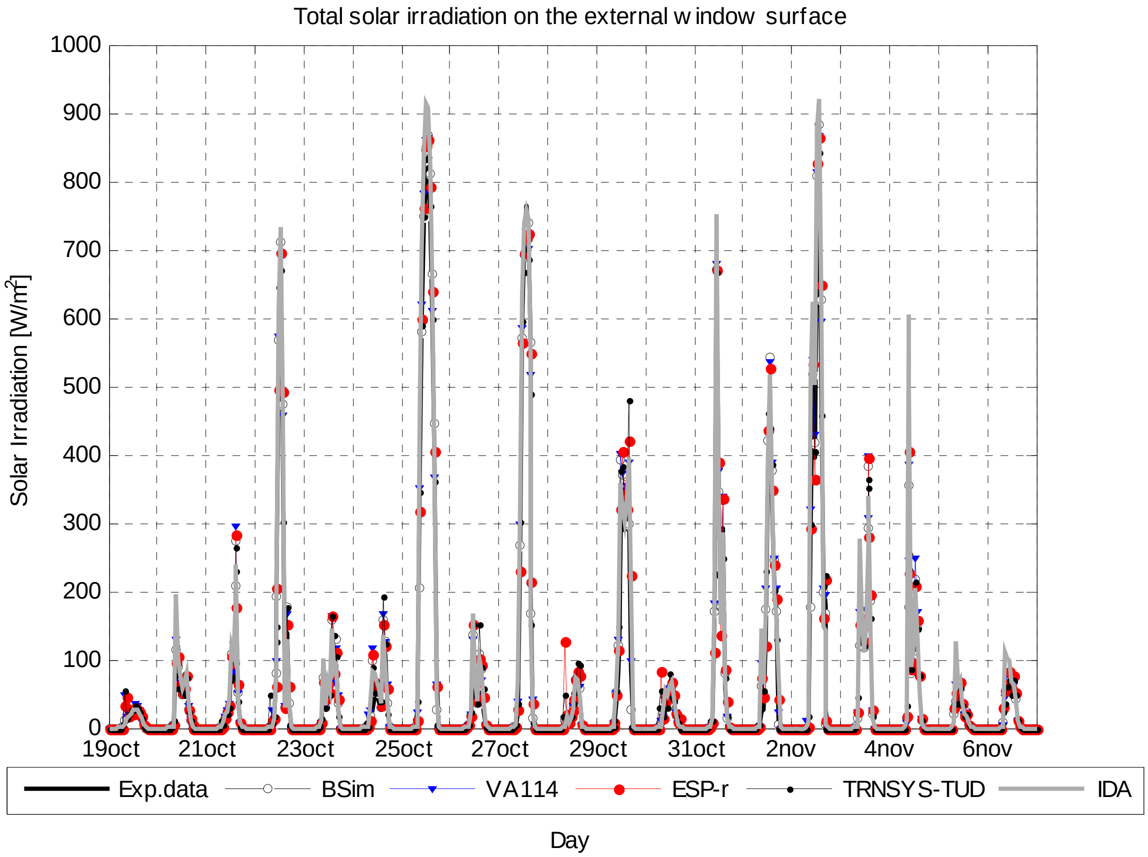

In general one can say that the correspondence of the results for total solar radiation on the external window surface between the models is good when comparing the mean values. The main deviations are characteristic for IDA when the maximum values are compared. Regarding the experimental data, the agreement is still very good for the mean values, comparing the maximum values the experimental data seem to be slightly lower.

Talking about the experimental data, it is necessary to mention that only the total solar irradiation was measured, thus there is no access to the direct and diffuse components on the vertical surface of the DSF. At the same time, the ground reflection in the models, was a fixed value, which can differ from the true experimental conditions, as only 0.5 of the DSF view factor was covered with the ground carpet. Moreover, the measurement accuracy can also have an impact, especially because of the often rain drops on the top of the pyranometer.

3.3.5 Solar radiation transmitted into the zone1 (first order of solar transmission)

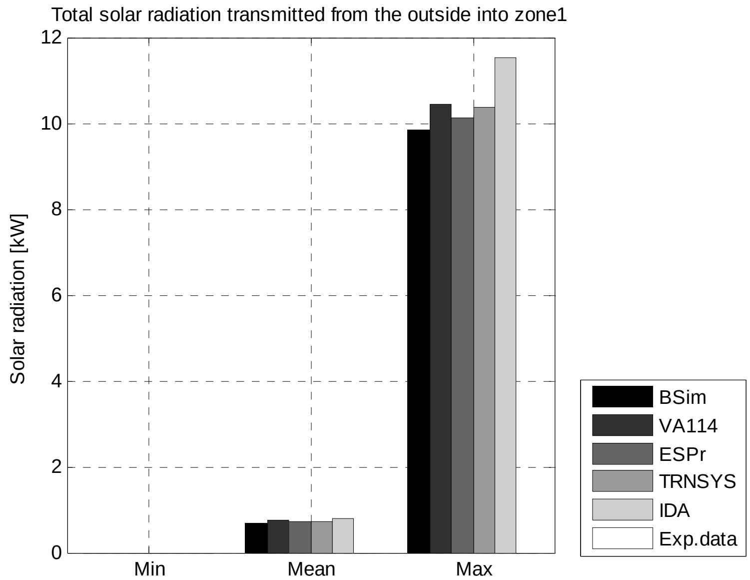

Solar rad. transmitted into the zone 1	BSim	VA114	ESP-r	TRNSYS-TUD	IDA
MIN, kW	0	0	0	0	0
MAX, kW	9.8	10.5	10.1	10.4	11.5
MEAN, kW	0.7	0.8	0.7	0.7	0.8

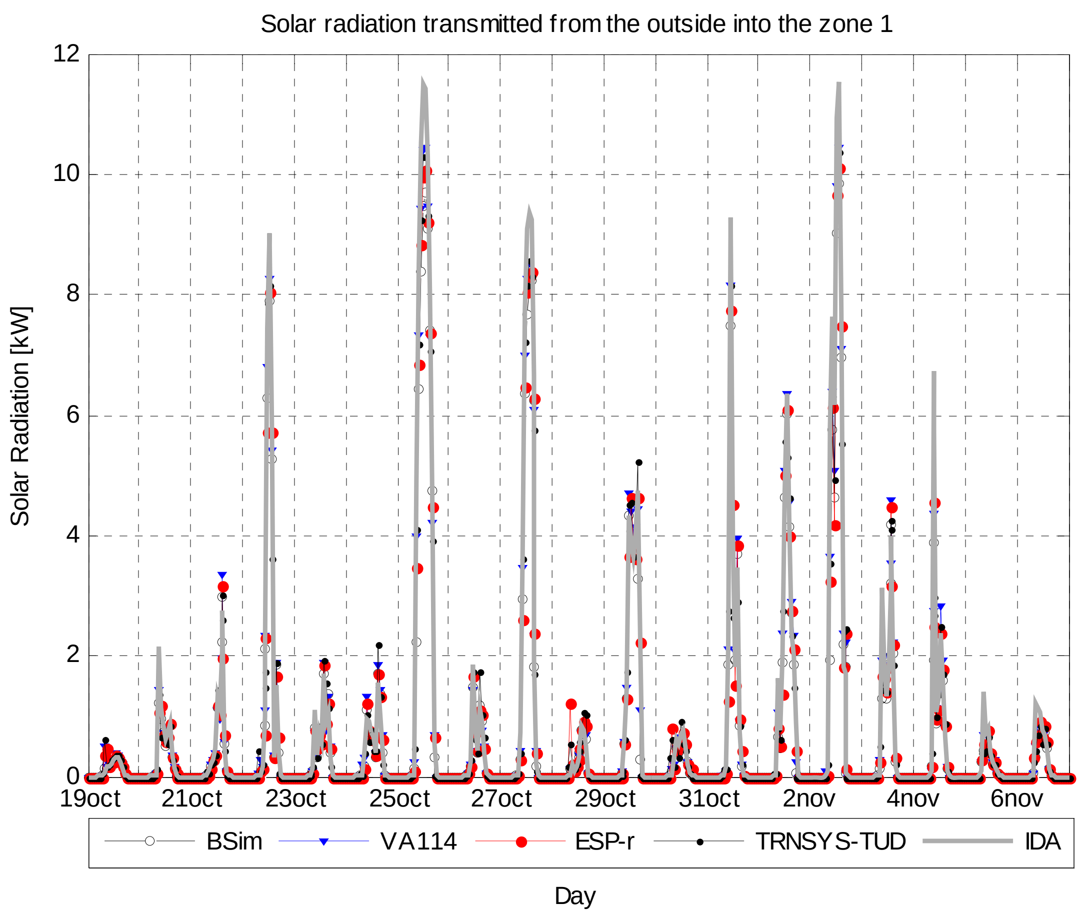

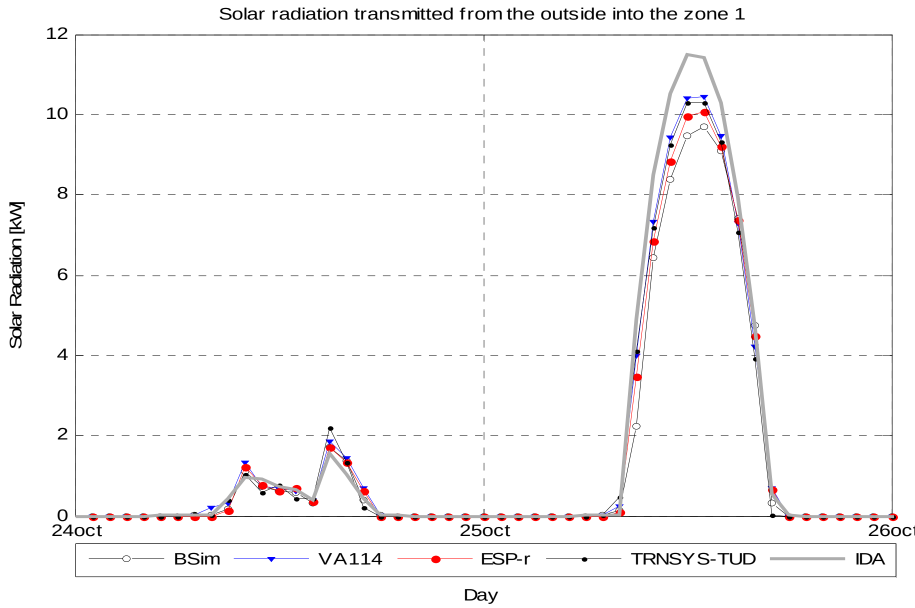

Transmission of solar radiation into the DSF (zone 1) shows good correspondence of the mean values. Again, IDA calculates the maximum values, which are the consequence of calculated maximum incident solar radiation. The quantitative comparison of the window model and transmitted solar radiation into the zones is performed in the following section.

3.3.6 Solar radiation transmitted from zone 1 into the zone 2 (first order of solar transmission)

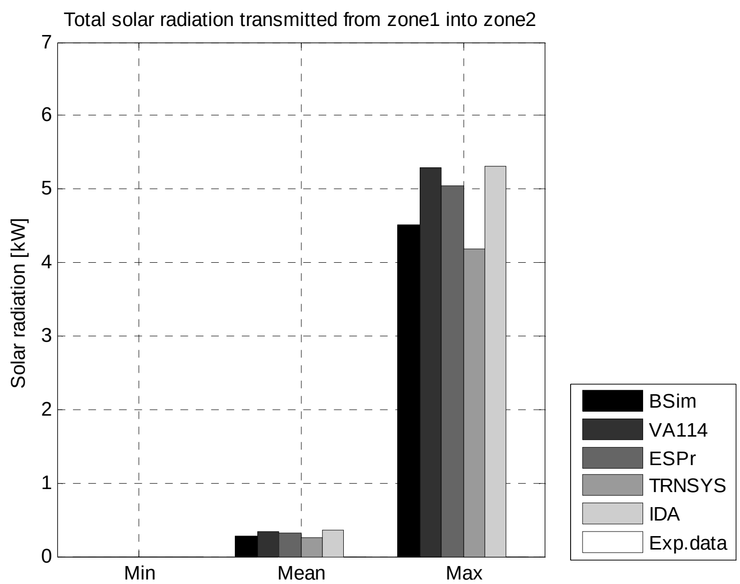

Solar rad. transmitted into the zone 2	BSim	VA114	ESP-r	TRNSYS-TUD	IDA
MIN, kW	0	0	0	0	0
MAX, kW	4.5	5.3	5.0	4.2	5.3
MEAN, kW	0.3	0.3	0.3	0.3	0.4

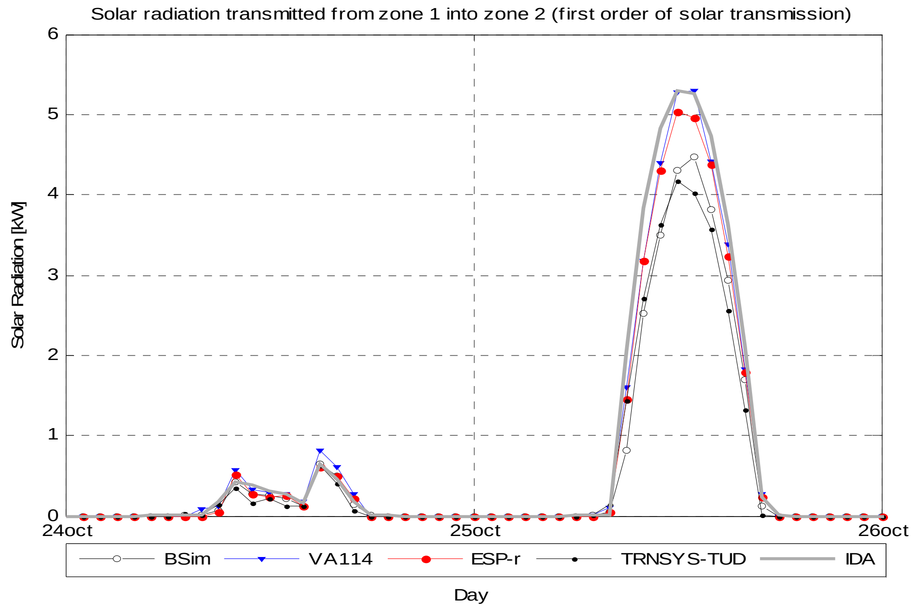

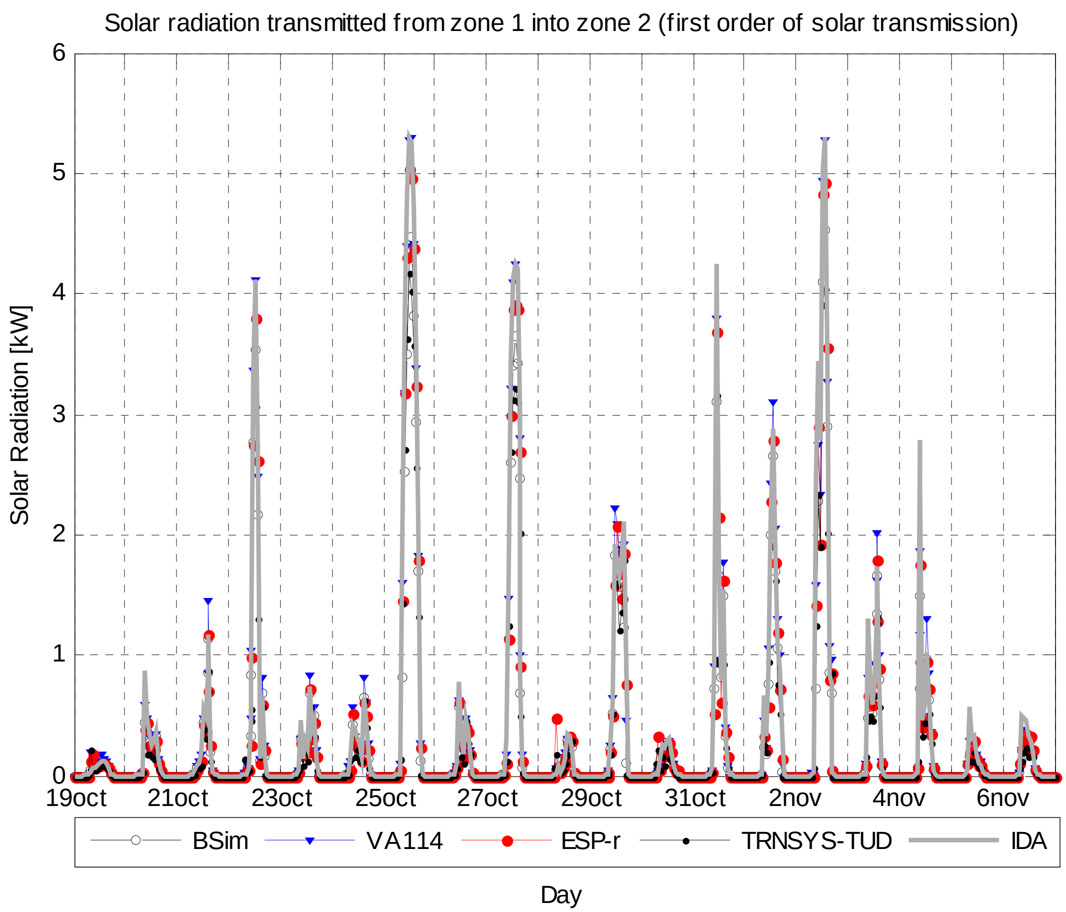

Comparative validation of the models is not a task of this exercise, but this is an important procedure when evaluate the modeling of the boundary conditions in a model. Transmission of the solar radiation was simulated with the good agreement between the programs when comparing the mean values, although the transmission/absorption property of the glazing was modeled with rather different inputs. Following part is used to perform the quantitative analysis and see whether the increase in the transmission property of glazing consequently results in the increase of transmitted solar radiation or not.

Investigation of the results starting with the solar radiation incident on the window surface, solar radiation transmitted into the zone 1 and the one transmitted into the zone 2 do not demonstrate any consistency in forming the groups of high an low values. Therefore, it is necessary to perform further analysis of the results applying some measures to complete the examination.

It is possible to assess how is the solar radiation received on the external window surface, reflected and transmitted into the zone 1 and into the zone 2. Total solar radiation received on the external surface, transmitted into the zone 1 and into the zone 2, calculated by IDA is considered as a reference, representing 100 % of solar radiation, consequently, received on the window surface, solar radiation transmitted into the zone 1 and the one transmitted into the zone 2 (see table below). Correspondingly, the external surface in BSim receives 4%, VA114 6%, ESP-r 6%, TRNSYS-TUD 9% less of solar energy compared to IDA.

Software	Maximum total solar radiation on external window surface		Maximum solar radiation transmitted into the zone 1		Maximum solar radiation transmitted into the zone 2	
	W/m^2	%	kW	%	kW	%
BSim	882	-4	9.8	-15	4.5	-15
VA114	866	-6	10.5	-9	5.3	0
ESP-r	864	-6	10.1	-12	5	-6
TRNSYS-TUD	841	-9	10.4	-10	4.2	-21
IDA	*921*	*0*	*11.5*	*0*	*5.3*	*0*

Although, it is obvious that the processing of solar radiation through the glazing differs between the software in the task, it is very difficult to get a general idea about it. Therefore the maximum of incident, transmitted into zone 1 and transmitted into zone 2 solar radiation calculated in each model has been made dimensionless to the value calculated by IDA and plotted in the below figure:

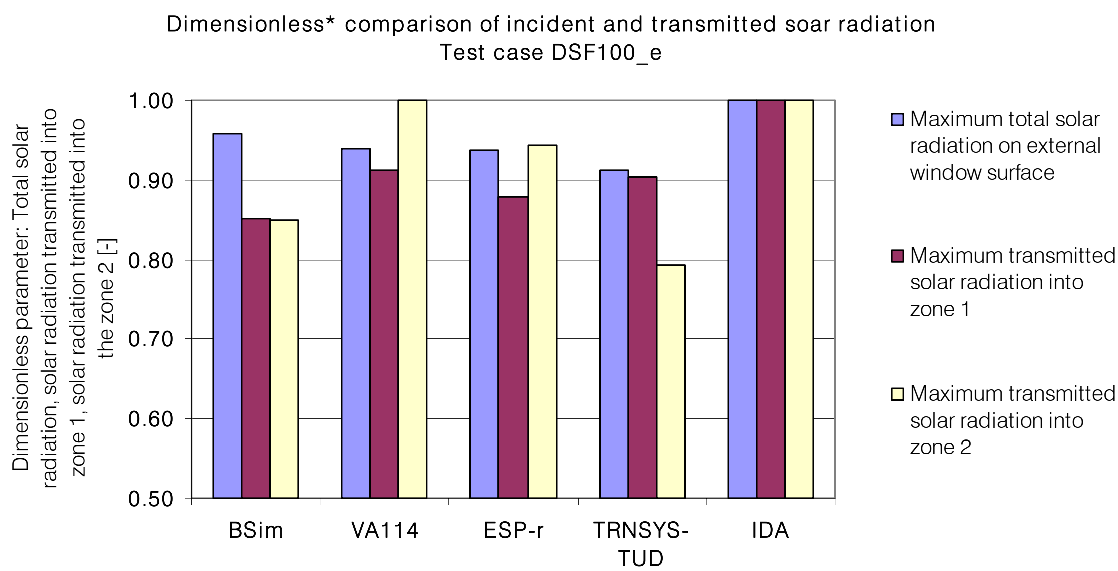

*- every parameter is dimensionless to IDA corresponding parameter

The above bar-plot demonstrates that there is no similarity between the software tools when processing the solar radiation through the glazing.

3.3.7 Summary over simulation of boundary conditions

One of the most essential measures for the validation of simulation programs for buildings with the double skin facade is their ability to predict air temperature and air flow in the double facade cavity, moreover the cooling/heating load to the adjacent room is significant. Therefore the differences in the boundary conditions, such as solar flux on the DSF surface, can be crucial. Glazing area of the double skin facade windows at the outer skin is 16.158m^2 and the differences in predictions of solar irradiation of $\pm$100 W/m^2 will result in $\pm$1.6 kW difference in received solar radiation on the glazing surface.

For the defined empirical test case DSF100_e the solar altitude was verified in the first place, it is unfortunate that it was possible to asses it only for three programs (TRNSYS-TUD, ESP-r and VA114). In further investigations the direct and diffuse solar irradiation demonstrated the deviations in the maximum values, but still these deviations are low. It is particularly noticeable the continuous overestimations of parameters in the boundary conditions by IDA.

By any means, comparing incident total solar radiation with the experimental data, the agreement is rather good, low values of MEANDT and DT95% support that conclusion.

Looking upon transmission of solar radiation, it has been shown that there are differences exist in window treatment between the models. However, the mean values are in good correspondence between the models, while the main difficulties appear when the maximum solar radiation transmitted into the zone 2 is compared between the models, caused by differences in the window models and the glazing properties used.

By any means, calculation of the incident, transmitted and distributed solar radiation is not the focus of these empirical exercises. However, the results of these calculations are the tool and the quality measure for completing the exercises.

3.3.8 Air temperature in the double façade cavity

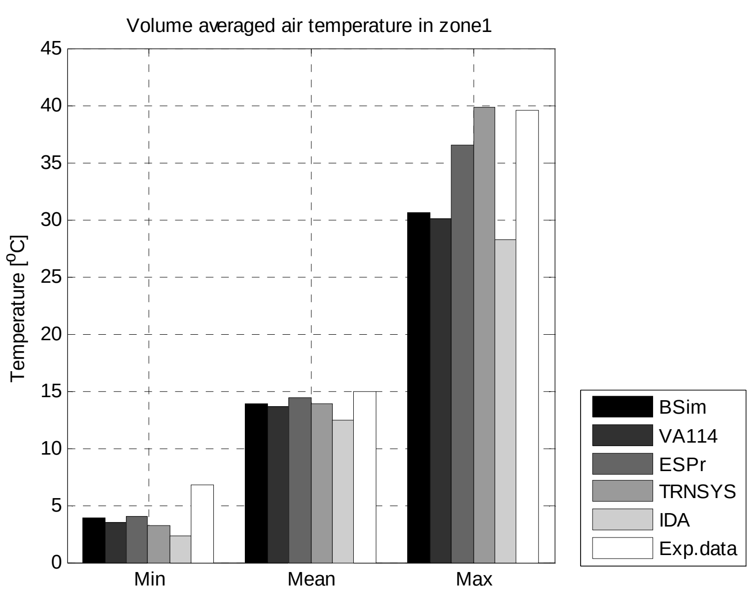

Volume averaged air temperature in zone 1	BSim	VA114	ESP-r	TRNSYS-TUD	IDA	Exp.
MIN, °C	3.9	3.4	4.1	3.2	2.4	6.7
MAX, °C	30.6	30.1	36.5	39.8	28.2	39.5
MEAN, °C	13.8	13.6	14.3	13.9	12.4	15.0
DT95, °C	-5.2	-5.1	-2.7	-3.9	-7.5	
DT5, °C	1.2	0.7	1.2	2.5	0.1	
MEANDT, °C	-0.6	-0.8	-0.3	-0.6	-1.9	
ABMEANDT, °C	1.2	1.1	0.8	1.4	2.0	
RSQMEANDT, °C	2.3	2.3	1.4	2.3	3.3	
STDERR, °C	2.3	2.2	1.4	2.2	2.7	

Discussion of the results of the air temperature measurement in the DSF cavity is appropriate to start with the remark about the procedure for the measurement of the air temperature in the test facility. The air temperature is a difficult matter to measure when a thermocouple is exposed to solar radiation, as explained in [3]. The bar-plot above demonstrates that the average values are in good correspondence between the programmes and experimental data. However the maximum values are represented by two groups of the results [ESP-r, TRNSYS-TUD, Exp. Data] and [BSim, VA114, IDA]. The first group demonstrates agreement with the experimental data. With regard to the table of statistics, one can note that the mean error (MEANDT) is always with the minus sign, which denotes that the measured values are generally higher than predicted ones.

Although the steps were undertaken to decrease the effect of the solar radiation when measuring the air temperature, it was not possible to ensure that the measured air temperature is exactly its true temperature [1], thus there is a possibility for an error caused by solar radiation. However, the experimental data demonstrates higher air temperatures in the DSF cavity at night and in the cloudy days compared to the predicted ones. Besides, the degree of error due to solar radiation in the experimental data is rather low according to the preliminary tests of air temperature measurement procedure (see [3]). Hence, the models underestimate the air temperature in the cavity.

From the statistical data ESP-r seems to perform well when consider dynamics of the system (lowest STDERR), this is probably due to the set of climate data, as ESP-r is only the one model using the 10min-step climate data. ESP-r is also the model that follows the slope of the plotted experimental data.

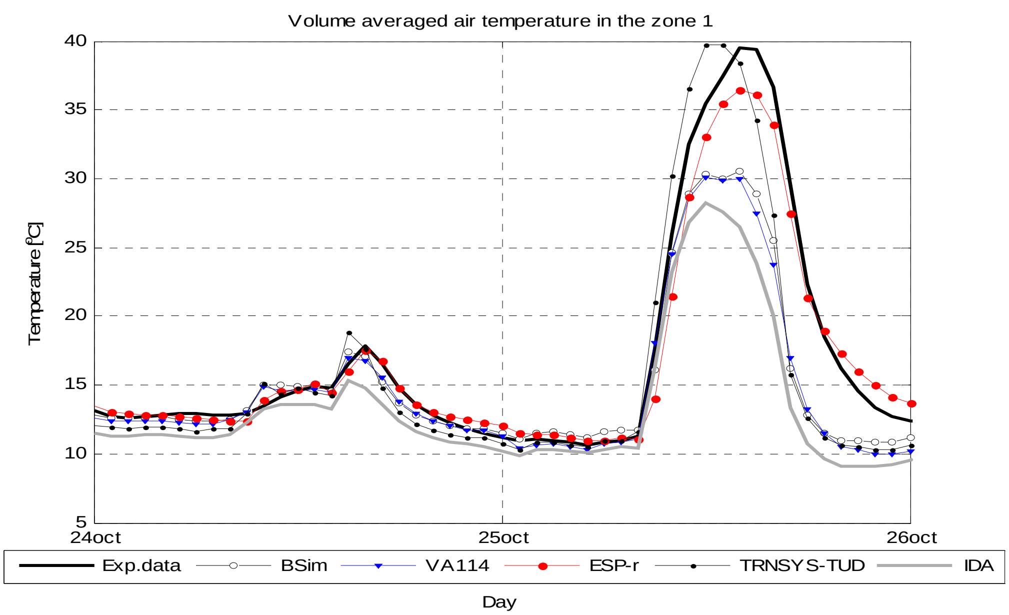

•

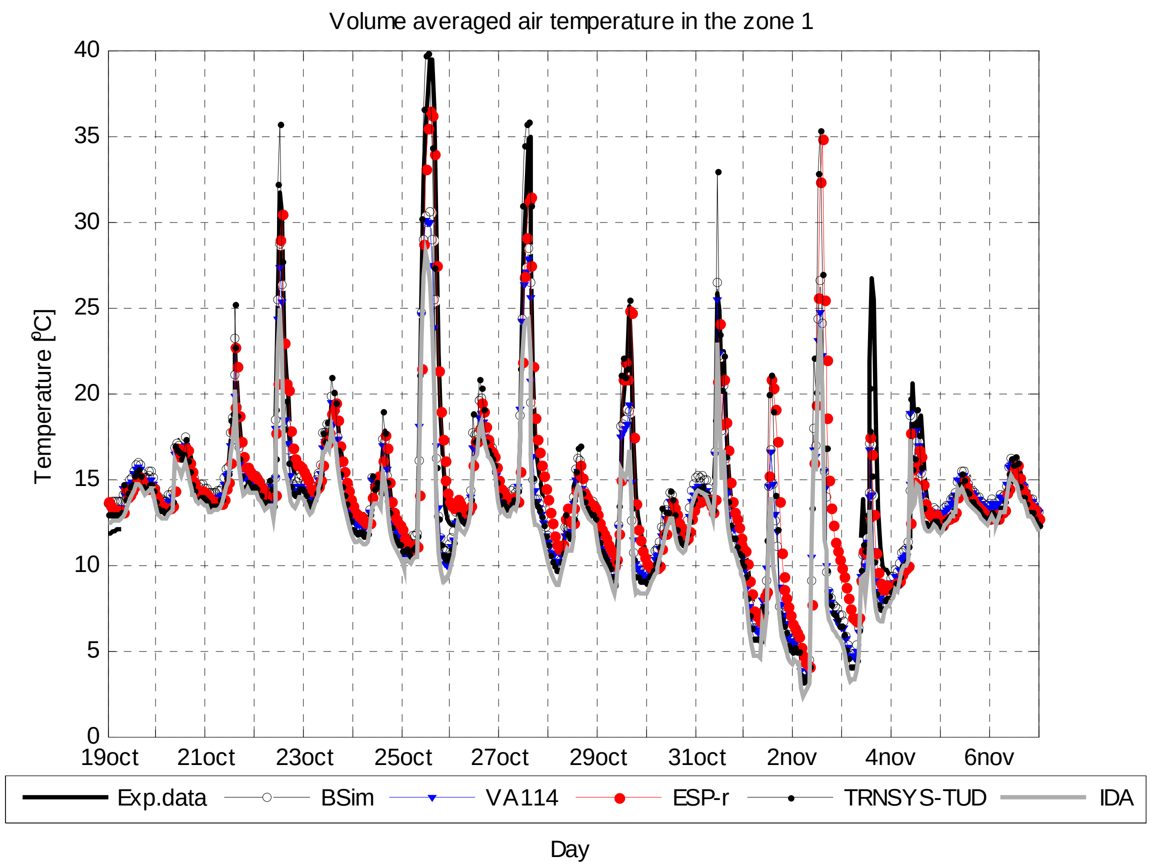

The temperature raise in the DSF cavity is used as one of the main measures in the case with the natural ventilation, that's why it is also reported for the test case DSF100_e.
May be move in appendix

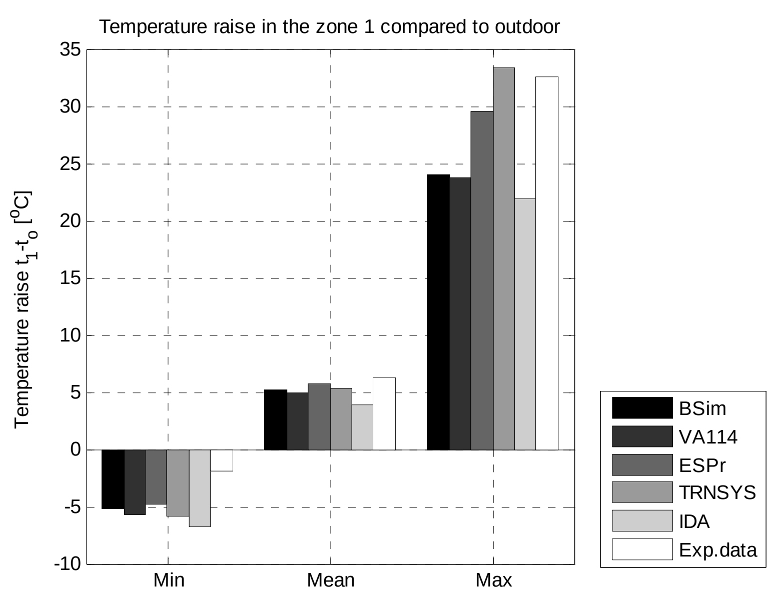

Temperature raise in the zone 1 compared to outdoor (t_1-t_o)	BSim	VA114	ESP-r	TRNSYS-TUD	IDA	Exp.
MIN, °C	-5.2	-5.7	-4.8	-5.9	-6.7	-1.9
MAX, °C	24.0	23.8	29.6	33.4	21.9	32.6
MEAN, °C	5.2	5.0	5.7	5.3	3.8	6.2
DT95, °C	-5.2	-5.1	-2.7	-3.9	-7.5	
DT5, °C	1.2	0.7	1.2	2.5	0.1	
MEANDT, °C	-0.6	-0.8	-0.3	-0.6	-1.9	
ABMEANDT, °C	1.2	1.1	0.8	1.4	2.0	
RSQMEANDT, °C	2.3	2.3	1.4	2.3	3.3	
STDERR, °C	2.3	2.2	1.4	2.2	2.7	

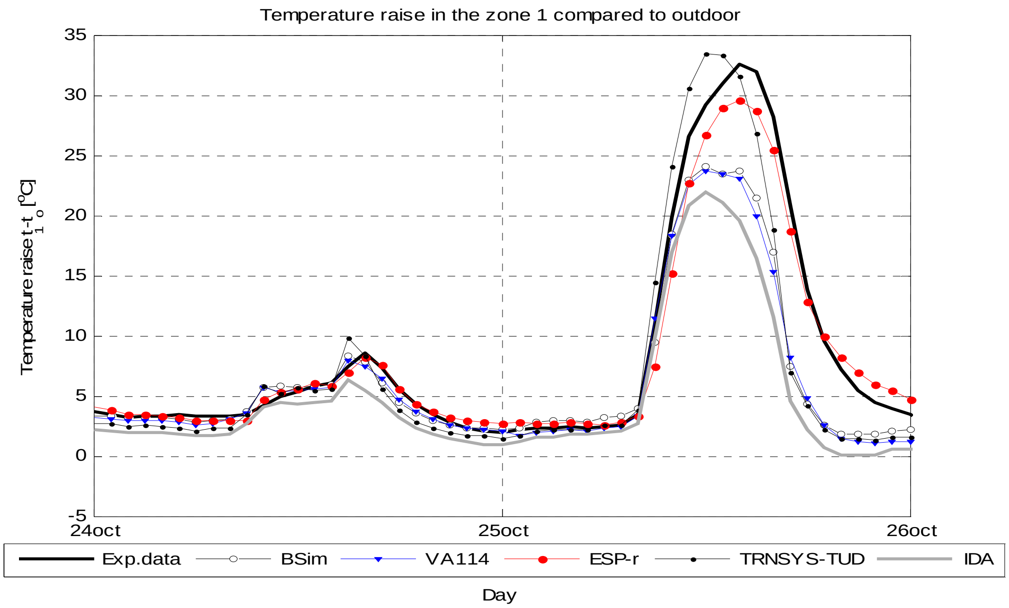

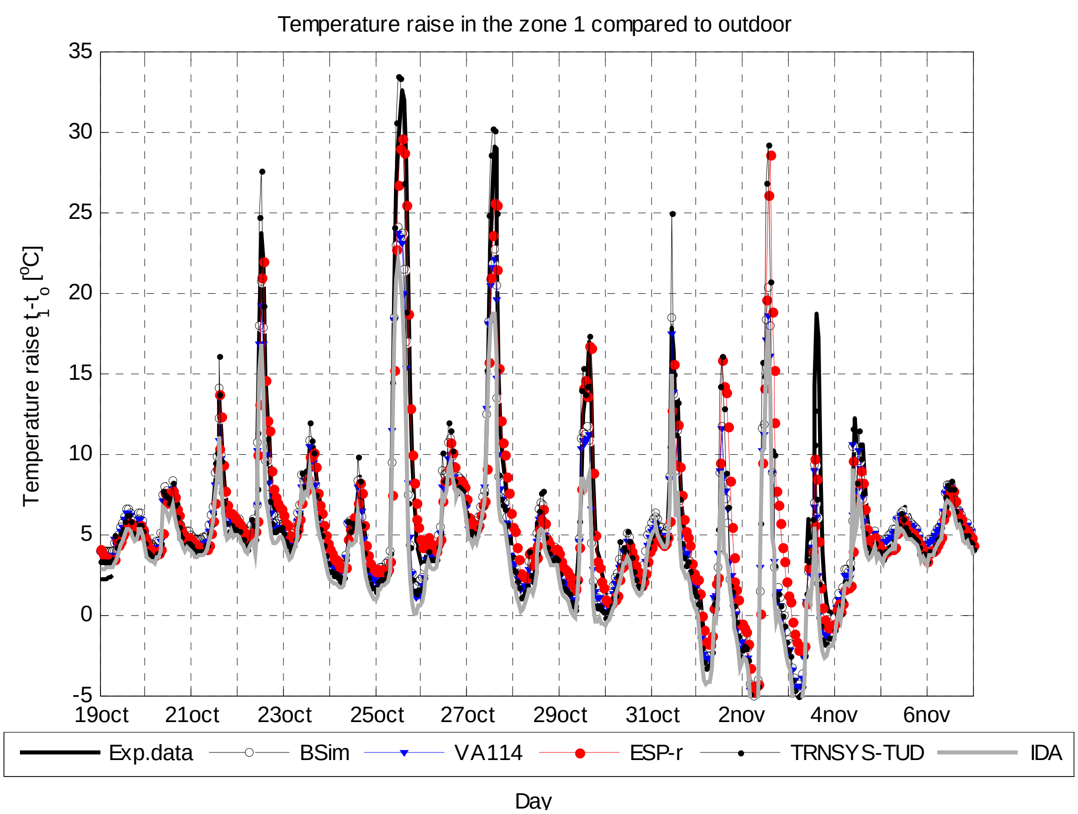

3.3.9 Energy load to the zone 2

Cooling load in zone 2

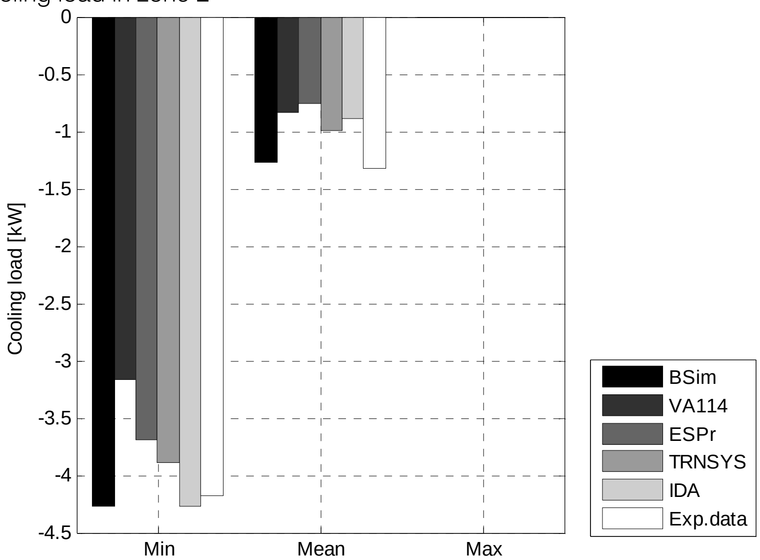

Cooling load in zone 2	BSim	VA114	ESP-r	TRNSYS-TUD	IDA	Exp.
MIN, kW	-4.28	-3.16	-3.69	-3.89	-4.27	-4.18
MAX, kW	-0.01	0.00	0.00	-0.01	0.00	0.00
MEAN, kW	-1.27	-0.83	-0.76	-0.99	-0.89	-1.33
DT95, kW	-0.52	-0.30	-0.57	-0.56	-0.80	
DT5, kW	0.32	0.96	1.00	0.67	0.29	
MEANDT, kW	-0.12	0.14	0.08	0.01	-0.14	
ABMEANDT, kW	0.22	0.32	0.35	0.26	0.25	
RSQMEANDT, kW	0.29	0.43	0.45	0.34	0.35	
STDERR, kW	0.27	0.41	0.45	0.34	0.32	

Looking upon the statistical analysis, most of the models underestimate the cooling load into the zone (positive MEANDT), mean values are in good correspondence between the models, but lower than measured. It is characteristic that BSim predicts the highest cooling loads, which are probably caused by the fact that all solar radiation approaching the surface is fully absorbed.

Heating load in zone 2

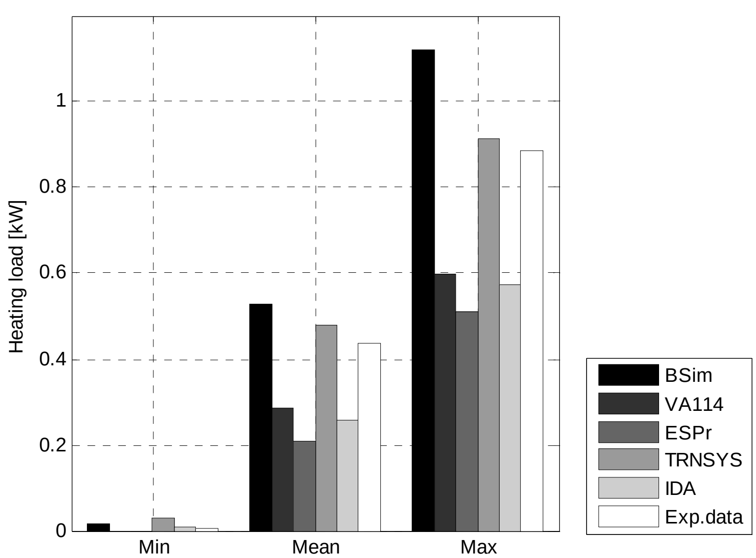

Heating load in zone 2	BSim	VA114	ESP-r	TRNSYS-TUD	IDA	Exp.
MIN, kW	0.02	0.00	0.00	0.03	0.01	0.01
MAX, kW	1.12	0.60	0.51	0.91	0.57	0.89
MEAN, kW	0.53	0.29	0.21	0.48	0.26	0.44
DT95, kW	-0.07	-0.28	-0.45	-0.23	-0.36	
DT5, kW	0.29	-0.07	-0.07	0.16	-0.09	
MEANDT, kW	0.09	-0.18	-0.26	0.01	-0.21	
ABMEANDT, kW	0.11	0.18	0.26	0.10	0.21	
RSQMEANDT, kW	0.15	0.19	0.28	0.13	0.23	
STDERR, kW	0.12	0.08	0.11	0.13	0.09	

More difficulties are noticeable in calculation of the heating load, two groups of the results are obvious: [BSim, TRNSYS-TUD, Exp. data] and [VA114, ESP-r and IDA]. The second group of the results differs up to 50% from the experimental data. In ESP-r, IDA- and VA114.-models this may be due to the fact the thermal bridges were ignored. Some preliminary heat loss experiments in 'the Cube' have demonstrated that the heat losses from the building are low, still the deviation between the models which include and ignore the heat losses is obvious, although the differences are in the range of 200W for the mean values.

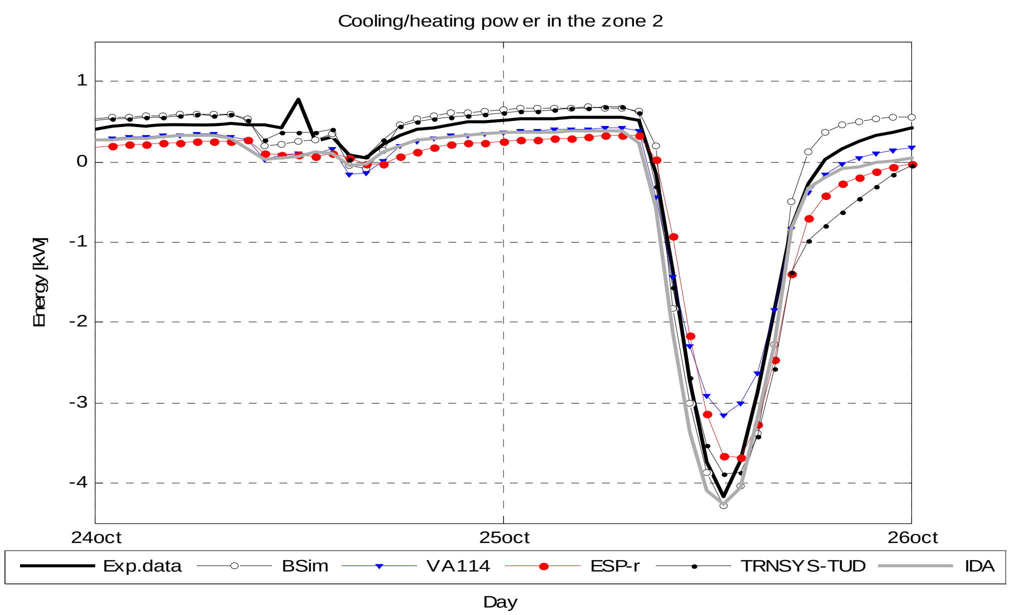

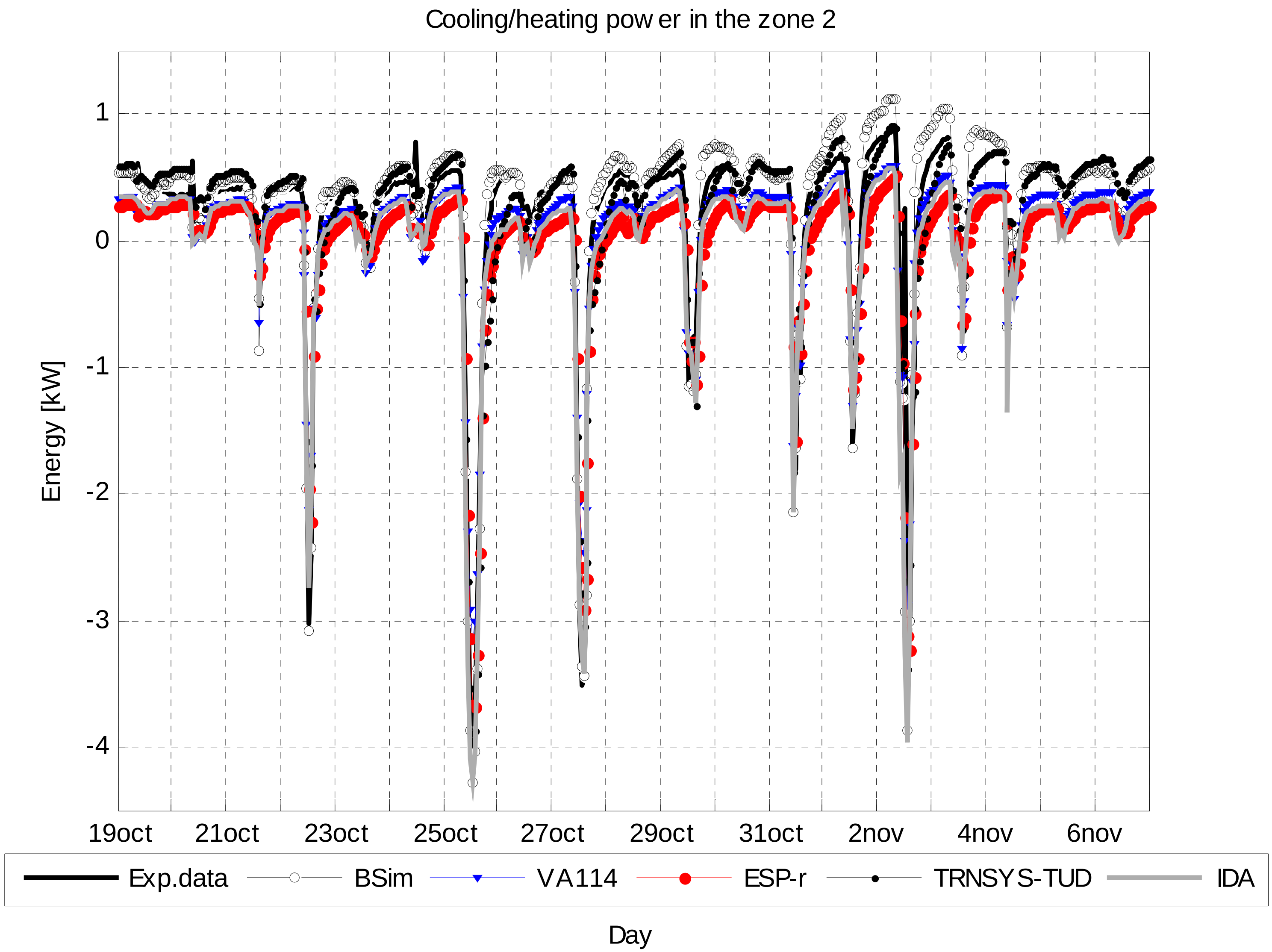

Cooling/heating pow er in the zone 2
1
0
-1
-2
-3
-4
Energy [kW]
19oct
21oct
23oct
25oct
27oct
29oct
31oct
2nov
4nov
6nov
Exp.data
BSim
VA114
ESP-r
TRNSYS-TUD
IDA
Day

DSF200_e

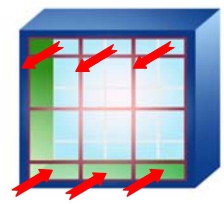

3.4 Test case DSF200_e

In this test case the most complex phenomenon of the double façade cavity is investigated – the naturally ventilated double skin façade, which includes impact both from the buoyancy and wind forces. The ventilation strategy in this test case belongs to the single sided ventilation with the openings in the different

3.4.1 Direct solar irradiation

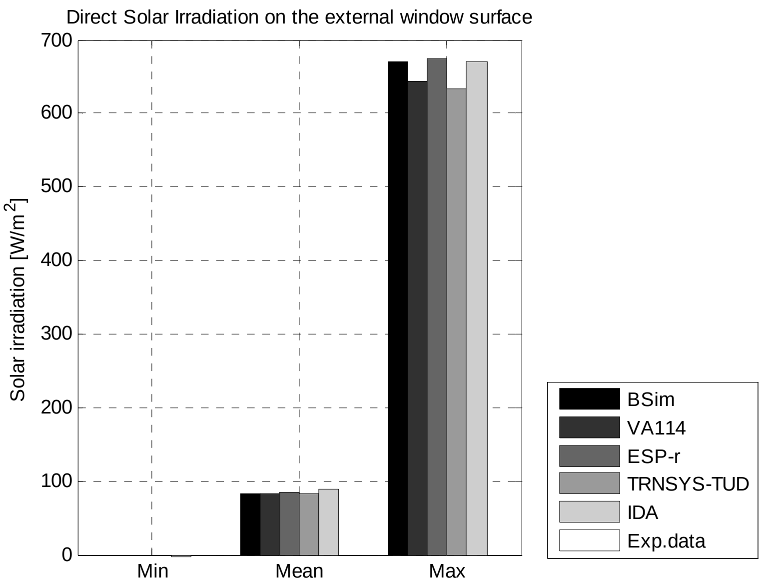

Direct solar rad. on ext window surface	BSim	VA114	ESP-r	TRNSYS-TUD	IDA
MIN, W/m^2	0	0	0	0	-3
MAX, W/m^2	670	643	675	634	669
MEAN, W/m^2	83	84	84	82	89

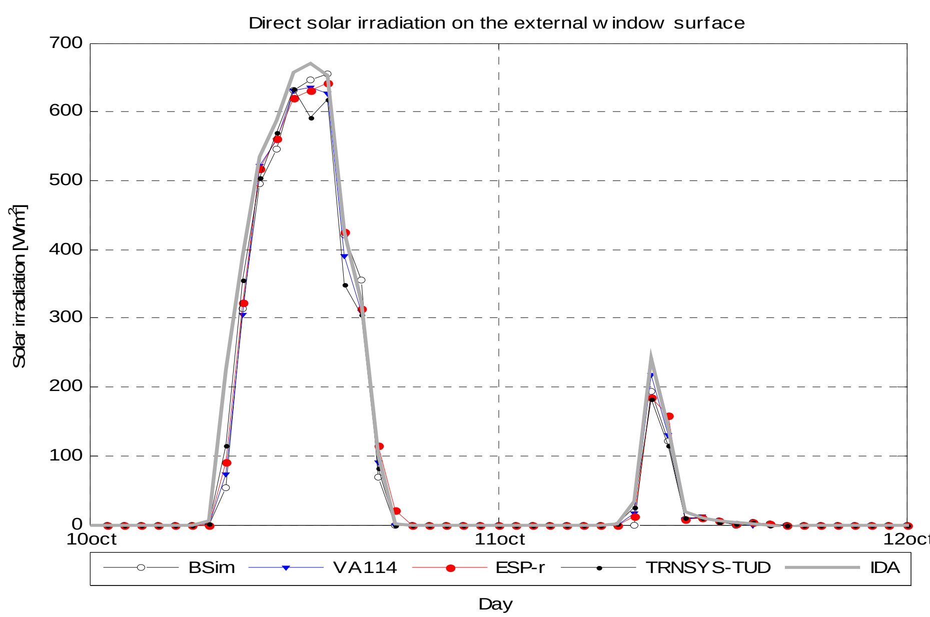

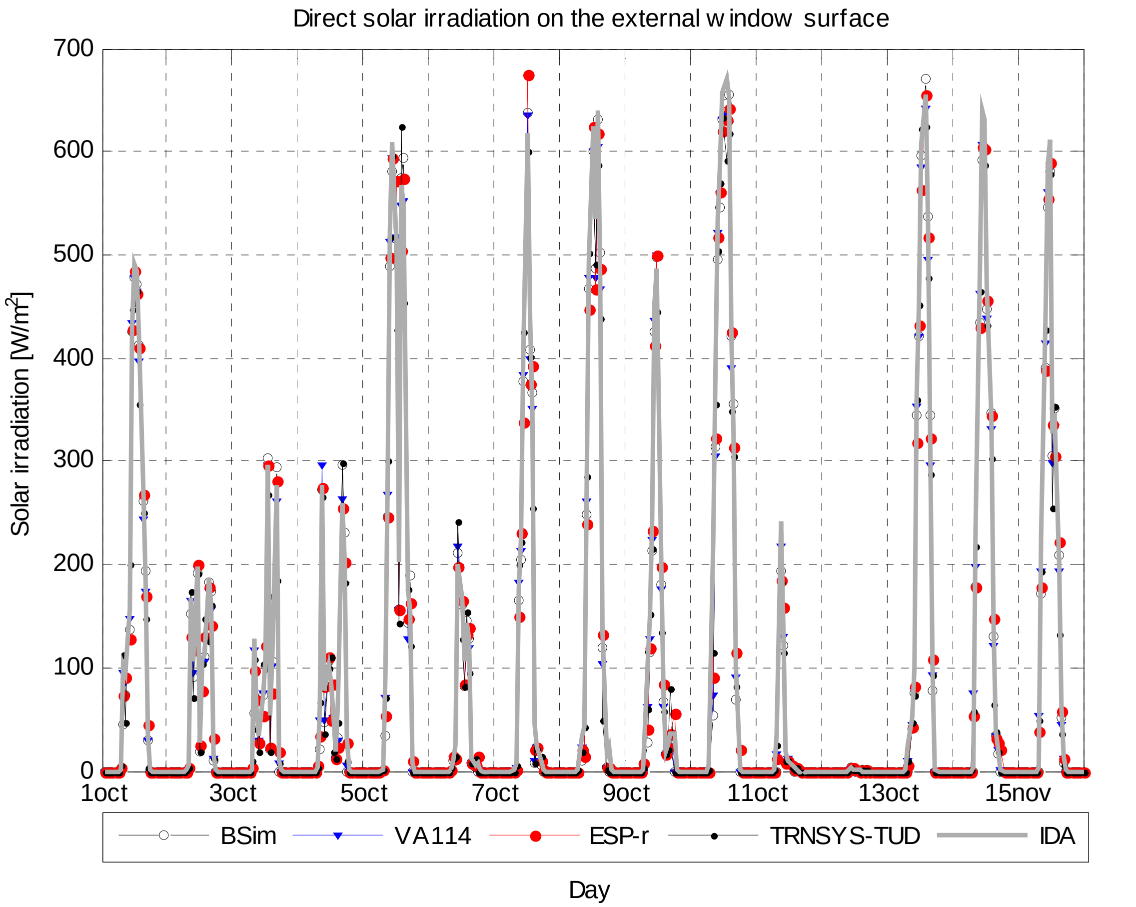

There are two groups of results for direct solar irradiation when compare the maximum values: the higher values belong to BSim, ESP-r and IDA, while the lower values belong to TRNSYS-TUD and VA114. Good correspondence of the results can be seen for the average values and especially for the days with the low solar intensity.

3.4.2 Diffuse solar irradiation

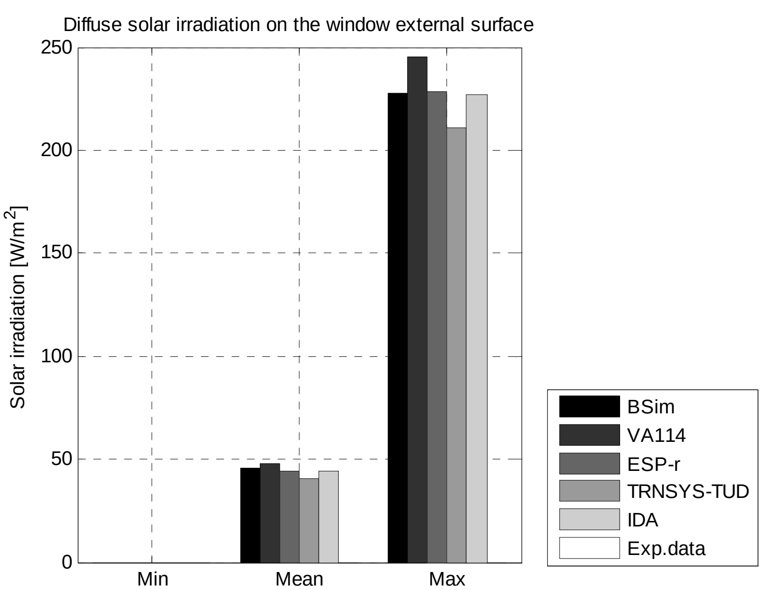

Diffuse solar rad. on the window ext. surface	BSim	VA114	ESP-r	TRNSYS-TUD	IDA
MIN, W/m²	0	0	0	0	0
MAX, W/m²	228	245	229	211	227
MEAN, W/m²	46	48	45	41	44

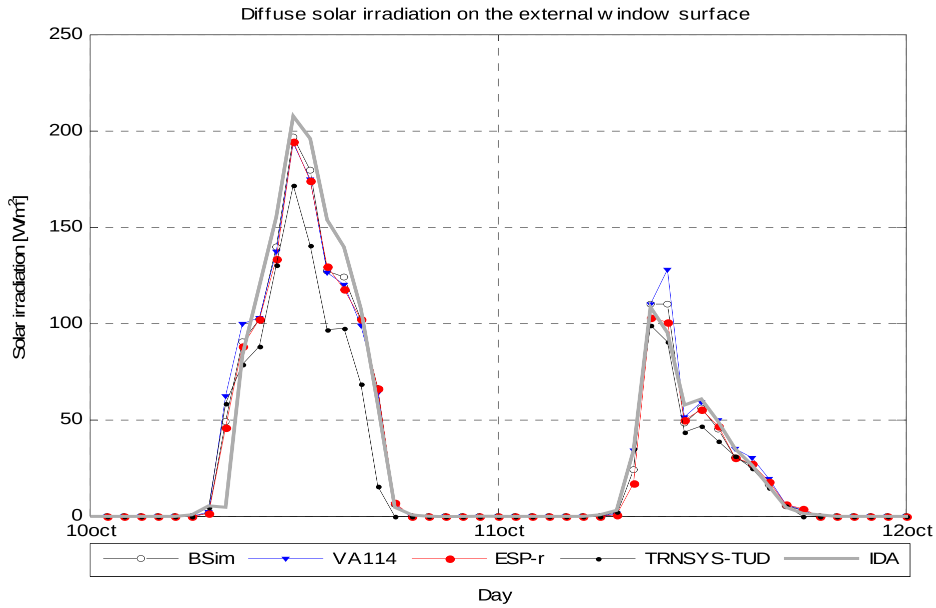

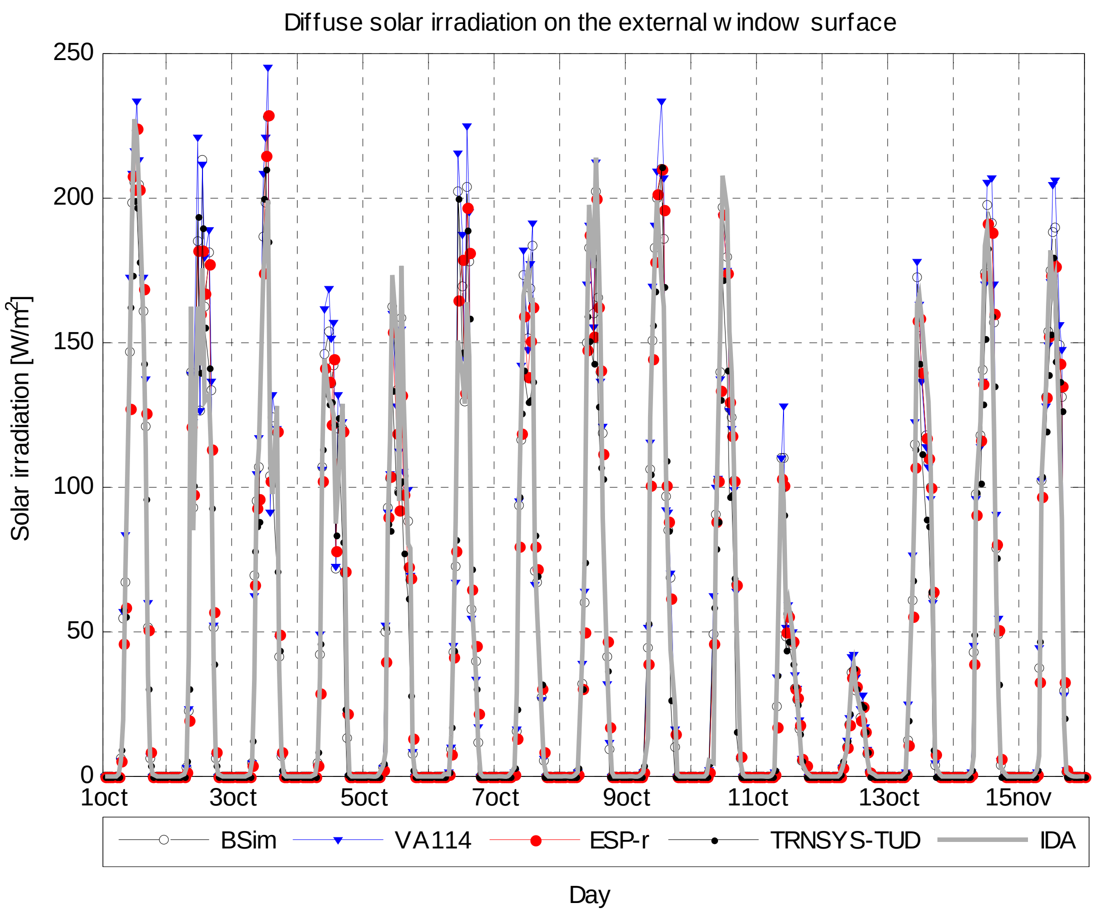

Simulations of the diffuse solar radiation shows generally good correspondence between the mean values, while the maximal differ: highest values belong to VA114 and the lowest to TRNSYS-TUD. Although it is possible to see the deviations between the programs, these are in the range of a few watts per square meter.

3.4.3 Total solar irradiation

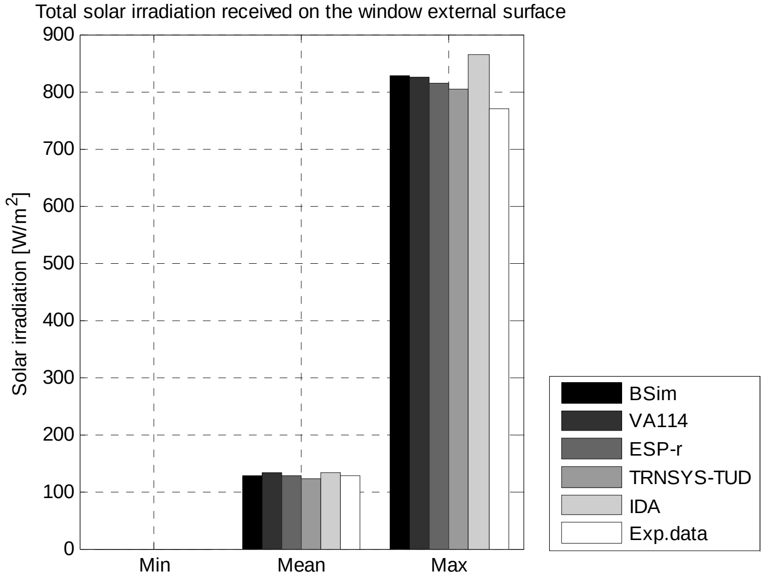

Total solar rad. on ext window surface	BSim	VA114	ESP-r	TRNSYS-TUD	IDA	Exp.
MIN, W/m^2	0	0	0	0	0	0
MAX, W/m^2	827	824	814	805	865	769
MEAN, W/m^2	129	132	129	123	133	128
DT95, W/m^2	-24	-9	-28	-57	-15	
DT5, W/m^2	49	39	41	32	66	
MEANDT, W/m^2	3	6	3	-3	8	
ABMEANDT, W/m^2	10	9	9	12	13	
RSQMEANDT, W/m^2	19	17	18	25	25	
STDERR, W/m^2	19	16	17	25	24	

Again, similar to the test case DSF100_e the maximum values of the total solar irradiation on the vertical surface of the DSF are overestimated in the models, especially in IDA model, while the average values are in a good agreement. The experimental data might include some level of error due to the imperfect experimental conditions and considering that the absolute mean error (ABMEANDT) is rather small.

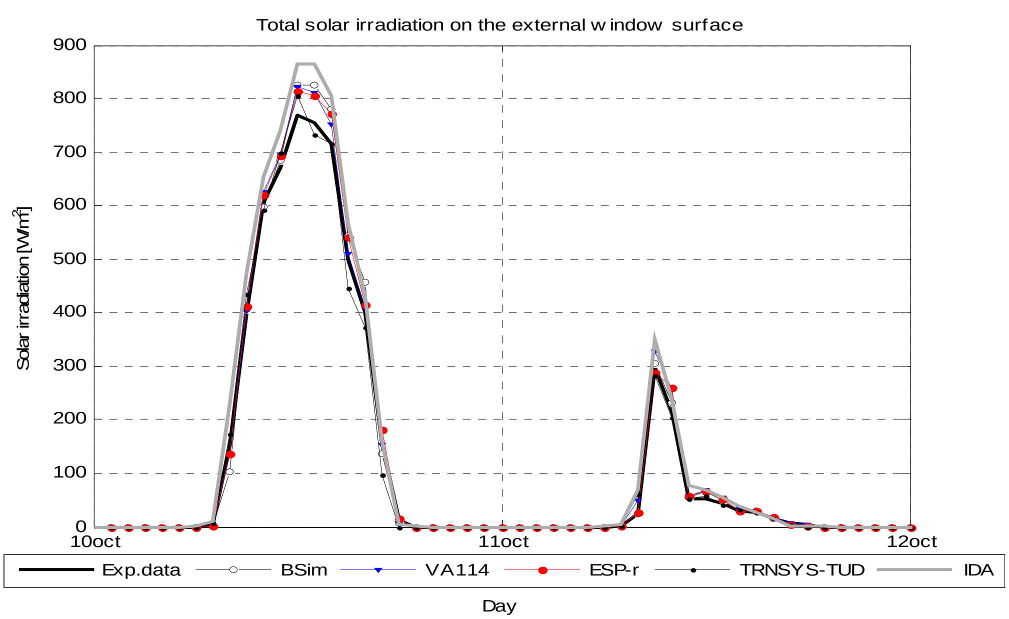

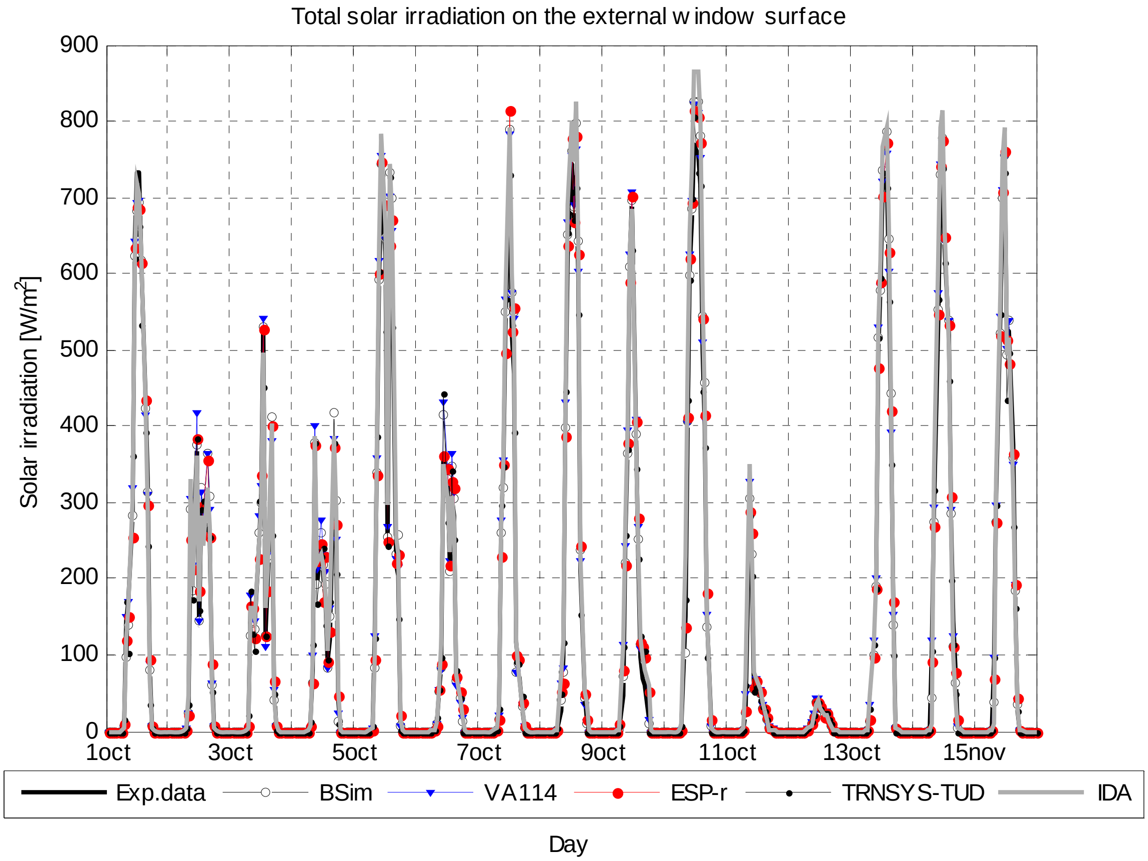

Total solar irradiation on the external w indow surface
Solar irradiation [W/m2]
900
800
700
600
500
400
300
200
100
0
1oct
3oct
5oct
7oct
9oct
11oct
13oct
15nov
Exp.data
BSim
VA114
ESP-r
TRNSYS-TUD
IDA
Day

3.4.4 Solar radiation transmitted into the zone1 (first order of solar transmission)

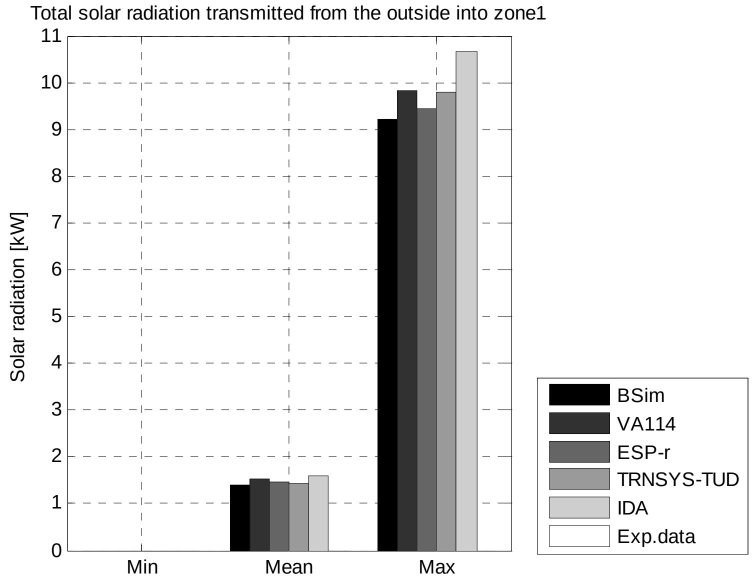

Solar rad. transmitted into the zone 1	BSim	VA114	ESP-r	TRNSYS-TUD	IDA
MIN, kW	0	0	0	0	0
MAX, kW	9.2	9.8	9.4	9.8	10.7
MEAN, kW	1.4	1.5	1.4	1.4	1.6

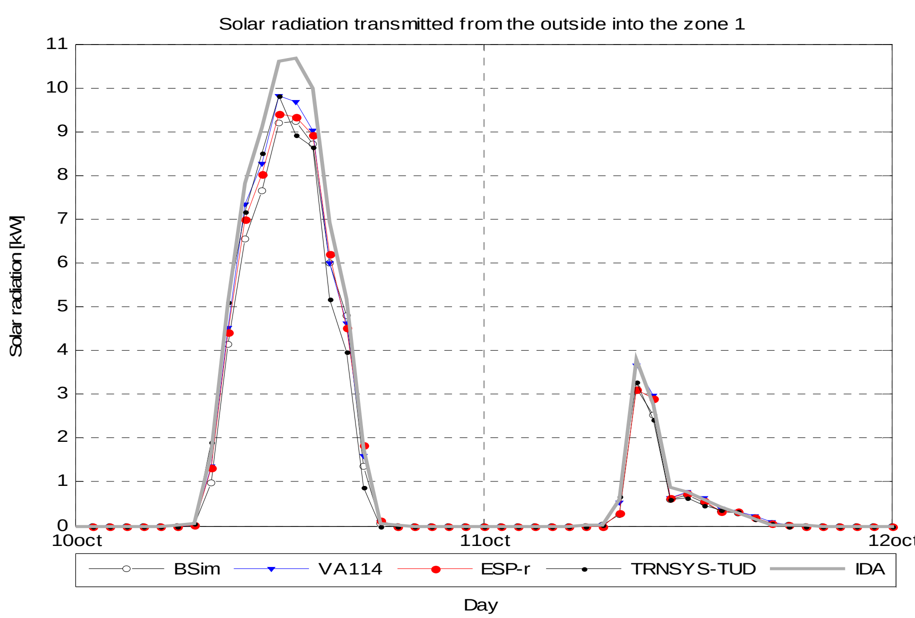

Transmission of solar radiation into the DSF (zone 1) shows good correspondence of the mean values. Again, IDA calculates the maximum values (same as in the test case DSF100_2), which are the consequence of calculated maximum incident solar radiation. Results are in exceptionally good agreement in the days with the low solar radiation intensity.

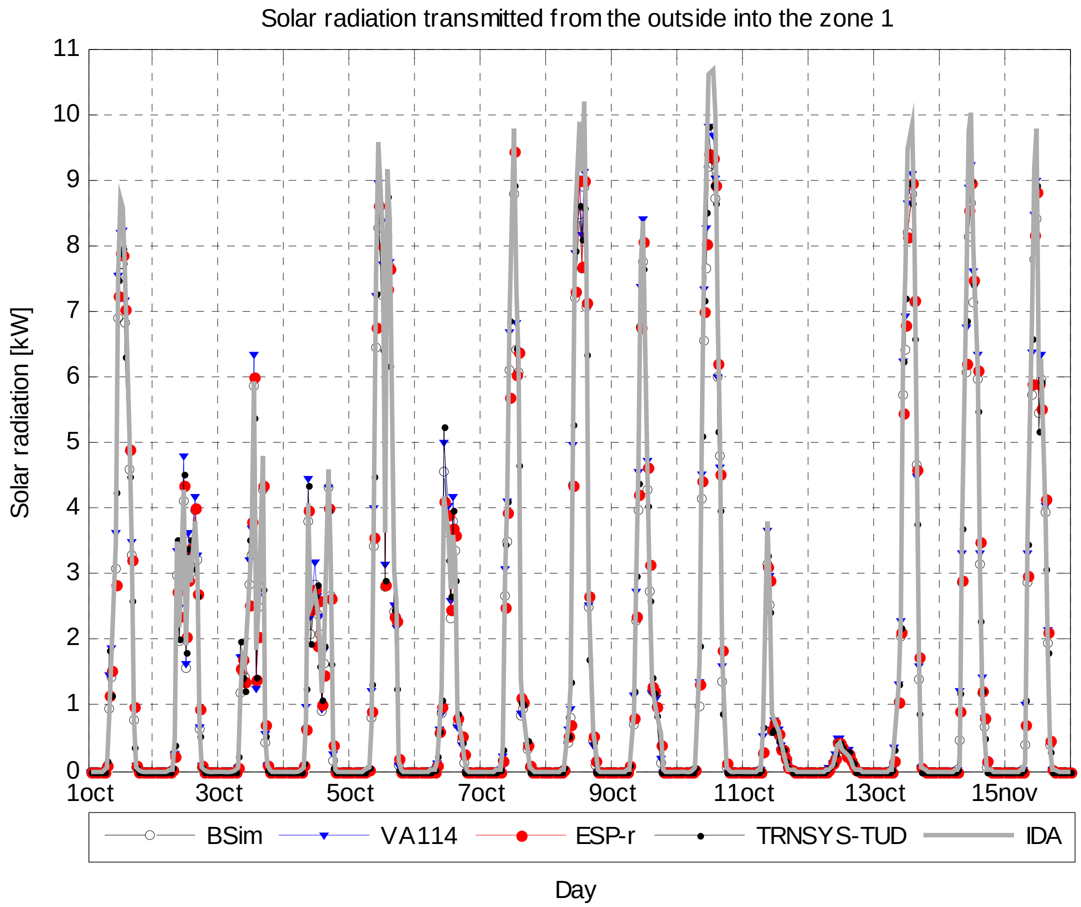

3.4.5 Solar radiation transmitted into the zone2 (first order of solar transmission)

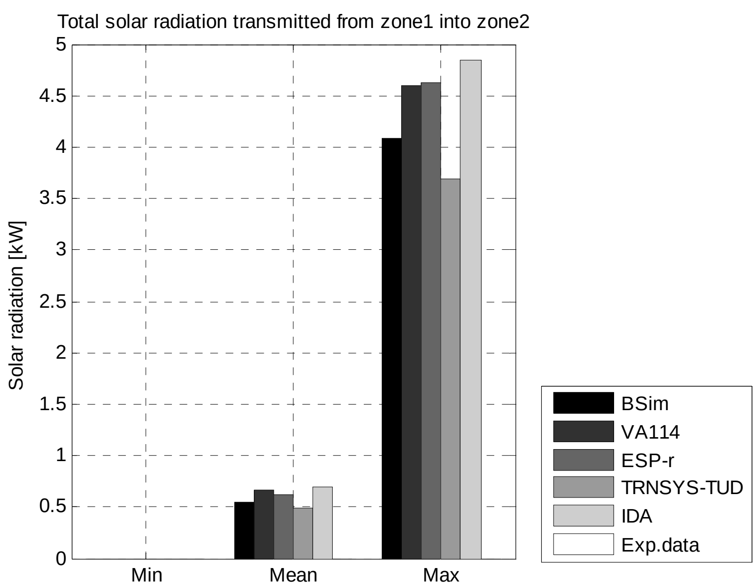

Solar rad. transmitted into the zone 2	BSim	VA114	ESP-r	TRNSYS-TUD	IDA
MIN, kW	0	0	0	0	0
MAX, kW	4.1	4.6	4.6	3.7	4.9
MEAN, kW	0.6	0.7	0.6	0.5	0.7

The situation is identical with the test case DSF100_e, where the relatively good agreement is achieved between the models when calculating the average of the transmitted solar radiation into the zone 2, while the situation is different with regard to the maximum values. There appear 2 groups of the results: low values are characteristic for TRNSYS and IDA and the maximum is calculated by VA114, ESP-r and IDA. Such a substantial deviation between the predictions (up to 1kW in max values) is probably caused by the differences in the window model and inputs in the glazing optical properties.

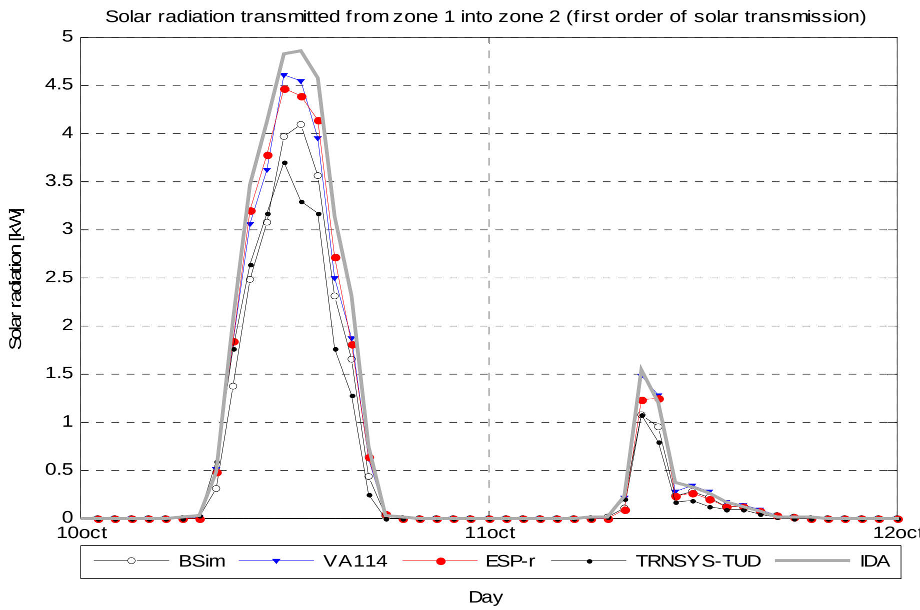

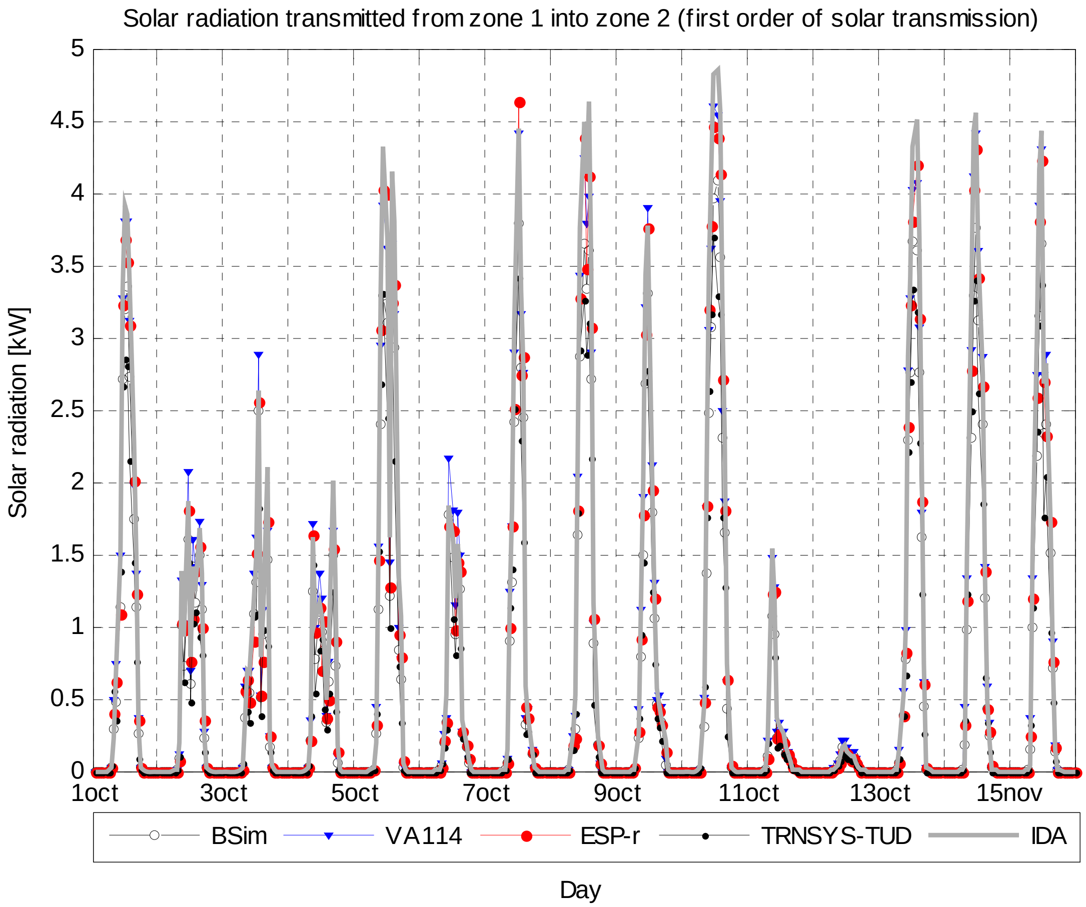

Investigation of the results starting with the solar radiation incident on the window surface, solar radiation transmitted into the zone 1 and the one transmitted into the zone 2 do not demonstrate any consistency in forming the groups of high an low values, however the consistency between the test cases is clear (see figure below) and the corresponding one for the test case DSF100_e in section 3.3.6.

It is possible to assess how is the solar radiation received on the external window surface, reflected and transmitted into the zone 1 and into the zone 2. Total solar radiation received on the external surface calculated by IDA is considered as a reference, representing 100 % of solar radiation received (see figure below).

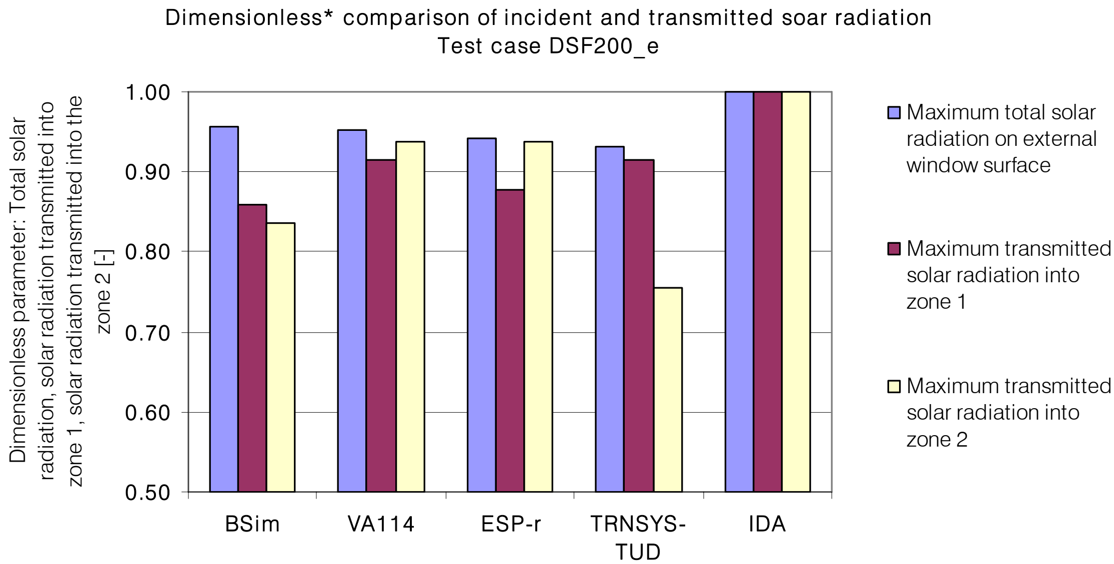

*- every parameter is dimensionless to IDA corresponding parameter

The above plot is almost identical with the one prepared for the test case DSF100_e, that proves the consistency of the simulations between the test cases, however it is also used to demonstrate the differences in the window models applied, as the above plot doesn't follow the differences between the models regarding the glazing optical properties, discussed in the section 3.2.1.

3.4.6 Air temperature in the double façade cavity

To include the air temperature-figures in appendix ?

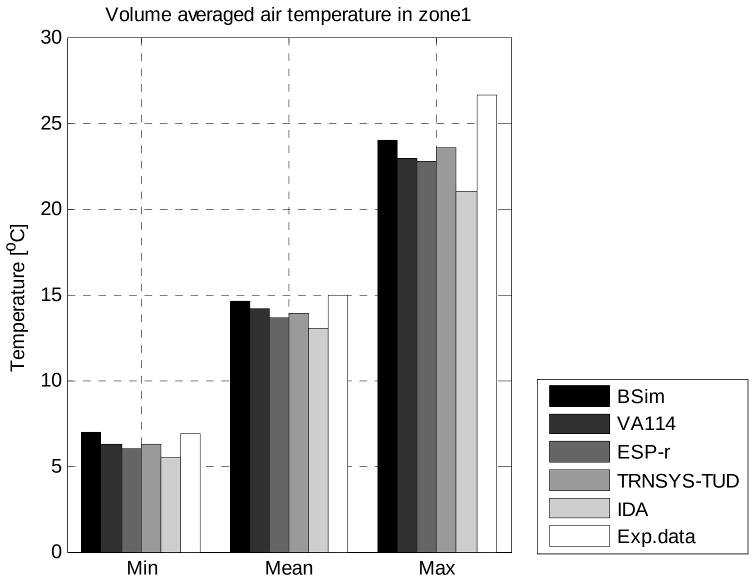

Volume averaged air temperature in zone 1	BSim	VA114	ESP-r	TRNSYS-TUD	IDA	Exp.
MIN, °C	7.0	6.3	6.0	6.3	5.5	6.9
MAX, °C	24.0	23.0	22.8	23.6	21.0	26.7
MEAN, °C	14.6	14.1	13.6	13.9	13.0	15.0
DT95, °C	-2.4	-3.6	-4.5	-3.4	-5.4	
DT5, °C	0.5	0.3	-0.1	0.0	-0.5	
MEANDT, °C	-0.3	-0.8	-1.3	-1.0	-1.9	
ABMEANDT, °C	0.6	0.9	1.3	1.0	1.9	
RSQMEANDT, °C	0.9	1.4	1.9	1.4	2.4	
STDERR, °C	0.9	1.1	1.4	1.1	1.5	

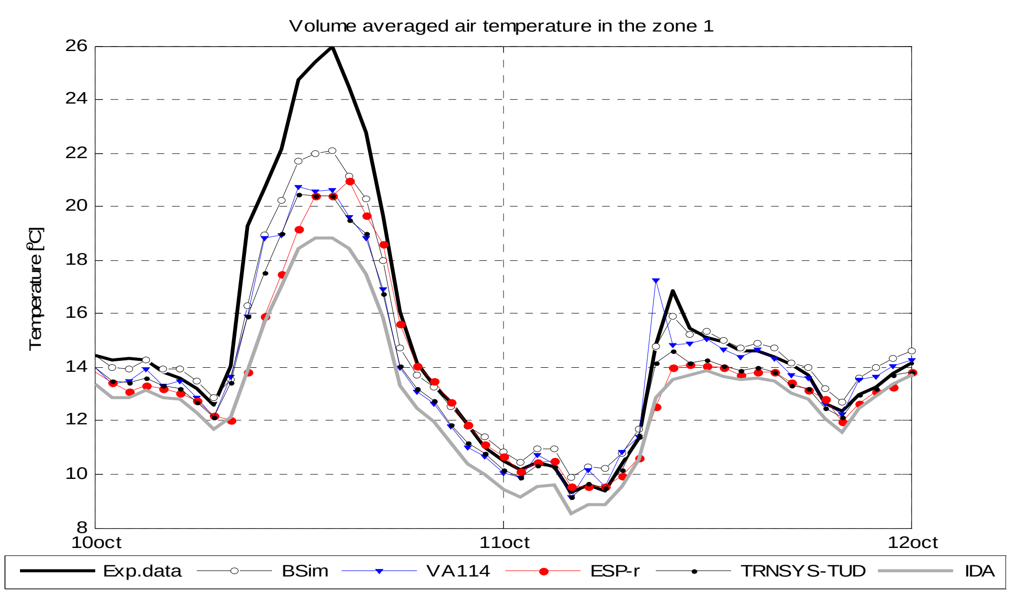

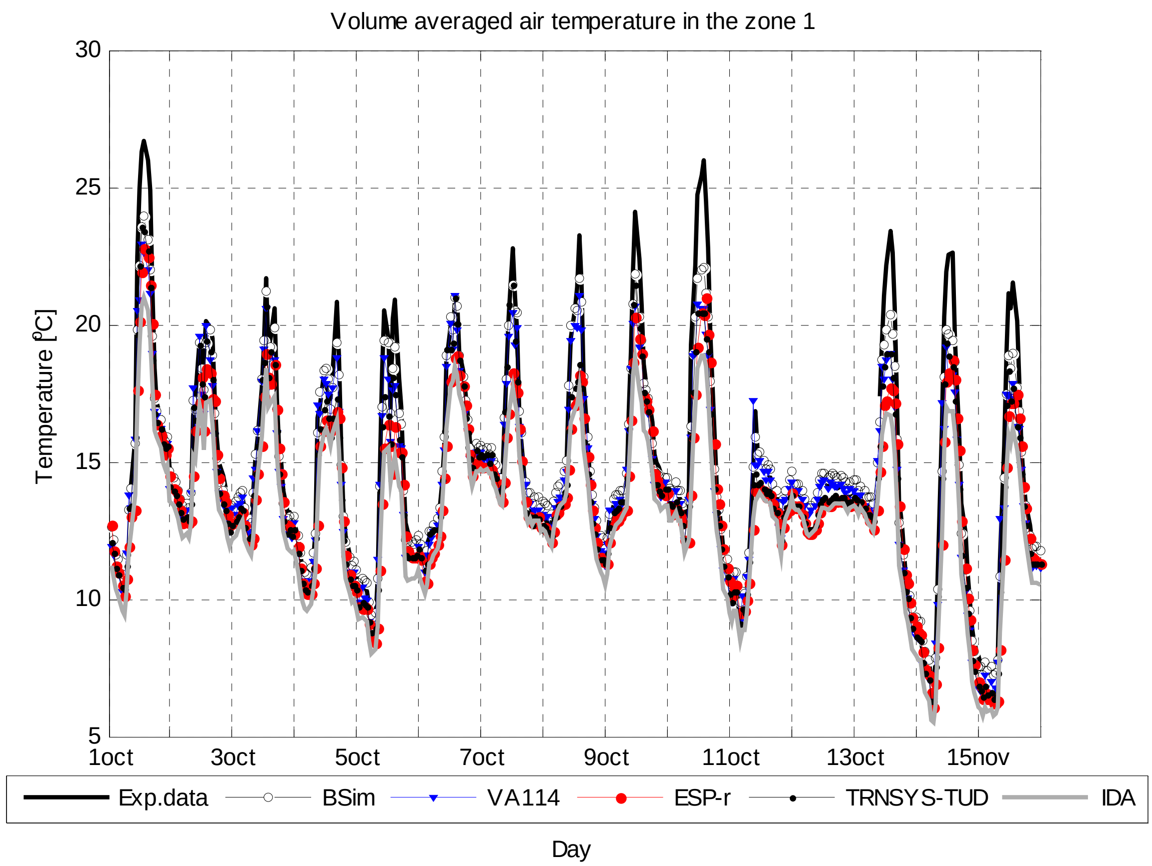

In view of fact that the air flow rate in a double skin facade cavity is rather high compared to the temperature difference between the air in the cavity and outdoor, it is essential to perform the empirical validation of the air temperature predictions in the models via *'the temperature raise in the zone1'*. The reason for that is amount of energy transported by the air flow. It is necessary to mention that an error in prediction of air temperature in the range of 1 degree Celsius can mean hundreds of watts of error in energy balance.

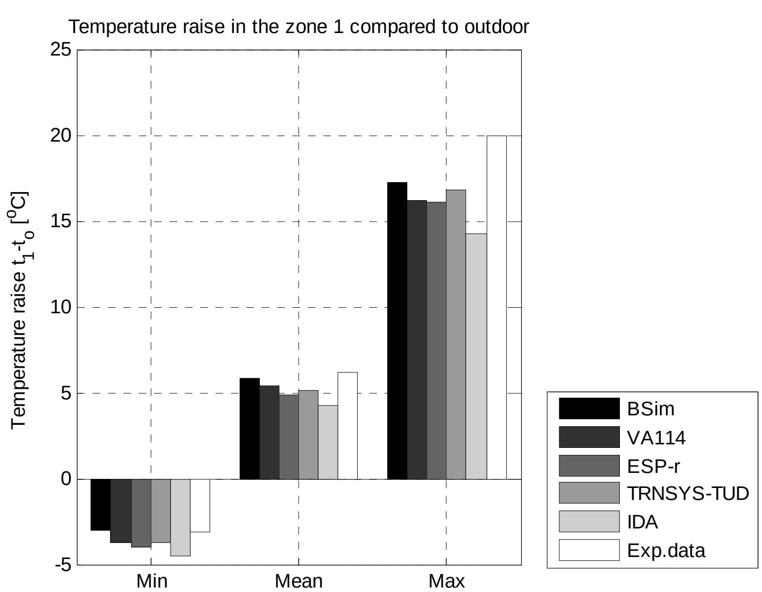

Temperature raise in the zone 1 compared to outdoor	BSim	VA114	ESP-r	TRNSYS-TUD	IDA	Exp.
MIN, °C	-3.0	-3.7	-4.0	-3.7	-4.5	-3.1
MAX, °C	17.3	16.2	16.1	16.8	14.3	20.0
MEAN, °C	5.9	5.4	4.9	5.1	4.2	6.2
DT95, °C	-2.4	-3.6	-4.5	-3.4	-5.4	
DT5, °C	0.5	0.3	-0.1	0.0	-0.5	
MEANDT, °C	-0.3	-0.8	-1.3	-1.0	-1.9	
ABMEANDT, °C	0.6	0.9	1.3	1.0	1.9	
RSQMEANDT, °C	0.9	1.4	1.9	1.4	2.4	
STDERR, °C	0.9	1.1	1.4	1.1	1.5	

The statistical data in the table above demonstrates that all of the models underestimate the air temperature in the cavity, all of the MEANDT values are negative and DT5 are close to zero. The absolute mean error is approximately 1°C, that corresponds to energy transport with the mass flow of apx 0.3kW, when the mass flow is 1000kg/h. Certainly the accuracy of the measurements become even more important, since we deal with rather small temperature range. From the 2-days plot it is seen that in a day with the low solar intensity the agreement between the experimental results and prediction is much better, however the experimental data is often higher.

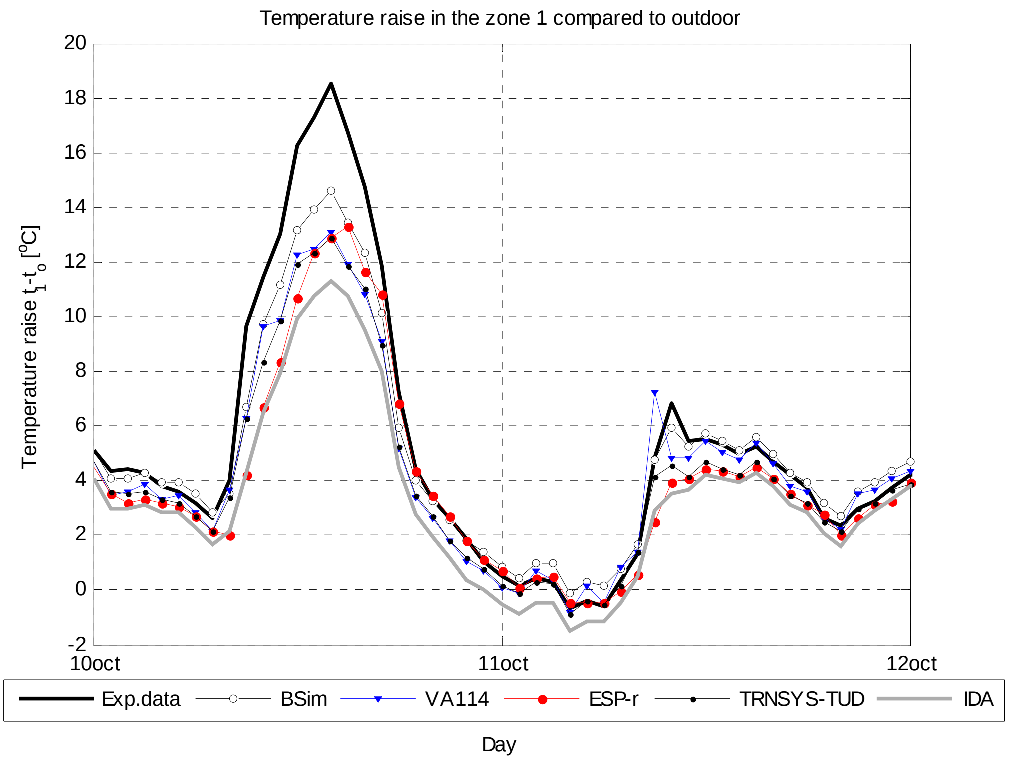

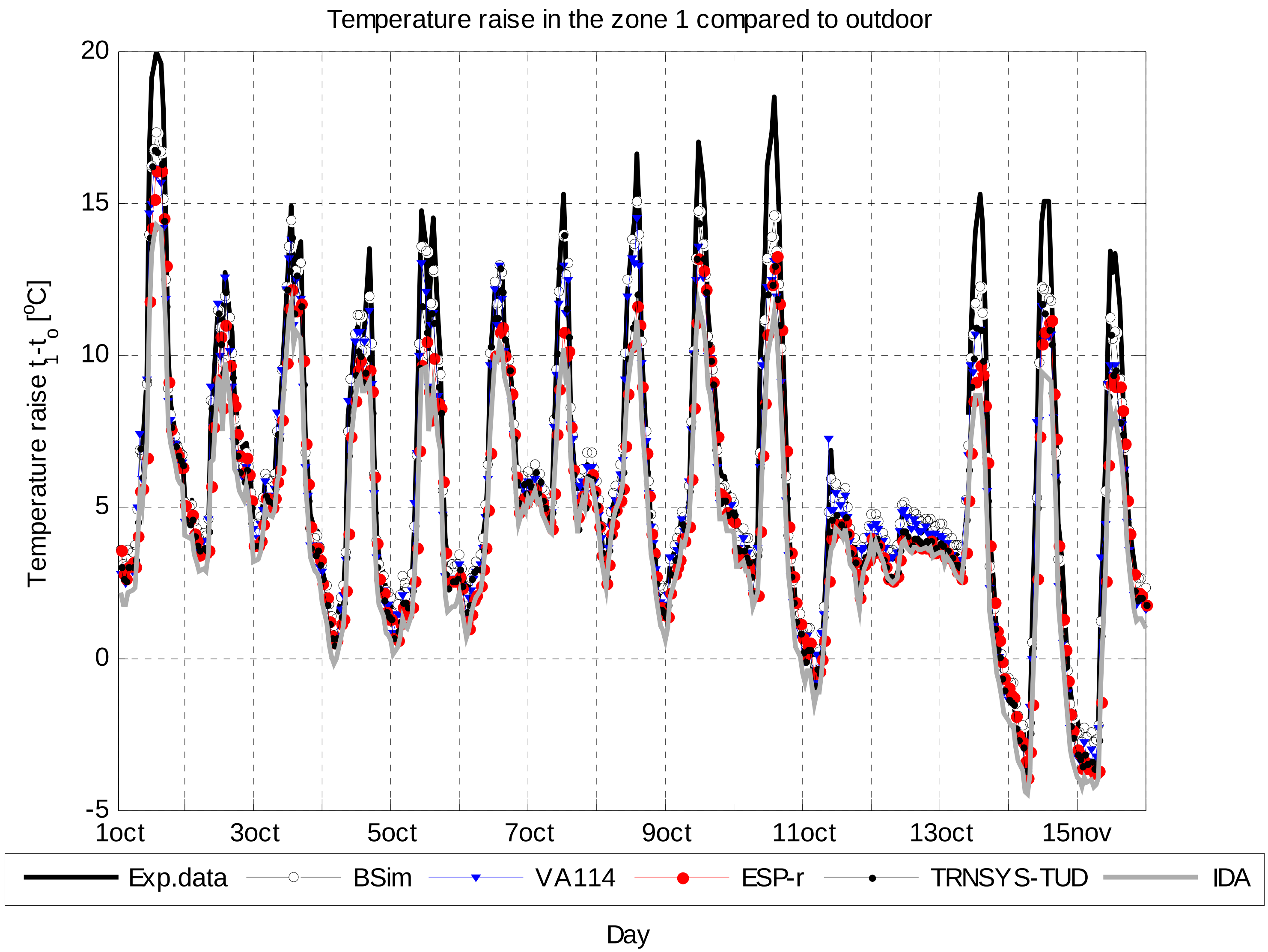

Temperature raise in the zone 1 compared to outdoor
Temperature raise t_1-t_o [^oC]
20
15
10
5
0
-5
1oct
3oct
5oct
7oct
9oct
11oct
13oct
15nov
Exp.data
BSim
VA114
ESP-r
TRNSYS-TUD
IDA
Day

3.4.7 Air flow rate in the zone 1

Before assessment of the results with the experimental data it is reasonable to start with the comparison of the results between the models. Previously in the comparative exercises it was shown that the deviation of predicted airflow between the programs was significant, but due to the lack of the experimental data there were no conclusions derived. Again, the same situation has occurred, as can be seen from a 2-days plot.

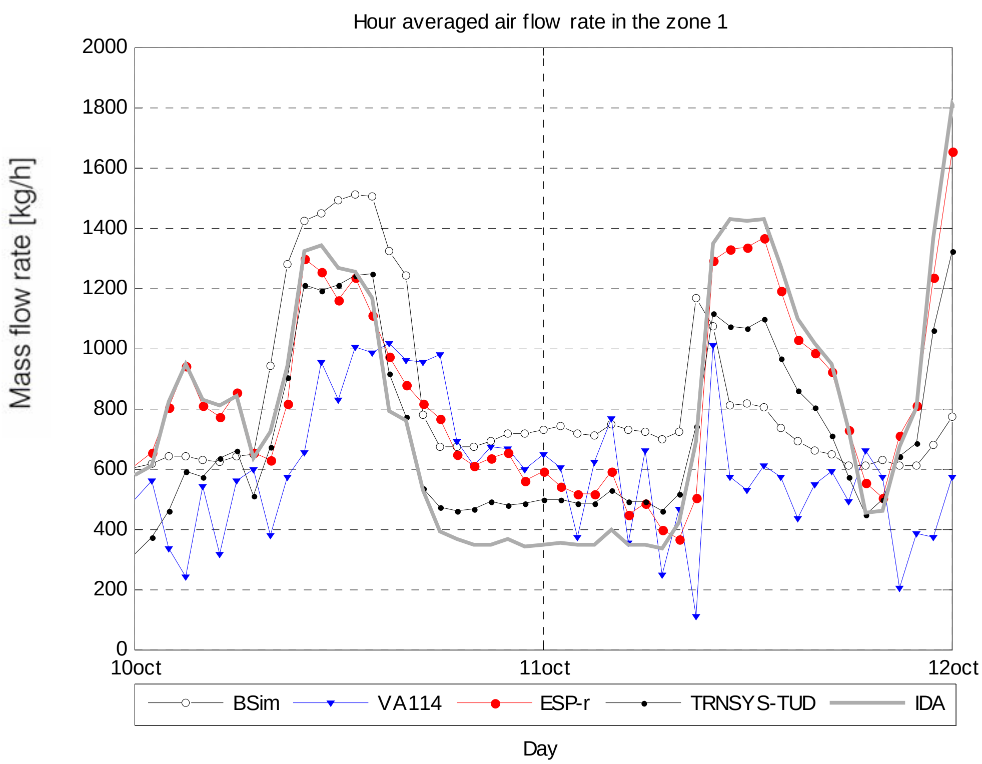

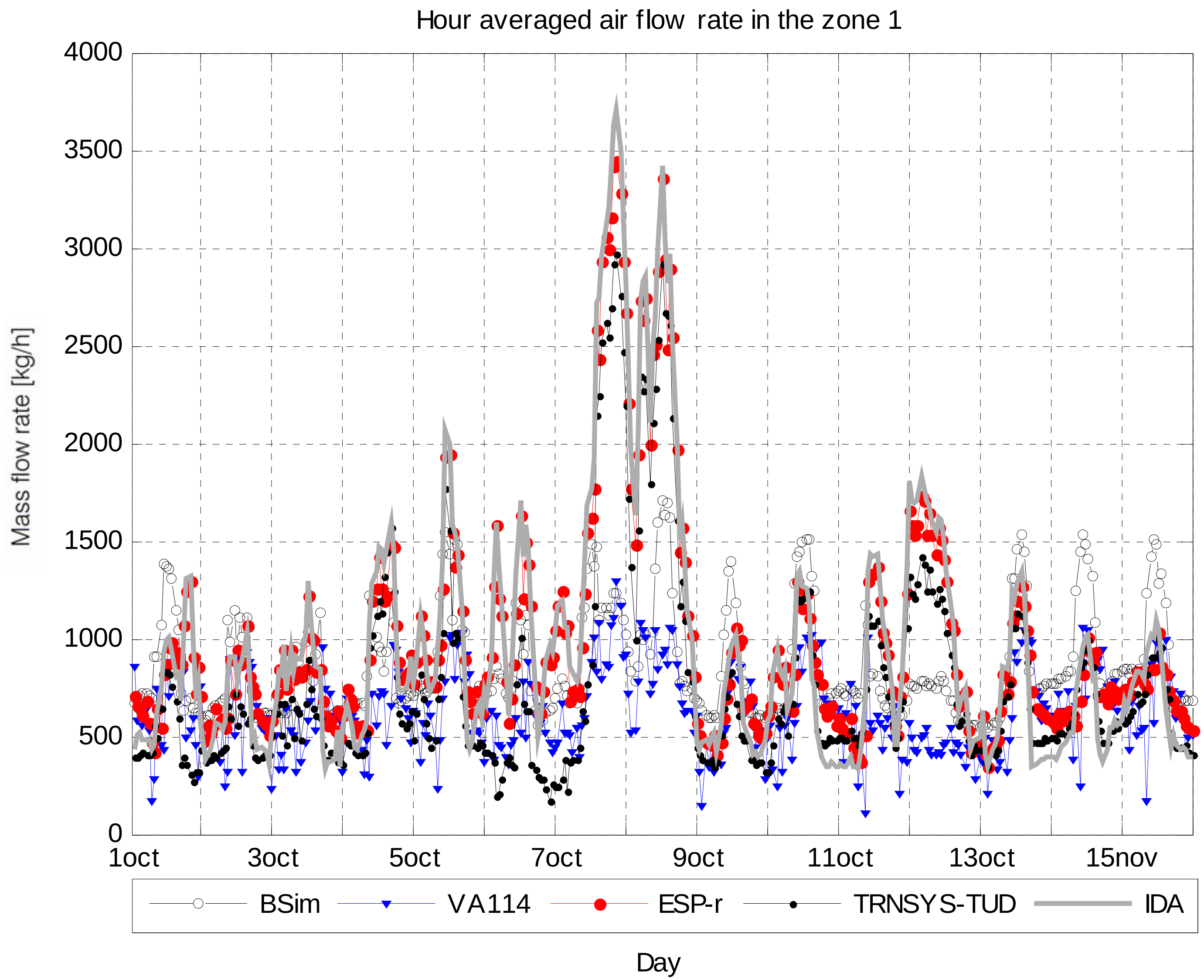
Hour averaged air flow rate in the zone 1
Mass flow rate [kg/h]
4000
3500
3000
2500
2000
1500
1000
500
0
1oct
3oct
5oct
7oct
9oct
11oct
13oct
15nov
BSim
VA114
ESP-r
TRNSYS-TUD
IDA
Day

Next, the discussion of the experimental data should take place. The mass flow rate measured with the three methods, explained in [3], however the results from only two of them are reported as reliable. These are the velocity profile method and the tracer gas method. As it is explained in the [3], the measurement of the air flow rate is very difficult and although the accuracy of the equipment is rather good, different measurement errors may appear.

In the tracer gas method, the errors could appear when the tracer gas is not well mixed with the entrance air or in the case of wind wash-out effects and the reverse flow appearance. In the latter cases the tracer gas is removed from the DSF cavity and, as a consequence, some measurement points are characterized with the air flow rate approximating the infinity.

The statistical analysis of this data is difficult and it can be unreliable for some statistical parameters, as it requires a flawless set of experimental data. However, the exact periods of wash-out effect and reverse flow occurrence aren't possible to recognize and therefore it is not possible to 'clean-up' the data properly. The authors have removed any points with the mass flow rate above 7000 kg/h, that corresponds to the mean velocity in the DSF cavity above 0.85m/s and air change rate in the cavity above 500 1/h. This is rather high limit to choose for the mass flow rate, therefore most of the parameters in the table of statistics are affected and can not be used for the assessment. An option of the lower limit wasn't considered since it would also require removing an important part of the reliable data too.

The occurrence of the reverse flow was experienced during the experiments, but it was not possible to visualize or record that phenomena. The detection of periods with the reverse flow from the experimental data can't be done accurately. However, it is worth mentioning that the greatest dilution of the tracer gas was noticed for the periods when the wind had exactly South direction (striking into the DSF openings). In that case, due to the shape of the wind profile, the wind became the dominating driving force causing flow reverse.

In the velocity profile method the errors are mainly caused by the approximation in the shape of the velocity profile and the convection boundary flow at the heated surfaces. Since, the velocity profiles were measured only in the central section of the DSF cavity then there is an assumption of equal flow conditions in all tree sections of the DSF cavity is applied, although there is no evidence that it was fulfilled during the experiments.

The application of the statistical analysis for the data obtained with the velocity profile is difficult, as the measured air flow can include periodical errors, such as overestimation of the flow rate due to the measurement of increased air speed at the surfaces in the convective boundary flow. Periodical character of the errors (errors are distinctive for the periods with the strong solar irradiation) forbids an application of the mean values as meaningless.

Tables with the statistical data are included into this report, but they will be disregarded in the further discussion for both sets of empirical data. Therefore, the main discussion will be made looking upon the plots of simulated and measured mass flow rates.

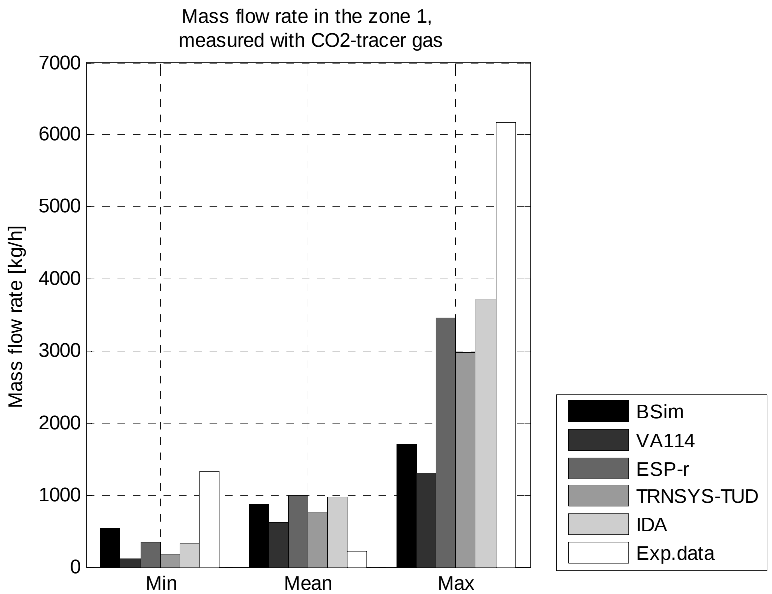

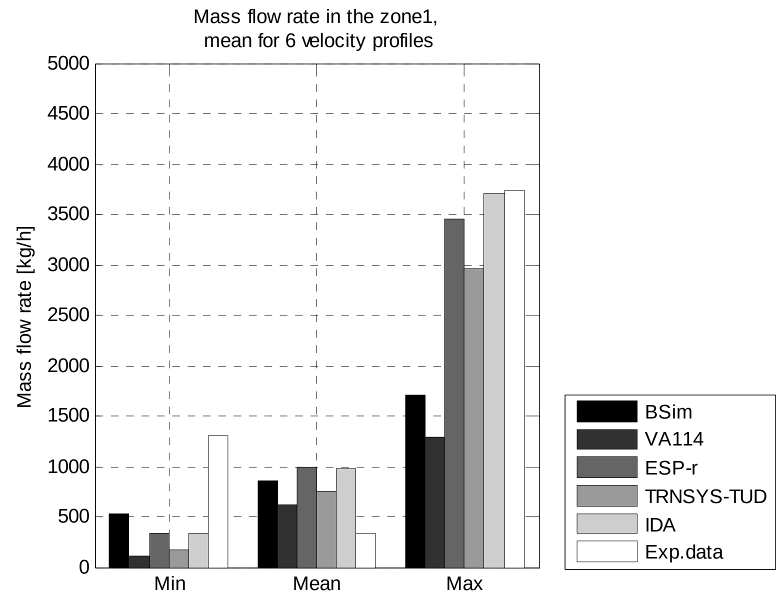

Mass flow rate in the zone 1, CO_2 tracer gas method	BSim	VA114	ESP-r	TRNSYS-TUD	IDA	Exp.
MIN, kg/h	537	108	342	171	333	229
MAX, kg/h	1707	1296	3450	2969	3711	6166
MEAN, kg/h	861	624	991	761	981	1324
DT95, kg/h	-3461	-3634	-2491	-2882	-2457	
DT5, kg/h	508	345	338	230	381	
MEANDT, kg/h	-442	-681	-299	-499	-312	
ABMEANDT, kg/h	752	813	526	598	512	
STDERR, kg/h	1187	1190	955	1033	942	

Mass flow rate in the zone 1, mean for 6 velocity profiles	BSim	VA114	ESP-r	TRNSYS-TUD	IDA	Exp.
MIN, kg/h	537	108	342	171	333	340
MAX, kg/h	1707	1296	3450	2969	3711	3744
MEAN, kg/h	861	624	991	761	981	1299
DT95, kg/h	-1792	-2080	-1379	-1709	-1565	
DT5, kg/h	302	147	326	126	377	
MEANDT, kg/h	-436	-668	-296	-531	-307	
ABMEANDT, kg/h	564	704	410	573	434	
STDERR, kg/h	674	681	540	635	563	

Hour averaged air flow rate in the zone 1
Measured with CO_2 tracer gas

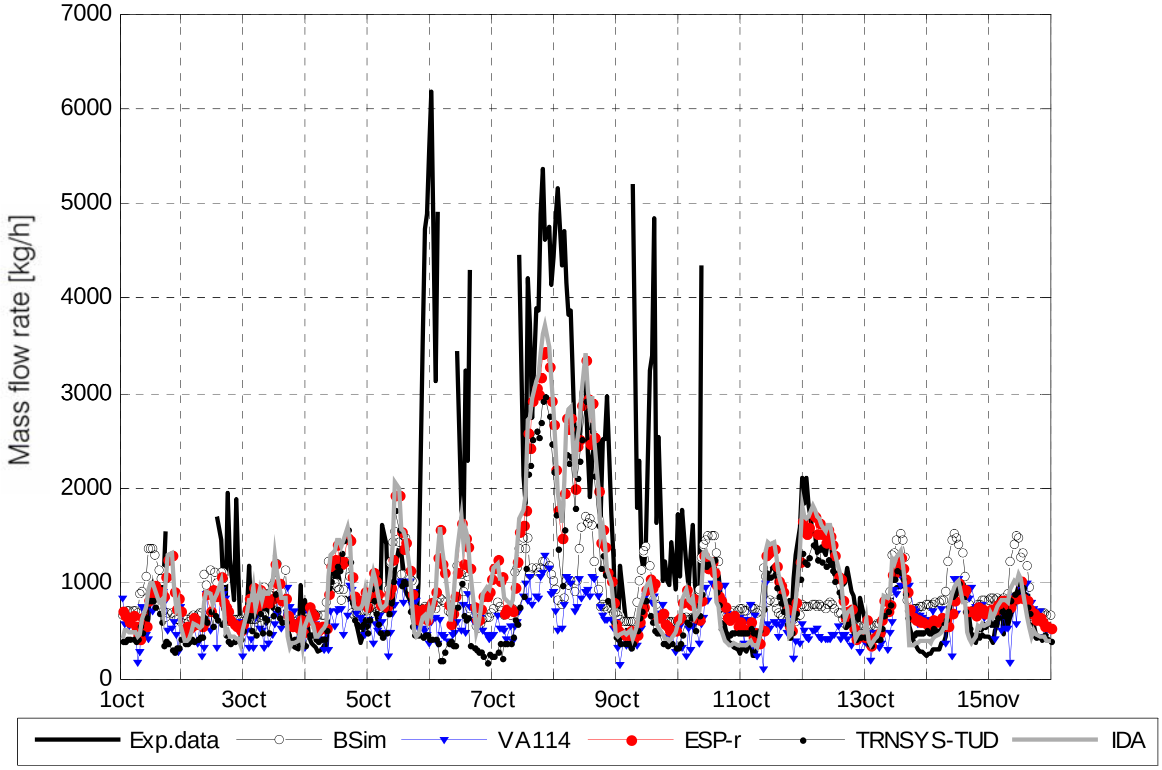

Hour averaged air flow rate in the zone 1
Mean for 6 velocity profiles

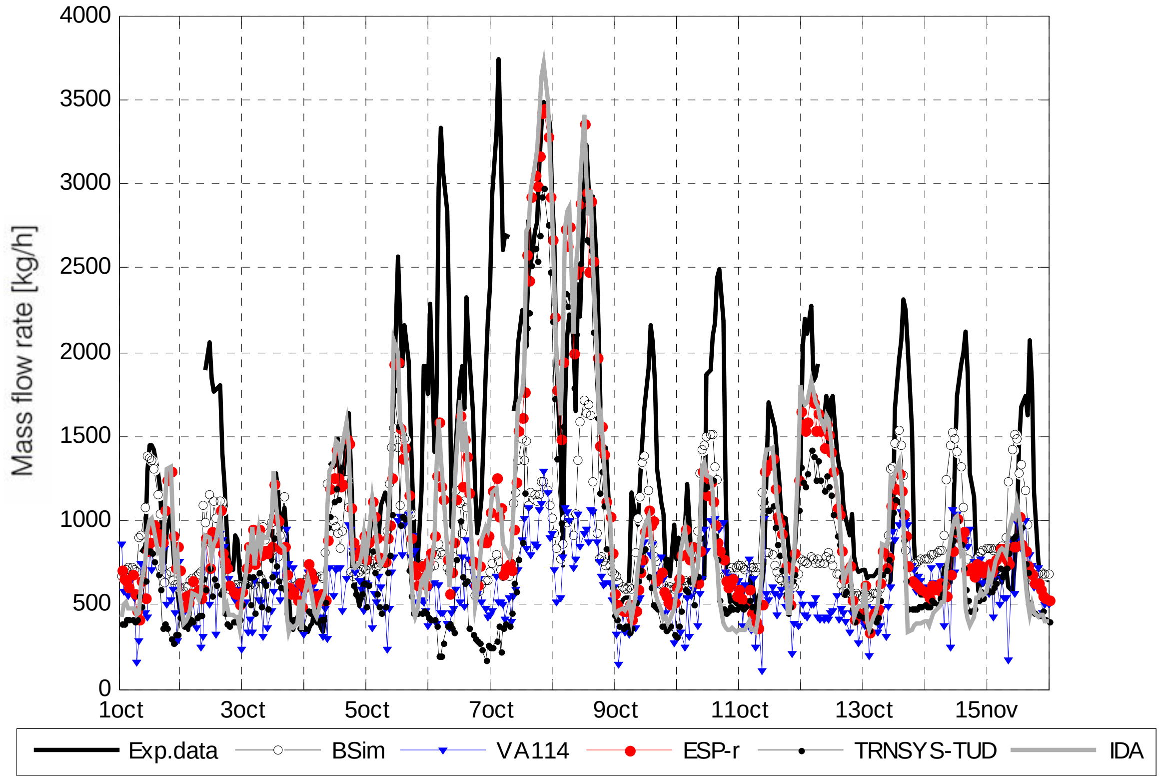

For the better visualization of the results, the above plots are divided into three periods, with the scale that is suitable for each period.

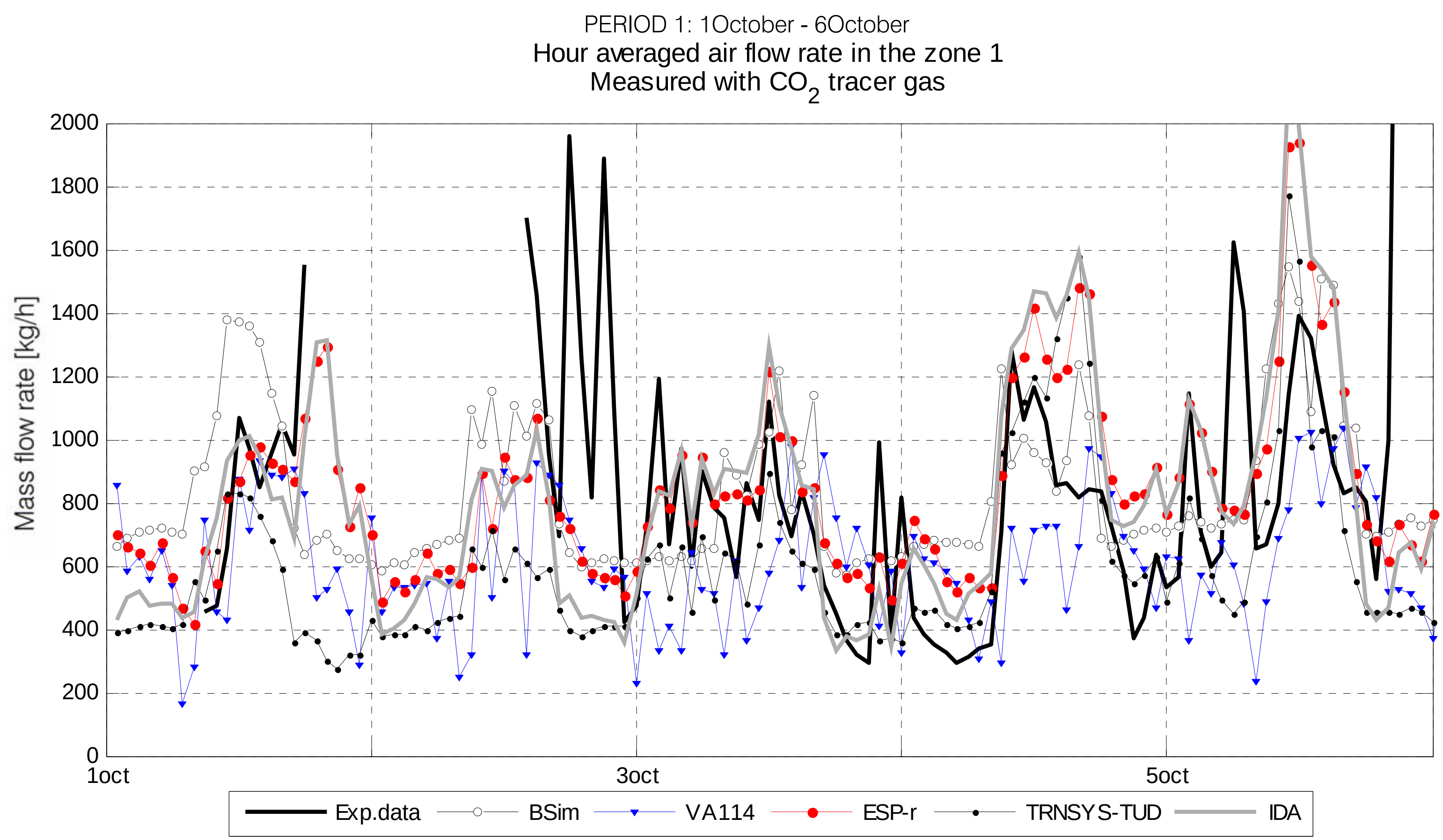

PERIOD 1: 1October - 6October
Hour averaged air flow rate in the zone 1
Measured with CO2 tracer gas
Mass flow rate [kg/h]
2000
1800
1600
1400
1200
1000
800
600
400
200
0
1oct
3oct
5oct
Exp.data
BSim
VA114
ESP-r
TRNSYS-TUD
IDA

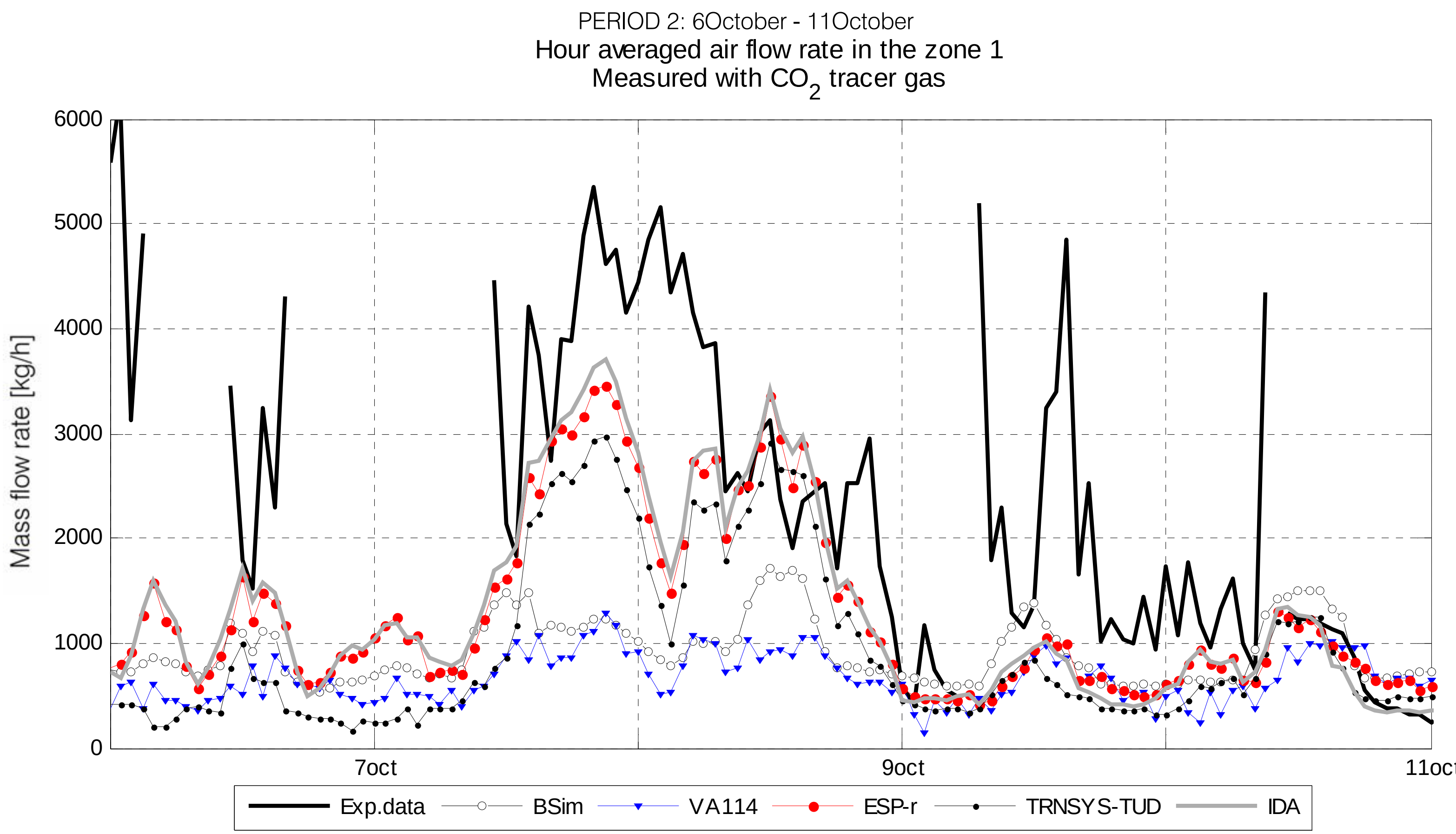

PERIOD 2: 6October - 11October
Hour averaged air flow rate in the zone 1
Measured with CO_2 tracer gas
Mass flow rate [kg/h]
6000
5000
4000
3000
2000
1000
0
7oct
9oct
11oct
Exp.data
BSim
VA114
ESP-r
TRNSYS-TUD
IDA

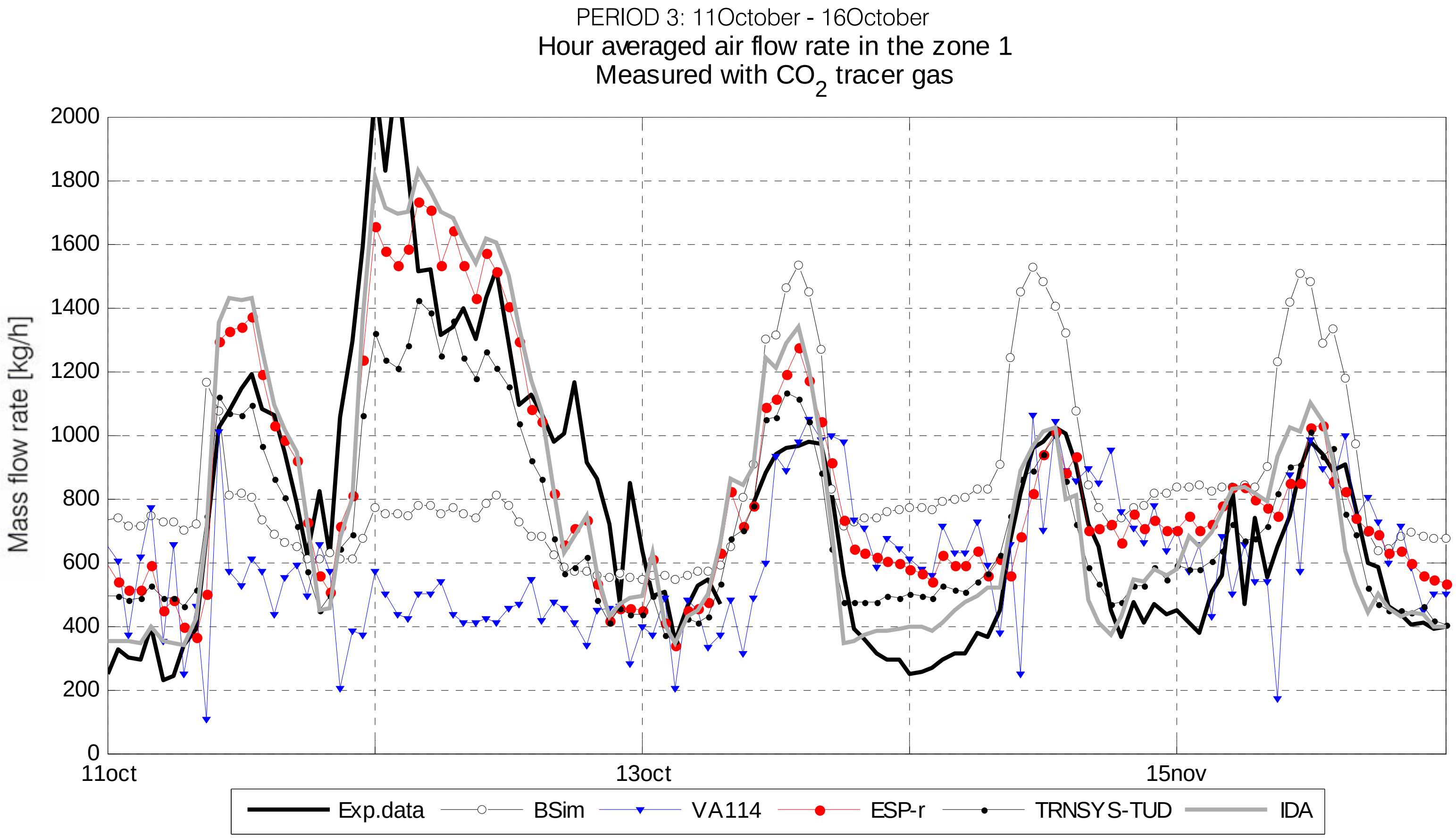

PERIOD 3: 11October - 16October
Hour averaged air flow rate in the zone 1
Measured with CO2 tracer gas
Mass flow rate [kg/h]
2000
1800
1600
1400
1200
1000
800
600
400
200
0
11oct
13oct
15nov
Exp.data
BSim
VA114
ESP-r
TRNSYS-TUD
IDA

Comparing the characteristics of expected errors in both experimental methods, it is necessary to note that the appearance of the reverse flow is periodical (South wind direction) and the periods are relatively easy to notice in the plots of the experimental results. The wind wash-out effect is the same phenomena as the reverse flow, but its occurrence is more random and originated from the highly fluctuating wind nature. However, this is a short-term phenomenon and therefore it doesn't have as much influence to the accuracy as the reverse flow does. Looking upon the bad mixing, it should be mentioned that it is not possible to evaluate the impact of this error, although a lot of effort was made during the experimental work to avoid this kind of error. With regard to the errors that could have appeared during the velocity profile measurement, the most significant of them is the impact of the boundary flow, as both in the days with the strong solar radiation or in the night time the boundary layer flow can result in overestimation of the air flow rate in the cavity and it is not possible asses the degree of error. Considering all of the arguments, it is relevant to use the experimental data obtained with the tracer gas method, as most of the errors are possible to detect, while in the case of the velocity profile method it is not.

First, the results of simulations are discussed upon the experimental data obtained with the tracer gas method. The result plots are subdivided into the three periods:

- 1October-6October
- 6October-11October
- 11October-16October

Results corresponding to the first two periods are very difficult to evaluate: both the results of simulations and experimental results seem to be very fluctuating and random, while in the third one it is easy to distinguish between the periods with the higher/lower solar irradiation, etc. It is likely that the haphazard air flow rate in the DSF cavity during the first to periods is caused by often variation in the wind directions between the South-East and South-West. Moreover during the second period was experienced high wind speed above 6m/s. More stable wind direction, relatively low wind velocity (below 6m/s), cooler outdoor temperature and less changeable solar irradiation have resulted in a more clear experimental data and simulation results. Therefore the third period is further used for the assessment of the results.

The night time ventilation of the DSF is mainly driven by wind, therefore the correspondence of the experimental results with the simulations in the night time periods, tells about proper estimation of the pressure difference coefficients in the empirical specification.

Predictions of the air flow rate for IDA, TRNSYS-TUD and ESP-r are often of the same shape and have close values. This is because of the similar flow model used in the simulations, still TRNSYS-TUD air flow is often lower than in ESP-r and IDA model, this is probably caused by the application of the fixed discharge coefficient in TRNYS-TUD, while the discharge coefficient defined in the specification was used in ESP-r and IDA.

The night/day –periods are almost unseen in VA114-results, this is due to the model which includes the impact of wind fluctuations on air flow rate in the cavity. At the same time this model doesn't include the direct influence of the wind forces, as $\Delta C_p=0$.

BSim often overestimates the air flow rate, both during the day and night time, but during the period of strong wind speed the air flow is underestimated, caused by the simplified empirical air flow model.

Similar to the tracer gas method, results of the velocity profile method are subdivided in the same periods, see figures below.

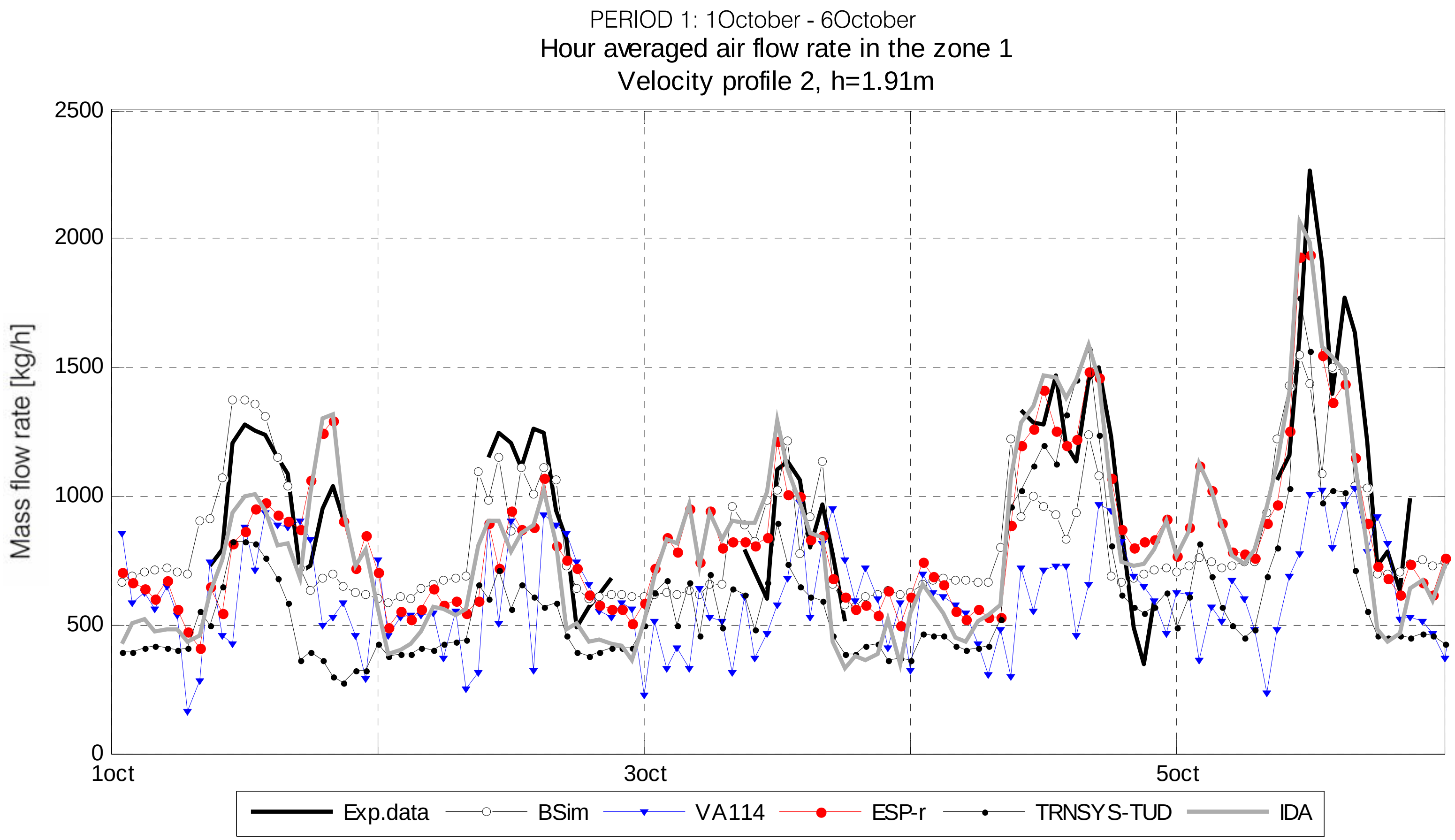
PERIOD 1: 1October - 6October
Hour averaged air flow rate in the zone 1
Velocity profile 2, h=1.91m
Mass flow rate [kg/h]
2500
2000
1500
1000
500
0
1oct
3oct
5oct
Exp.data
BSim
VA114
ESP-r
TRNSYS-TUD
IDA

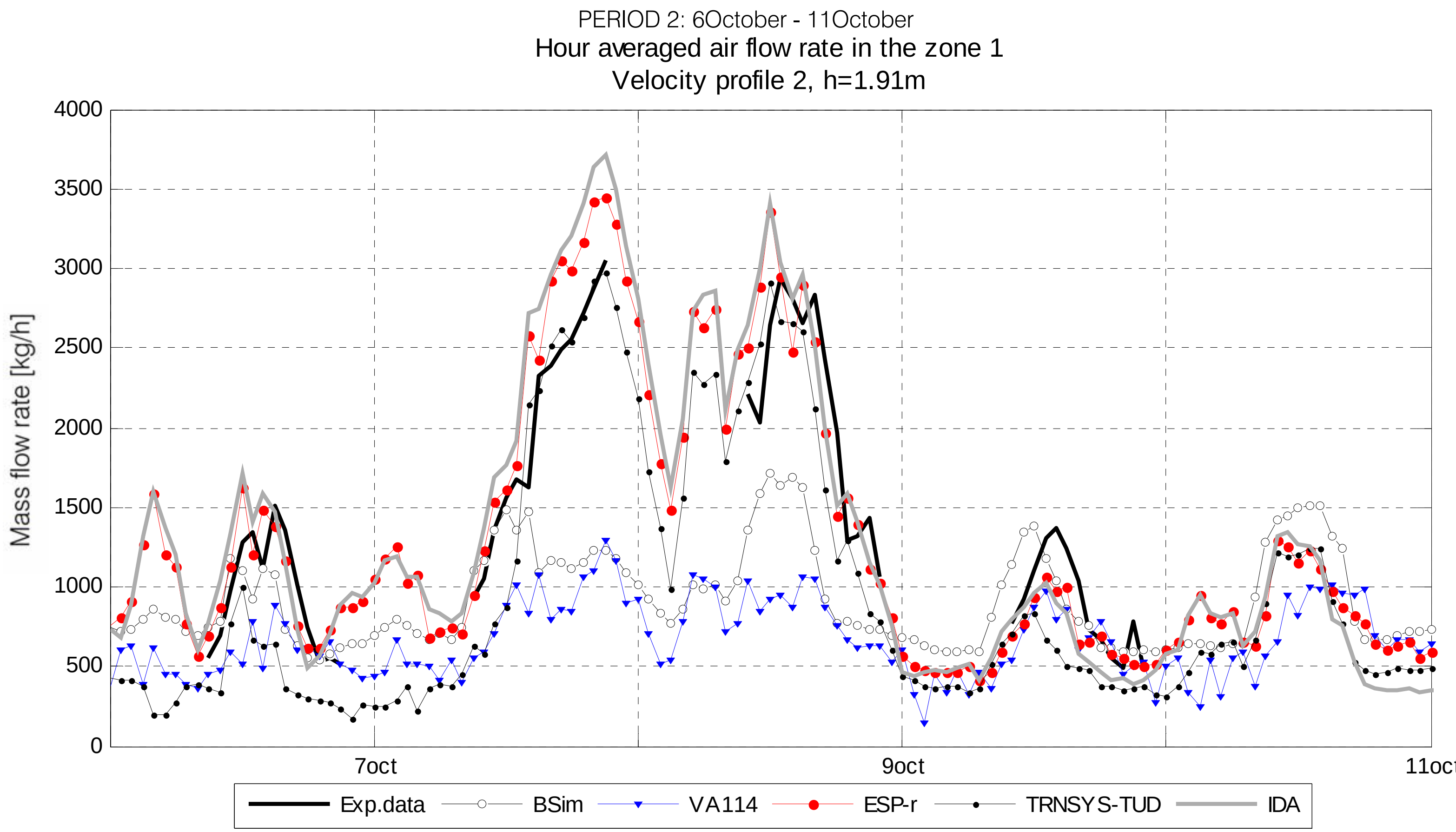
PERIOD 2: 6October - 11October
Hour averaged air flow rate in the zone 1
Velocity profile 2, h=1.91m
Mass flow rate [kg/h]
4000
3500
3000
2500
2000
1500
1000
500
0
7oct
9oct
11oct
Exp.data
BSim
VA114
ESP-r
TRNSYS-TUD
IDA

PERIOD 3: 11October - 16October

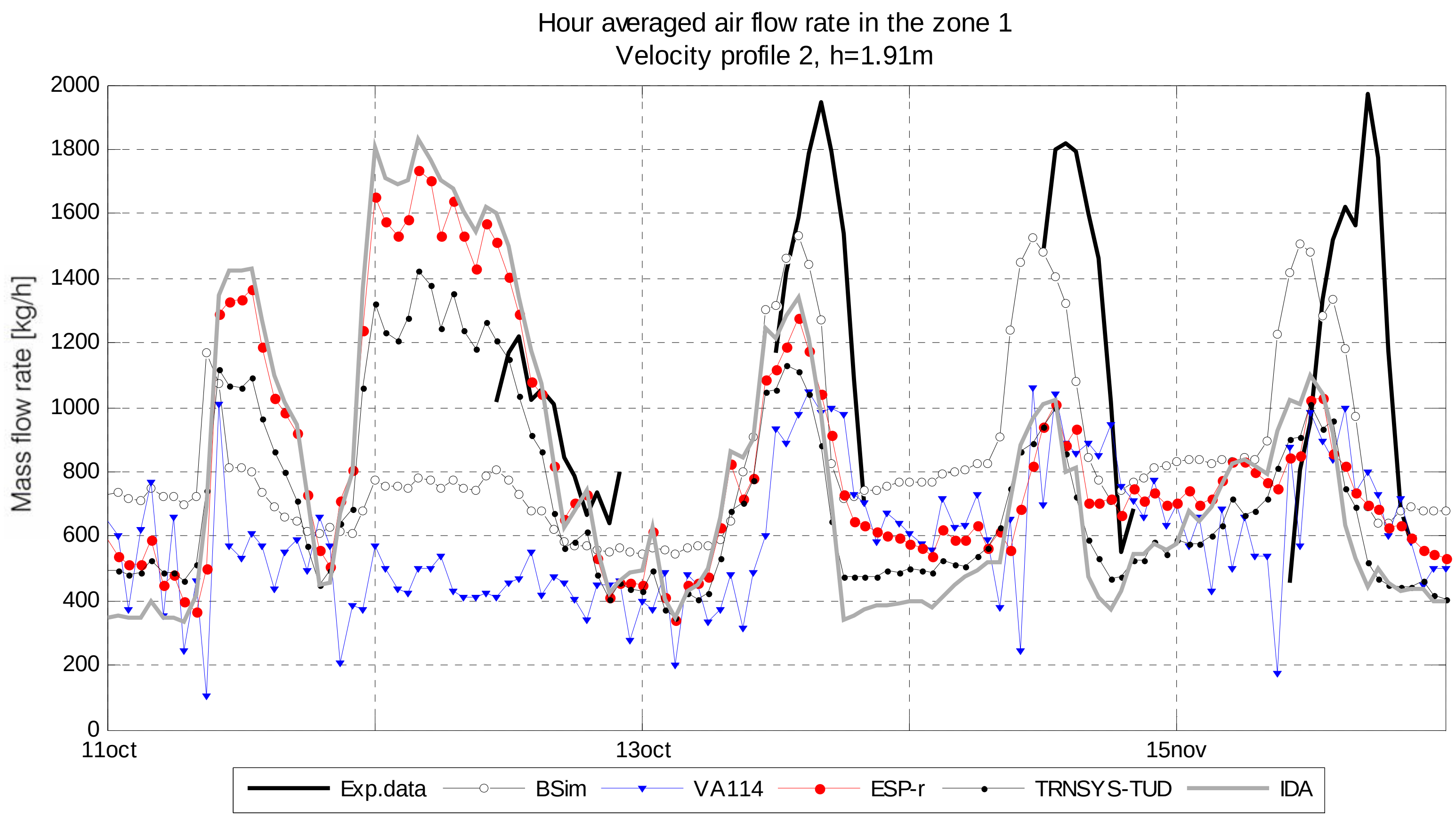

The differences between the results obtained with the tracer gas method and the velocity profile method (mean value for all six velocity profiles) are evident: the air flow rates during the days with relatively high solar radiation are notably higher at the noon compared with the tracer- gas results. Also during the night time the air flow rate in the cavity is higher for the velocity profile method, while the tracer gas method includes different periods with the enormous flow rates, which are remarkably higher.

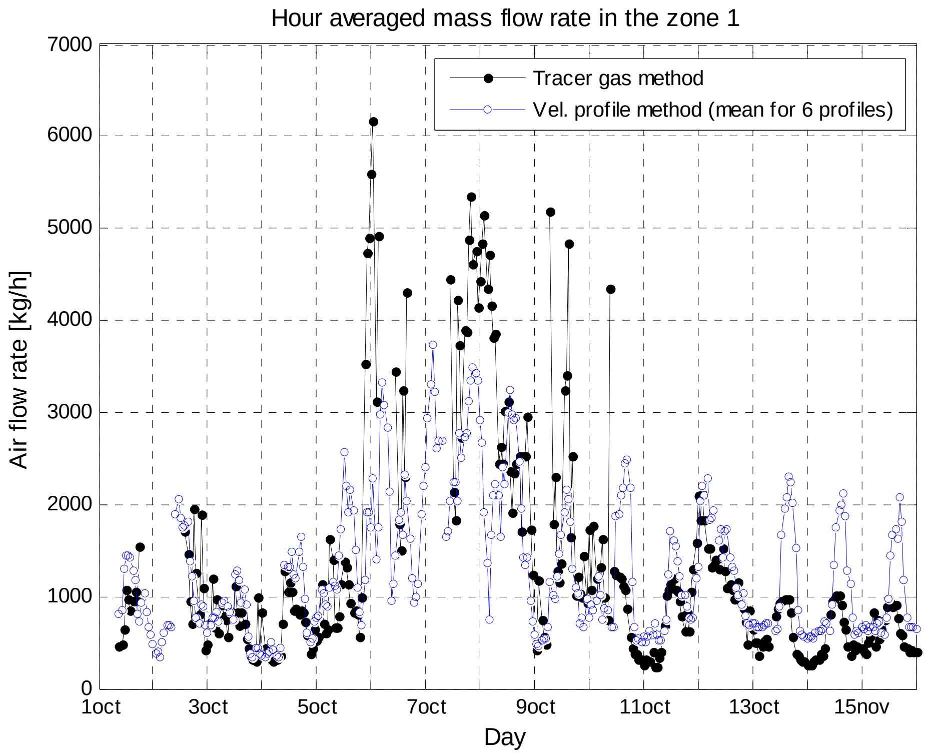

The overestimation of the air flow rate can occur when using the velocity profile method, due to the boundary layer flow. Moreover the boundary layer thickness increases with the distance from the origin and with increase of surface temperature. Since the velocity profiles in the DSF cavity were measured at six different heights, then the error due to the convection at the boundary layer should increase with the height of the velocity profile measurement.

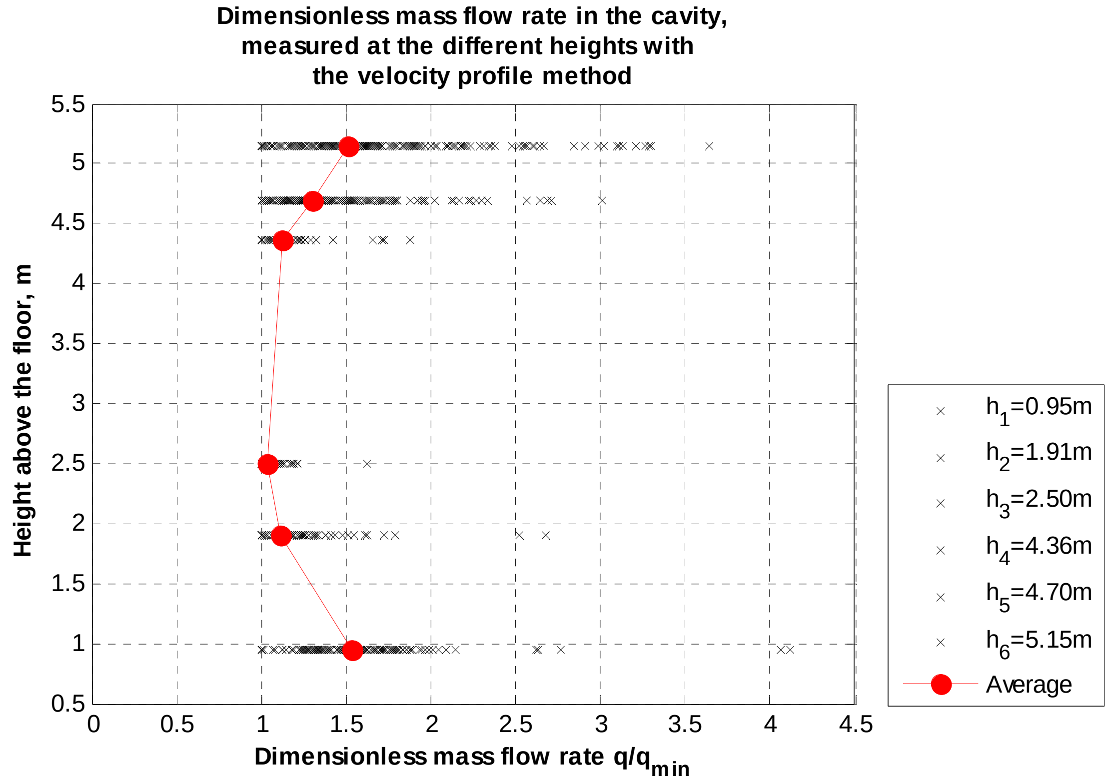

In the figure above the air flow rate in the cavity is dimensionless, where the value of 1 corresponds to the minimum air flow rate measured with one out of six velocity profiles. The figure demonstrates that actually the mass flow rate at the bottom of the cavity is not minimal; this is probably due to the bending of the jet when entering the cavity and wind wash-out effects. The dimensionless mass flow rate at the height of 2.5m and 4.36m is close to 1, this is probably due to the close location of the measurement points to the window frame, which destroys the boundary layer flow. Again, after passing the window frame, the development of the boundary layer should begin and this can be seen in the above figure for the height 4.70m ad 5.15m. As a consequence, in order to minimize the influence of the boundary flow the mass flow rate in the DSF cavity should be calculated on the basis of the velocity profile at the height 1.91m, as there is a lack of measurements for the height 2.50m.

Comparison of the experimental results obtained with the tracer gas and velocity profile method can be seen in the figure below, for the velocity profile measured at the height 1.91m.

From the figure below it can be seen that from the 11th of October, the velocity profile method predicts higher air flow rates in the cavity during the daytime. For the night time periods the mass flow rate for the velocity profile method at the height 1.91m is unavailable, as well as for many other periods. Thus the evaluation of the simulation results upon the experimental data is difficult,

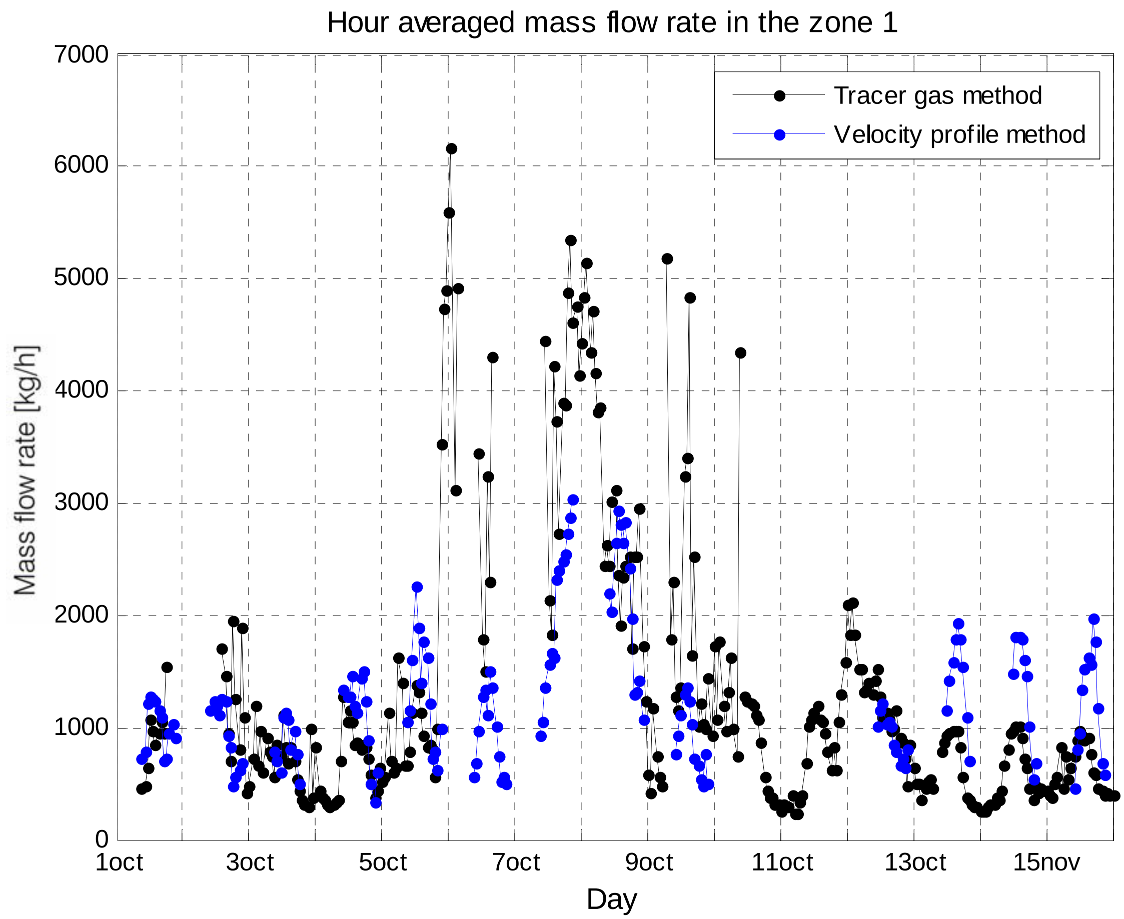

*FIGURE: Hour averaged mass flow rate in the zone 1. The mass flow rate measured with the velocity profile method is plotted for the velocity profile measured at 1.91m height (Profile II).

3.4.8 Energy load to the zone 2

Cooling load in zone 2

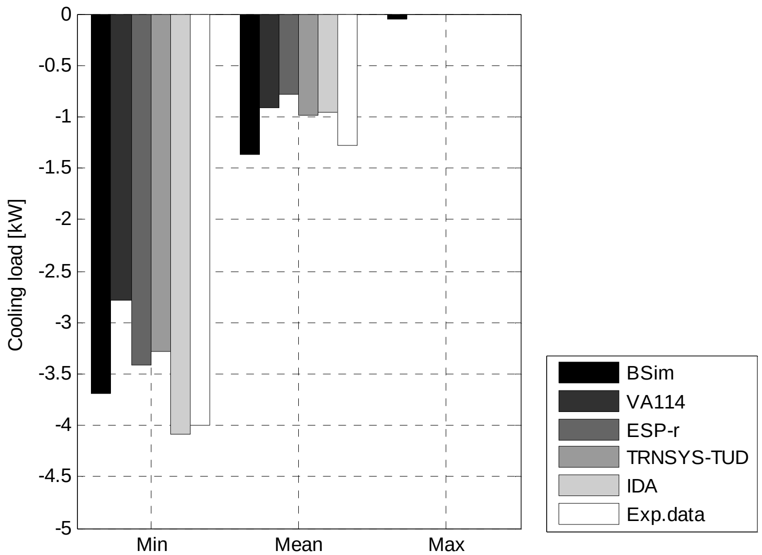

Heating load in zone 2

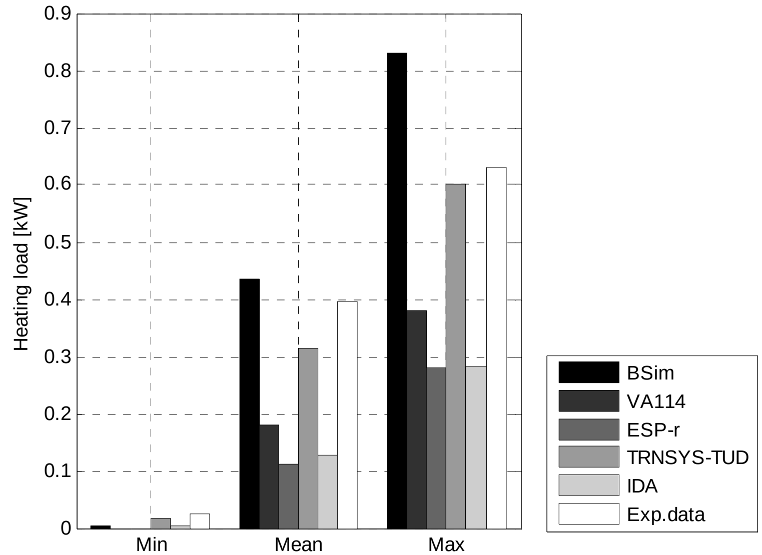

Cooling load in zone 2	BSim	VA114	ESP-r	TRNSYS-TUD	IDA	Exp.
MIN, kW	0.00	0.00	0.00	0.02	0.00	0.02
MAX, kW	0.83	0.38	0.28	0.60	0.28	0.63
MEAN, kW	0.44	0.18	0.11	0.32	0.13	0.40
DT95, kW	-0.05	-0.33	-0.45	-0.34	-0.44	
DT5, kW	0.20	-0.16	-0.21	0.08	-0.17	
MEANDT, kW	0.04	-0.25	-0.34	-0.11	-0.33	
ABMEANDT, kW	0.06	0.25	0.34	0.13	0.33	
RSQMEANDT, kW	0.08	0.26	0.35	0.16	0.33	
STDERR, kW	0.07	0.05	0.07	0.12	0.08	

Heating load in zone 2	BSim	VA114	ESP-r	TRNSYS-TUD	IDA	Exp.
MIN, kW	-3.70	-2.79	-3.41	-3.28	-4.09	-4.00
MAX, kW	-0.05	0.00	0.00	-0.01	0.00	-0.01
MEAN, kW	-1.37	-0.91	-0.79	-0.99	-0.95	-1.28
DT95, kW	-0.38	-0.39	-0.69	-0.58	-0.73	
DT5, kW	0.27	0.82	0.72	0.64	0.12	
MEANDT, kW	-0.07	0.05	-0.02	0.00	-0.32	
ABMEANDT, kW	0.15	0.31	0.33	0.27	0.35	
RSQMEANDT, kW	0.19	0.40	0.41	0.35	0.42	
STDERR, kW	0.18	0.40	0.41	0.35	0.27	

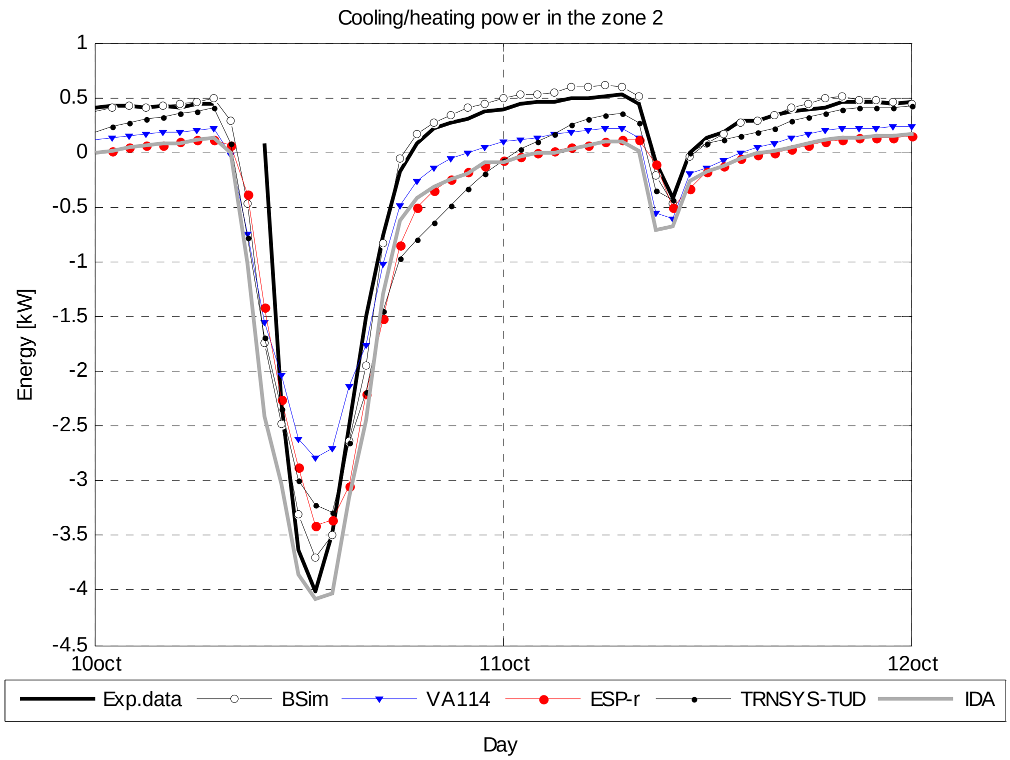

Cooling/heating pow er in the zone 2
Energy [kW]
1
0.5
0
-0.5
-1
-1.5
-2
-2.5
-3
-3.5
-4
-4.5
10oct
11oct
12oct
Exp.data
BSim
VA114
ESP-r
TRNSYS-TUD
IDA
Day

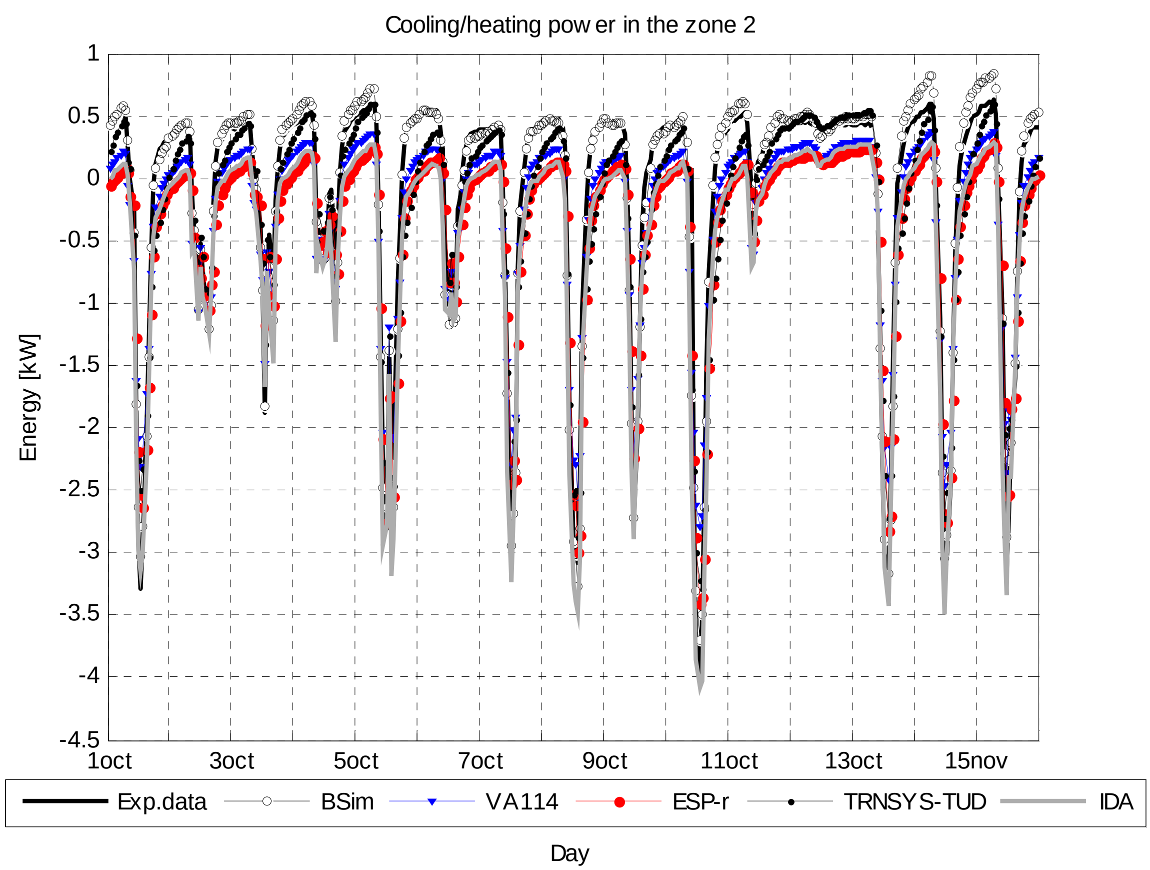

Cooling/heating pow er in the zone 2
Energy [kW]
1
0.5
0
-0.5
-1
-1.5
-2
-2.5
-3
-3.5
-4
-4.5
1oct
3oct
5oct
7oct
9oct
11oct
13oct
15nov
Exp.data
BSim
VA114
ESP-r
TRNSYS-TUD
IDA
Day

The underestimation of the heating load to zone 2 became characteristic for most of the models. Also the same two groups of results formed similar to the test case DSF100_2: [BSim, TRNSYS-TUD, Exp. data] and [VA114, ESP-r and IDA]. Models represented in the first group together with the experimental data use the simplified methods to calculate the heat loss through the thermal bridges, while the thermal bridges were not included in the models from the other group of the results.

The cooling load to the zone 2 is often underestimated in the models, although the best performing are IDA and BSim. The smallest values are obtained by VA114, while ESP-r and TRNSYS-TUD have close results.

Talking about the risk of errors during the measurements of energy consumption in the zone 2, it is relatively easy to state that this set of measurements is free for errors, except for the errors caused by the short-term visits to the zone 2. On the other hand, the great care was taken to remove these periods from the final data set.

3.4.9 The other parameters in the empirical and simulation results

Besides the global parameters such as an air temperature, mass flow rate, energy load in a zone, modelers had to report the surface temperature of constrictions if possible. The surface temperatures of the constructions were measured during the experiments together with many other parameters. However the plots of the results and their assessment are not included into the main report, but into the appendix.

Less attention is paid to these data, since the measurement of the surface temperatures of the constructions is very complex and the results can include errors, which are not possible to detect or asses. Moreover, the modeling of the surface temperatures is very sensitive to assumptions made towards the convective and radiative heat transfer at the surfaces. And, finally, it is not crucial to use these parameters for the empirical validation of building simulation software, since the assumptions vary from one tool to another, but the building simulation tools stay focused on the predictions of energy consumption and occupants' comfort and therefore the quantitative measure for the validation were chosen between the global parameters. However, it is desirable to develop a tool that is able not only to predict the energy consumption, but also to be able to provide a reasonable level of accuracy of other parameters.

If the surface temperature results are to be used, then it is necessary to consider possible measurement errors and limitations in the experimental setup.

A measurement of the surface temperature requires a good junction between the surface and the temperature sensor and in case of a bad junction will occur a measurement error, which is not possible to quantify. The risk of error during the measurements was minimized by means of thermal paste of high heat transmitting property, which was used to attach the sensors to a surface.

Measurement of the surface temperature of the glazing requires shielding of the thermal sensor from the solar radiation, as the solar absorption property for thermal sensor is considerably higher then for the glass. The details on shielding the sensors and on measurements of a surface temperature are given in [3].

The limitations in the experimental setup and correspondingly caused errors are normally described by the numerous cables, measurement devices and equipment placed around. Moreover, this kind of errors can occur due to the experimental conditions, which are in many cases are different from the normal situation. For example the temperature in the test room was kept constant during the whole period of experiments. In order to fulfill that, four fabric ducts were placed on the floor of the zone 2. Since the air in the ducts was slightly cooler or warmer (depending on the temperature in the zone), the concrete floor in the zone was heated up or cooled down. Correspondingly the measurement of the surface temperature in the zone 2 was affected by the air temperature in the ducts and therefore it is not reliable to conduct any comparison between simulated and measured floor surface temperature in the zone 2 [3].

Moreover, the modelers had to take additional steps in order to model the actual situation in the zone 2 ,with the floor shadowed from the longwave and short wave radiation by the fabric ducts. As a consequence, in some models an additional layer of insulation on the floor was used in order to simulate the effect of the ducts (ESP-r), while in VA114 this was done via the definition between convective and radiative form of solar gains in to the zone (the convective part vas increased from 0 to 10%). Meanwhile in TRNSYS-TUD model, the thermal conductivity of Rockwool insulation was used 0.0468 W/mK instead of 0.039 W/mK as defined by the specification, to simulate the thermal bridge heat loss effect. As a conclusion it is necessary to state that the reported and measured floor temperature in the zone 2 are incomparable.

The situation is similar for the floor temperature measurements in the zone 1, as a big number of cables were placed on the floor of the DSF cavity and therefore the measurement of this surface temperature is erroneous. [3].

3.5 Discussion and summary for the empirical validation test cases

As explained in the literature review [1], the physics of the double skin façade involves complex processes and therefore require detailed calculations of optics, flow regime, convection, natural air flow etc. Often, building simulation software is not able to perform such detailed level of computations. When the detailed computations are not possible, then the simplified models are used as an alternative and it is not always possible to validate the advanced physical processes, however, this is not the objective. The building simulations must be validated on their performance *together with their limitations,* yet the best possible software performance must be achieved.

Prior to empirical validation, the completed set of comparative exercises have demonstrated the magnitude of differences between different building simulation tools and have confirmed the complexity of the task to simulate building with a double skin façade. Certainly, the procedure of validation a building simulation tool involves not only the program, but the modeler, his personal opinion, experience and time spent on modeling. The most important achievement in the comparative exercise was than the experience gained by the modelers in the DSF modeling, the justification of their models against each other and finally the demonstration of how important it is to conduct the empirical validation for modeling of buildings with the DSF, and thus to provide the reference against which modeling predictions could be compared.

The empirical exercises were completed in the 'blind'-form, which means that the modelers received the experimental results only after submitting their results of simulations.

Similar to the comparative validation only the results for the global parameters were included into the main report, such as energy consumption, air temperature and air flow rate, but not in the surface temperatures. The reason for that is that the resulting surface temperatures, for example, depend on computations and assumptions in a model, such as distribution of solar radiation and shadow to the surfaces, level of detail in longwave radiation exchange, flow regime at the surface and assumptions made for calculation of the convective heat exchange at the surface etc. These computations and assumptions vary from one tool to another, but the building simulation tools stay focused on the predictions of energy consumption and occupants' comfort and therefore the quantitative measure for this empirical validation were chosen between the global parameters.

In the empirical validation procedure it is necessary to keep in mind that the validation procedure is actually two-sided, as not only the accuracy of the model is to be validated, but also the accuracy of the measurements and the material in the specification as well. Thus, in case of disagreement between the model and the experimental data, it is necessary to examine possible reasons of deviations, both if the software doesn't perform the proper calculations and also if the experimental data is inaccurate.

Before comparing the global parameters, it was necessary to perform the verification of the boundary conditions, which was done in two steps:

- Evaluation of the boundary external conditions. If an agreement is achieved in computations of solar radiation striking to the surface, then it can be demonstrated that the models perform computations for the same external boundary conditions

- Validation of the boundary internal conditions. If an agreement is achieved in computations of solar radiation transmitted into the zone (first order of solar transmission), then it can be agreed that the models perform computations for the same initial boundary conditions and the final validation can take place

The above two steps were used in the comparative validation exercises, and provide similar results in the empirical ones, as the programs use the same techniques and methods. A good agreement was achieved between the simulation tools to model the solar radiation incident on the vertical surface of the double skin façade. With regard to the empirical data, lower solar irradiation was measured compared to the results of simulations. As explained earlier, it could be caused by differences in the ground reflection properties in the models and at the experimental setup, since the ground carpet covers only 0.5 of the DSF view factor to the ground, etc.

The second step is more indefinite, as various software apply different window models, used in different software. Although this step has already been completed during the comparative validation, it was necessary to repeat it for the empirical exercises, as the detailed spectral properties of the glazing in the test facility were now given in the empirical specification [3] and, as a result, models were adjusted to the specified properties. The dimensionless analysis of the incident and transmitted solar radiation has demonstrated that there is no similarity between the software tools when processing the solar radiation through the glazing. On the other hand, previously, it was argued that the modeling of transmission of solar radiation is not the main focus of the validation exercise, as these depend on the assumptions and limitations in the model and software. Since, there is no experimental data available about the solar radiation transmitted into the zone 1 and zone 2, then the accurate modeling of these parameters is not actually the focus of the validation exercise, but a tool for its completion. Although, the calculated boundary conditions in the models demonstrate some deviations, these were evaluated as acceptable for further comparison.

When the results of simulations are compared against the experimental data, then the information about the measurement procedure and experimental set-up can be critical for evaluation of the measurement accuracy and possibility for the error. On the whole, the main details of measurement procedure were mentioned in the report when compare plots of the simulation and experimental results. Even more details about the experimental setup and experiments can be found in [3].

The air temperature in the DSF is evaluated via the temperature raise in the cavity compared to the outdoor air temperature, this is essential, especially for the test case DSF200_e, which is characterized with the low temperature raise due to the high air change rate in the cavity. Regarding the air temperature in the zone 1, the test case DSF100_e and the test case DSF200_e are principally different, as in the first case the calculated air temperature depends mainly on assumptions made towards the convective heat transfer and in the other case it comprises a complete set of heat transfer processes characteristic for the double skin façade, which includes the mass flow rate. Correspondingly all of the models perform differently in each of the test cases. In the test case DSF100_e, TRNSYS-TUD and ESP-r represent the group of the results which are most alike with the experimental results, while all other models underestimate the air temperature in the cavity. On the contrary, in the test case DSF200_e, all models highly underestimate the air temperature in the cavity in the days with the strong solar irradiation. In the periods of weak solar radiation and at night, results of simulations and experimental data are in better agreement.

Regarding the mass flow rate in the DSF cavity it was difficult to attain a final conclusion, due to the extreme complexity of the long time monitoring and measurement of the naturally induced air flow rate in the cavity. Although it is difficult to measure the air flow in a naturally ventilated double skin façade cavity, as there is no easy method either no accurate one exists, results obtained with the velocity profile method and the tracer gas method show reasonable agreement. However, due to the risk of error in each of the methods, the preference of one method in front of the other one can be given only upon personal opinion. The authors have pointed out all of the possible risks of error during the experiments and, for now, the final conclusion is left upon the reader. At the same time it is important to point out that such conditions of experimental and simulation results argue for further experimental studies and empirical test case for validation of the building simulation software to conclude the subtask assignment.

The deviations between the measured and simulated energy load to the zone 2 are obvious. Most of the models underestimate the cooling loads to the zone especially in the days with intensive solar irradiation, while at night the heating load is often a problem, probably due to disregarded thermal bridges. The difficulties with the simulation during the day time periods are the consequence of the greater deviations in predicted air temperature and mass flow rates in the cavity.

As it was argued before, the energy consumption is one of the global parameters which represent the performance of the buildings simulation software when modeling a building with DSF. The great deviation in the energy consumption in the zone is a result of interplay of many parameters, such as air flow rate, convection and radiation heat transfer, transmission of solar radiation etc. At the same time it is not possible to validate all of the inter-related parameters in this subtask, as many of those are the challenge for the whole field of building simulations. However, the air flow rate is particularly interesting and influencing factor for the DSF performance, moreover the airflow in the DSF is unavoidable part of the whole DSF concept. Thus the air flow rate was chosen as one of the main targets in evaluation and validation of Building simulation software for buildings with DSF. Despite the fact that more empirical test cases are needed to complete the validation assignment, the discussion of the mass flow models upon the results of simulations and empirical results should be made.

3.5.1 Discussion of the airflow models and influencing matters in the air flow modeling.

It is well known that any model for calculations of natural air flow is very sensitive to number of empirical parameters such as the discharge coefficient, the wind pressure coefficients, the terrain parameters, coefficients in the power-law equations etc. The situation is extremely rare when the experimental data for estimation of these coefficients exists for a particular building which is to be modeled. In real life the modeling takes part prior to construction and therefore a user of the simulation tool takes the decision upon different recommendations, standards and experience.

In order to avoid or minimize the sensitivity of the air flow models to the input parameters, these were specified in the empirical test case specification (discharge coefficient, pressure difference coefficients, tightness characteristics of the building and the function of the wind reduction according to the type of terrain). The discharge coefficients, the function of wind reduction and building tightness were obtained empirically for the experimental setup.

The pressure difference coefficients were specified on the basis of literature study for a building of the same shape as the experimental test facility. The sensitivity of the flow models to the pressure difference coefficients is very significant and therefore the truthfulness of the defined pressure difference coefficients is essential. This is verified via wind driven night time ventilation in the test case DSF200_e, for the models using the same pressure difference coefficients as in specification (TRNSYS-TUD, ESP-r, IDA), which results demonstrate almost identical mass flow rate in the cavity as measured.

It is not always possible to use the specified data; therefore the discharge and the pressure coefficients for the openings used in all models were also compared. In fact, the differences in input values for the discharge and pressure difference coefficients are noteworthy. Furthermore, they could have played a vital role in calculations and can be a reason for disagreements in predicted air flow rate due to the sensitivity of the air flow models to these parameters. As for example in VA114 the difference between the pressure coefficients is set to zero, and as a result the wind pressure force is left out of consideration. In BSim an empirically obtained relationship is used to calculate wind induced air flow rate. ESP-r, TRNSYS-TUD and IDA use the same pressure difference coefficients, but not the discharge coefficients, thus no correspondence of the results are to be expected.

Earlier, it was mentioned that the application of the orifice model assumes the fully developed turbulent flow and in most of the cases this assumption is valid as even the laminar flow regime turns to turbulent due to the opening size, sharp edges of the opening etc. However, the orifice equation is not accurate enough when the laminar flow or flow in transition to turbulent occurs. In this case the power-law model has the priority as it can be adjusted to one or another regime as long as it is know what flow regime one deals with. Yet, there is no empirical data available to verify the application of one or another relationship (orifice or power-law).

Compare the application of different relationship: power-low and orifice…What is the model used by TRNSYS-TUD??

Another issue to discuss is the consideration of the wind turbulence effect on the air flow rates in the DSF cavity. Only one of the models in the empiricalexercises considers the wind fluctuations as a contributor to the total air flow rate in the cavity (VA114 uses the wind fluctuation model described in [9,10]). At the same time the design of the DSF in many cases represents a construction with the openings at the different levels of the same surface. This is also the case in the comparative exercises. Although, the openings located at different levels (single-sided ventilation), the wind pressure, does not have as much effect on the air flow, as in case of cross ventilation. From this point of view the wind fluctuation effect can have an increased importance and can influence the accuracy. Another expression for taking into account the wind fluctuations can be used, it is developed by Larsen [11] and it takes into consideration the location of the opening (windward/leeward side) and a combination of wind pressure and temperature differences.

Previously, it was explained that the air temperature in the DSF cavity is the result of the convective heat transfer between the glass surfaces and the cavity air. The surface temperature of the glass can become relatively high and as a part of convective heat transfer appears the boundary layer flow. The air flow rate in the boundary flow normally increases with the distance from the inlet opening and in some circumstances it is likely that the air flow in the boundary layer can exceed the main flow rate in the cavity. This can cause the appearance of the reverse flow and even more intricate the flow field in the cavity.

At the moment the network method and the loop method are the best suitable for the calculation of the dynamic air flow rate in a naturally ventilated space. The network method is also the one used for almost all models in the empirical exercise. However, one of the limitations of this method is that it is not suited to model the airflow patterns within the zone [12], such as reverse flow, local recirculation, etc.

Often this limitation is solved by dividing a zone into several sub zones, as explained in the modeler reports for TRNSYS-TUD and ESP-r models. The DSF is differently subdivided in ESP-r and TRNSYS-TUD models: there are three equal zones in ESP-r and 4 zones in TRNSYS-TUD, where two of the smaller zones located at the bottom and at the top and two bigger ones located in the middle of the cavity. Splitting up the cavity into a few zones stacked on the top of each other can highly improve the accuracy of simulation, but this solution is more suitable when it is necessary to count on the vertical temperature gradient only, as this doesn't solve the complexity of the local recirculation.

3.6 Summary

Looking upon the topics of the discussion in the previous section, one can argue that the subject of naturally driven flow is complex and it is not easy to model the naturally driven flow in the DSF cavity. Moreover, considering the results of simulated and measured global parameters, one can note that the main difficulties experienced in predictions (or measurements) are characteristic for the periods with the intensive solar radiation, however the night time periods, or the days with the low solar intensity are relatively easy to model, both from the heat transfer and mass transfer point of view. The most serious difficulties for those periods are experienced in underestimation of the heating load in zone 2, which are explained by disregarded thermal bridge calculations.

Good performance of the models in periods of lower solar intensity indicate that the building simulation tools perform very well, but in the periods of higher solar intensity more detailed calculations or models should be applied, as the presence of solar radiation is an essential element for the double skin façade operation (only the period with the moderate solar intensity was modeled in the empirical test cases) and the models in the present validation task do not provide results of superior accuracy compared to empirical results.

Certainly, the accuracy and quality of the experimental results must be also evaluated, as these are the main measures in empirical validation procedure. Most of the details about the accuracy and risk of error during the measurements are mentioned in the report, while more information is given in [3] It is apparent that the described measurement methods in [3] have sources of error and compared to laboratory conditions have relatively large uncertainties, but on the other hand these experimental results represent the full-scale outdoor measurements, with well controlled and measured internal conditions and with the measurement errors one can be aware of.

The result of the comparative exercises was that the comparative validation was regarded as the main argument to continue the validation of the building simulation software for the buildings with the double skin façade with the empirical validation test cases. The results of the empirical validation can be regarded as arguments for further empirical and comparative validation, which should include some sensitivity studies of the parameters involved into the simulation of the DSF performance (or expanded number of the test cases), including wind pressure coefficients, discharge coefficients, spectral properties of the glazing along with the analysis of influence of the DSF-geometry *in the model* in means of partitioning the DSF in 2 or more zones stacked on the top of each other, equal and different size of these zones, application of shading device, etc.

Another, extremely important subject in the DSF modeling is modeling of shading device in the cavity (zone 1). The predictions made for the double skin façade in the empirical test cases DSF100_e and DSF200_e do not include the shading device, despite that fact, the complexity of the processes in the DSF appeared to be strict enough to result in deficient accuracy of simulations. Shading device is a distinctive element of DSF application and, in addition, it is an important contributor to the double skin façade physics. Its contribution to the DSF physics is expressed by means of an additional heat source in the DSF cavity and therefore more complex longwave radiation exchange, increased air temperature in the cavity and thus the increased buoyancy effect, etc. In view of these facts, the modeling can become even more intricate. Therefore it is desirable to continue with the empirical validation of building simulation software, including the solar shading devices, their properties and positioning in the cavity.

Completing of the validation procedure with the above suggestions would allow to finalize whether it is possible to perform the DSF modeling within the software tools available on the market, by means of improved model geometry and definitions, minimized error due to the model sensitivity to the input parameters and whether the solar shading device intricate the modeling procedure. And, finally, the additional test cases would clarify whether a new computation model is required to perform an accurate modeling of the double skin façade buildings and what are the improvements should be made in the new model compared to the existing ones.

LITERATURE

1. Poirazis H. (2006). "Double Skin Facades for Office Buildings - Literature Review Report" (9.86MB). Division of Energy and Building Design, Department of Construction and Architecture, Lund Institute of Technology, Lund University, Report EBD-R—04

2. Kalyanova, O., & Heiselberg, P. (2007). Empirical Test Case Specification: Test Cases DSF200_3 and DSF200_4 : IEA ECBCS Annex43/SHC Task 34 : Validation of Building Energy Simulation Tools. Aalborg: Aalborg University : Department of Civil Engineering. ISSN 1901-726X DCE Technical Report No.033

3. Kalyanova O. (2007). Experimental set-up and full-scale measurements in 'the Cube'. Aalborg:Aalborg University: Department of Civil Engineering. ISSN 1901-726X DCE Technical Report No.034.

4. Kalyanova, O. & Heiselberg, P. (2007). Comparative validation of building simulation software: Modeling of Double Facades: FINAL REPORT. Aalborg: Aalborg University: Department of Civil Engineering. ISSN 1901-726X DCE Technical Report No.024.

5. Clarke J.A. (1985). Energy Simulation in building design. Adam Hilger Ltd. Bristol and Boston.

6. ASHRAE (1997) Handbook of fundamentals, Atlanta, 1997

7. Perez R., Ineichen, P., Seals, R., Michalsky J. & Stewart, R. (1990) Modelling Daylight Availability and Irradiance Components from Direct and Global Irradiance, Solar Energy, Vol. 44, pp. 271-289

8. Perez et al., (1987) R. Perez, R. Seals, P. Ineichen, R. Stewart and D. Menicucci, A new simplified version of the Perez diffuse irradiance model for tilted surfaces, Solar Energy 39 (1987) (3), pp. 221–232.

9. Phaff et al., (1980). The ventilation of buildings. Investigation of the consequences of opening one window on the internal climate of the room, TNO report C448.

10. Awbi, H.B. Ventilation of Buildings. Air infiltration and natural ventilation (chapter 3). F&FN Spon. ISBN 0-419-15690-9.

11. Larsen, T.S. (2006). Natural Ventilation Driven by Wind and Temperature Difference. Aalborg : Department of Civil Engineering : Aalborg University, 2006. 140p.

12. Walton G.N. (1989)Airflow Network Models for Element-Based Building Airflow Modeling. ASHRAE Transactions: 1989, Vol.95, Part 2, pp.611-620.

APPENDIX: Surface Temperatures

Test case DSF100_e

Surface temperature of the glazing

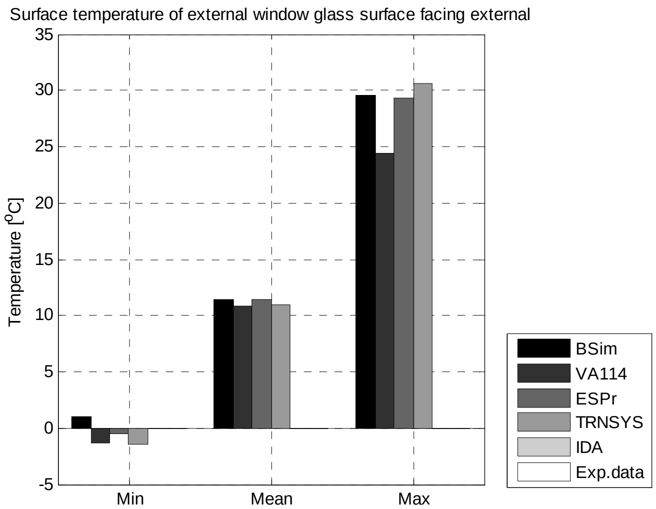

Temperature of external widow glass surface facing external	BSim	VA114	ESP-r	TRNSYS-TUD	IDA	Exp.
MIN, °C	1.1	-1.4	-0.5	-1.5	-	-
MAX, °C	29.6	24.4	29.4	30.6	-	-
MEAN, °C	11.5	10.9	11.4	11.0	-	-

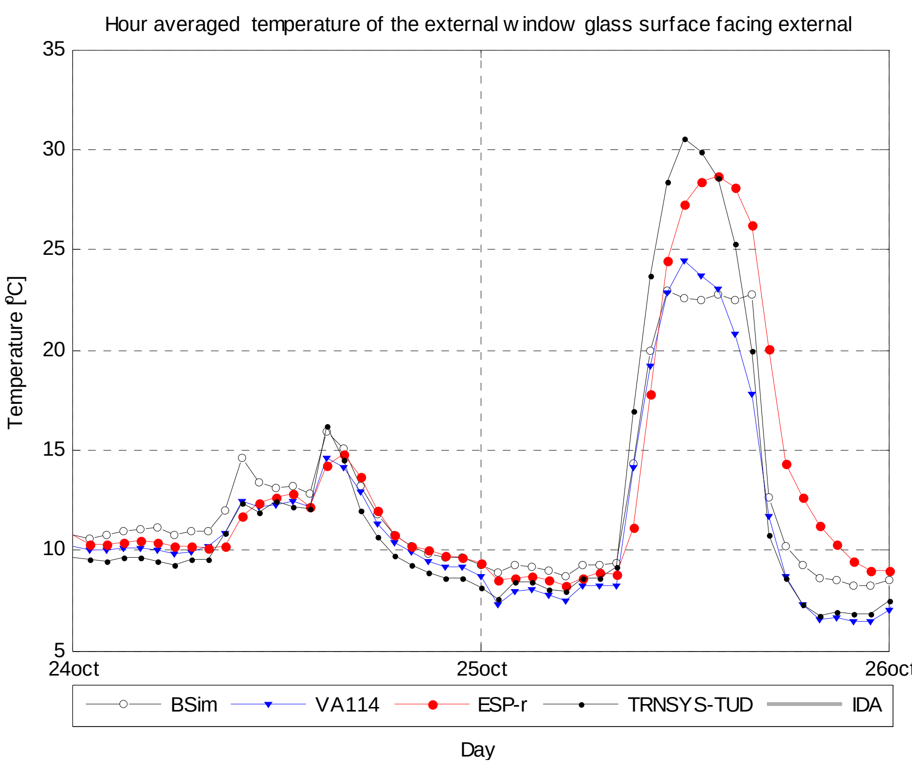

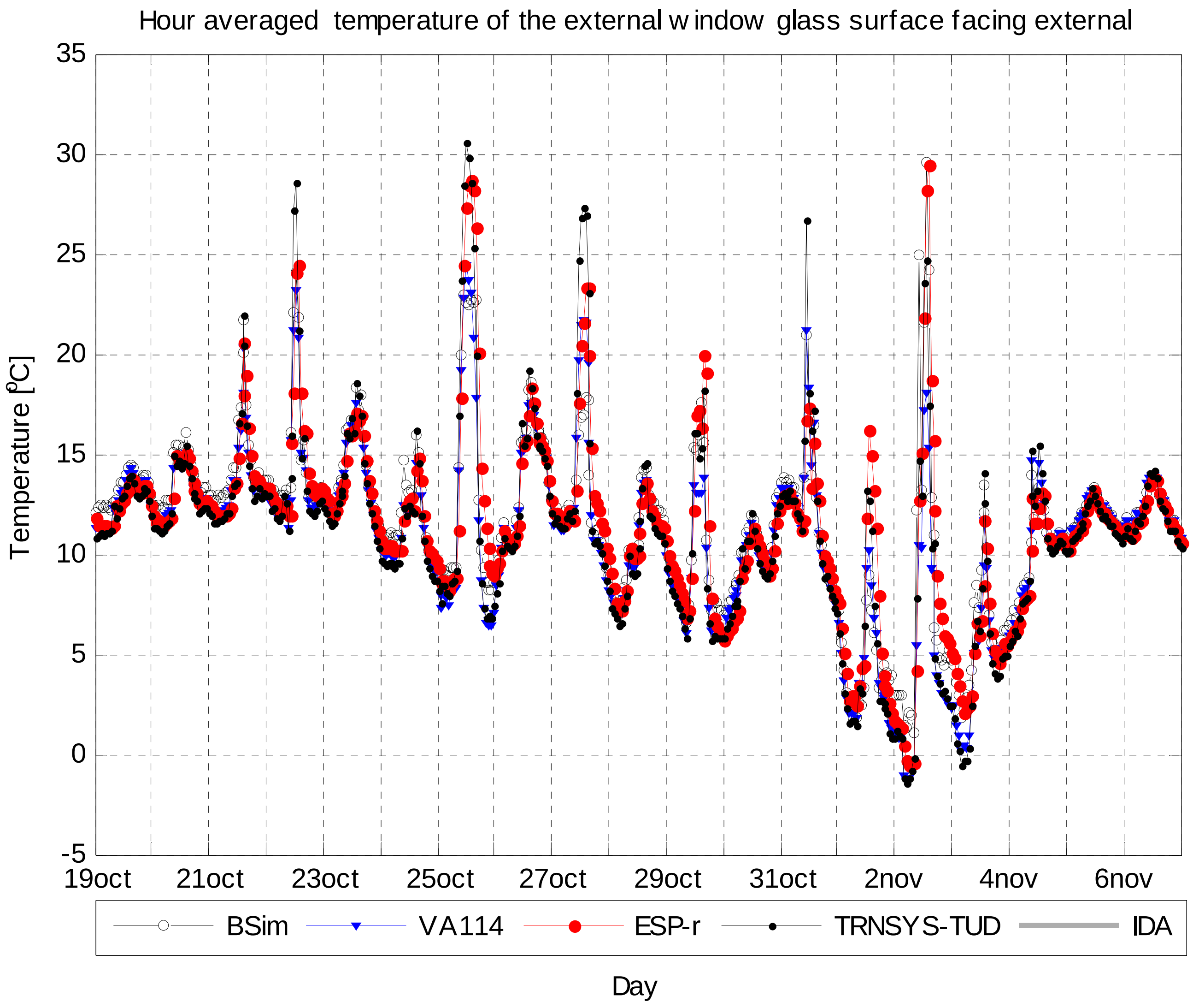

Hour averaged temperature of the external w indow glass surface facing external
Temperature [°C]
35
30
25
20
15
10
5
0
-5
19oct
21oct
23oct
25oct
27oct
29oct
31oct
2nov
4nov
6nov
BSim
VA114
ESP-r
TRNSYS-TUD
IDA
Day

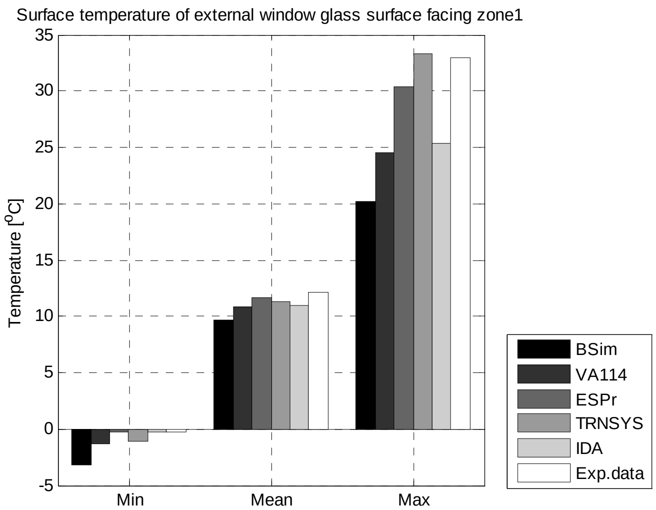

Temperature of external widow glass surface facing zone 1	BSim	VA114	ESP-r	TRNSYS-TUD	IDA	Exp.
MIN, °C	-3.2	-1.3	-0.3	-1.1	-0.3	-0.3
MAX, °C	20.2	24.6	30.4	33.3	25.3	33.0
MEAN, °C	9.7	10.9	11.6	11.4	10.9	12.2
DT95, °C	-9.0	-6.0	-2.6	-3.8	-5.7	
DT5, °C	-0.5	0.1	1.0	2.5	0.4	
MEANDT, °C	-2.5	-1.3	-0.5	-0.8	-1.3	
ABMEANDT, °C	2.5	1.4	0.9	1.4	1.4	
RSQMEANDT, °C	3.8	2.5	1.4	2.3	2.5	
STDERR, °C	2.9	2.2	1.3	2.1	2.2	

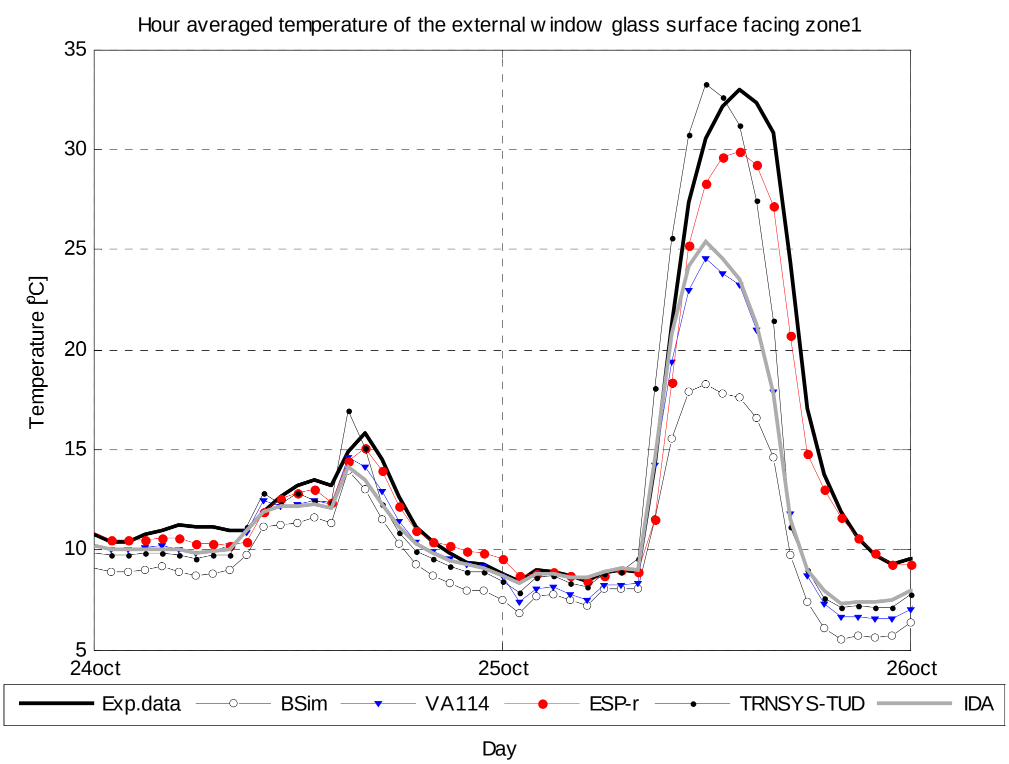

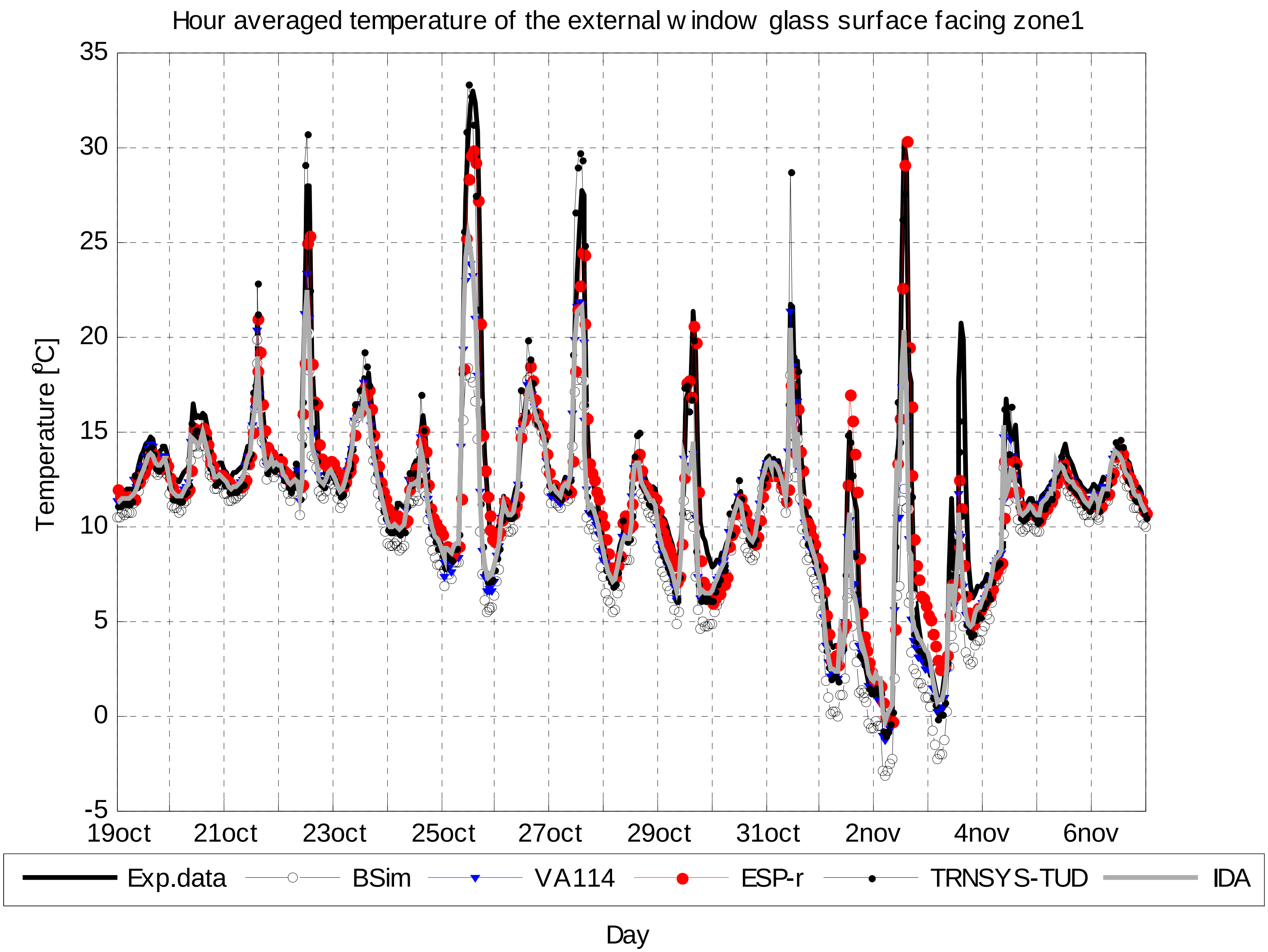

Hour averaged temperature of the external window glass surface facing zone1
Temperature [°C]
35
30
25
20
15
10
5
0
-5
19oct
21oct
23oct
25oct
27oct
29oct
31oct
2nov
4nov
6nov
Exp.data
BSim
VA114
ESP-r
TRNSYS-TUD
IDA
Day

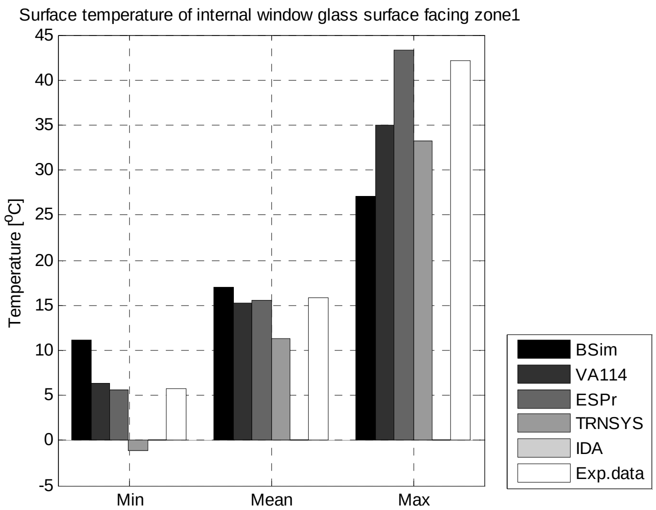

Temperature of internal widow glass surface facing zone 1	BSim	VA114	ESP-r	TRNSYS-TUD	IDA	Exp.
MIN, °C	11.1	6.4	5.6	-1.1		5.7
MAX, °C	27.0	35.0	43.4	33.3		42.2
MEAN, °C	17.0	15.2	15.6	11.4		15.8
DT95, °C	-7.0	-5.2	-1.4	-10.7		
DT5, °C	4.5	1.3	1.9	-1.1		
MEANDT, °C	1.2	-0.6	-0.2	-4.4		
ABMEANDT, °C	2.9	1.2	0.9	4.5		
RSQMEANDT, °C	3.7	2.5	1.4	5.4		
STDERR, °C	3.5	2.5	1.4	3.1		

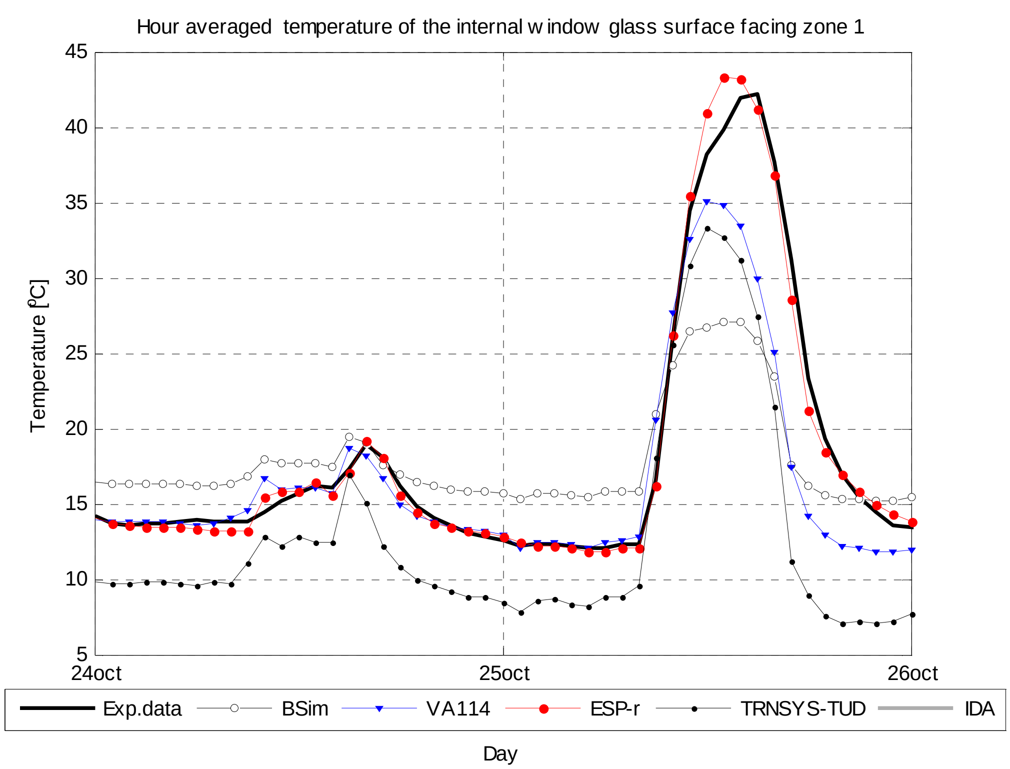

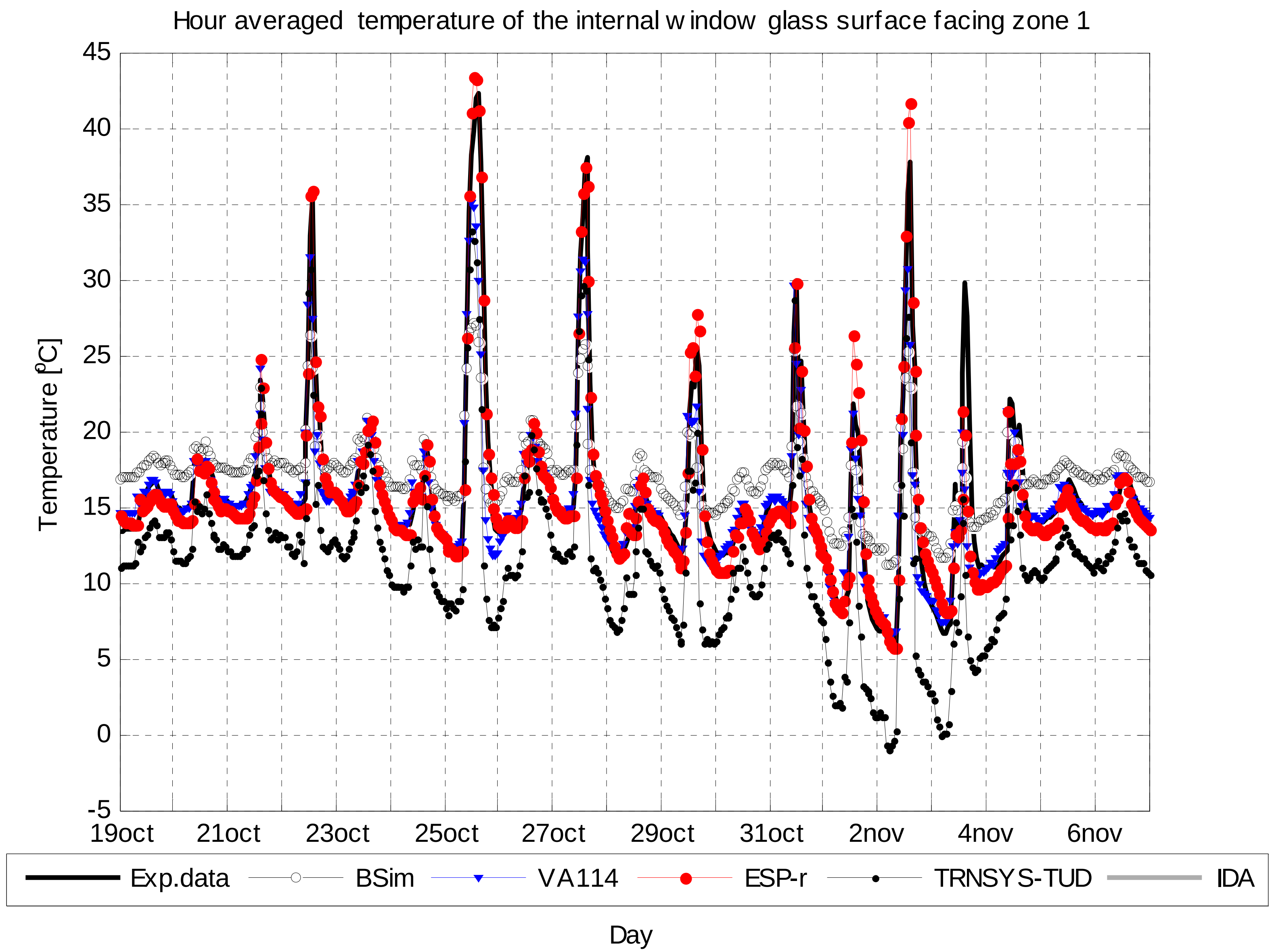

Hour averaged temperature of the internal window glass surface facing zone 1
Temperature [ºC]
45
40
35
30
25
20
15
10
5
0
-5
19oct
21oct
23oct
25oct
27oct
29oct
31oct
2nov
4nov
6nov
Exp.data
BSim
VA114
ESP-r
TRNSYS-TUD
IDA
Day

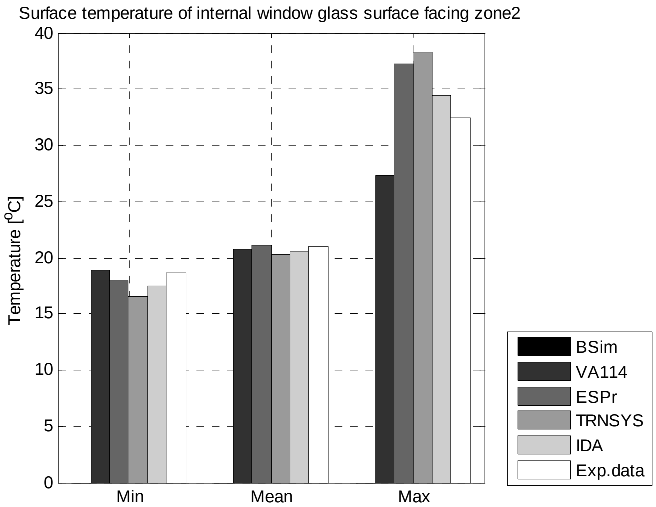

Temperature of internal widow glass surface facing zone 2	BSim	VA114	ESP-r	TRNSYS-TUD	IDA	Exp.
MIN, °C	14.7	18.9	18.0	16.6	17.5	18.6
MAX, °C	25.2	27.3	37.2	38.4	34.4	32.5
MEAN, °C	18.6	20.7	21.1	20.2	20.5	21.0
DT95, °C		-2.5	-0.7	-2.1	-1.4	
DT5, °C		0.3	3.3	2.4	2.0	
MEANDT, °C		-0.2	0.1	-0.7	-0.4	
ABMEANDT, °C		0.4	0.8	1.4	1.0	
RSQMEANDT, °C		1.0	1.2	1.8	1.3	
STDERR, °C		1.0	1.2	1.6	1.2	

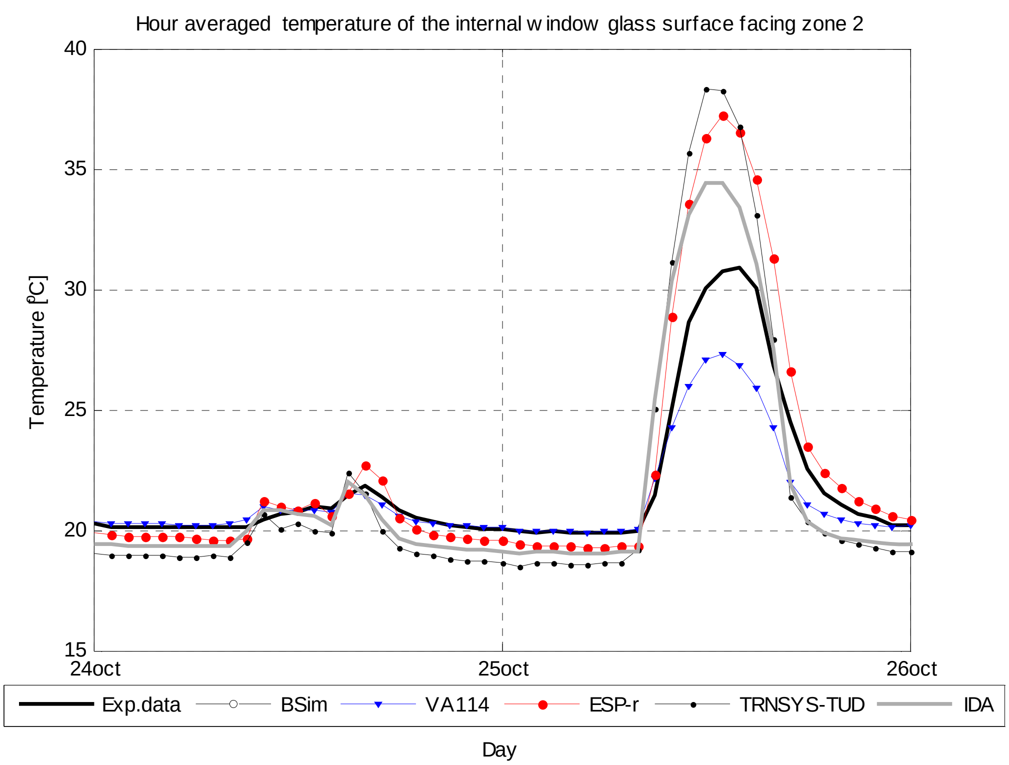

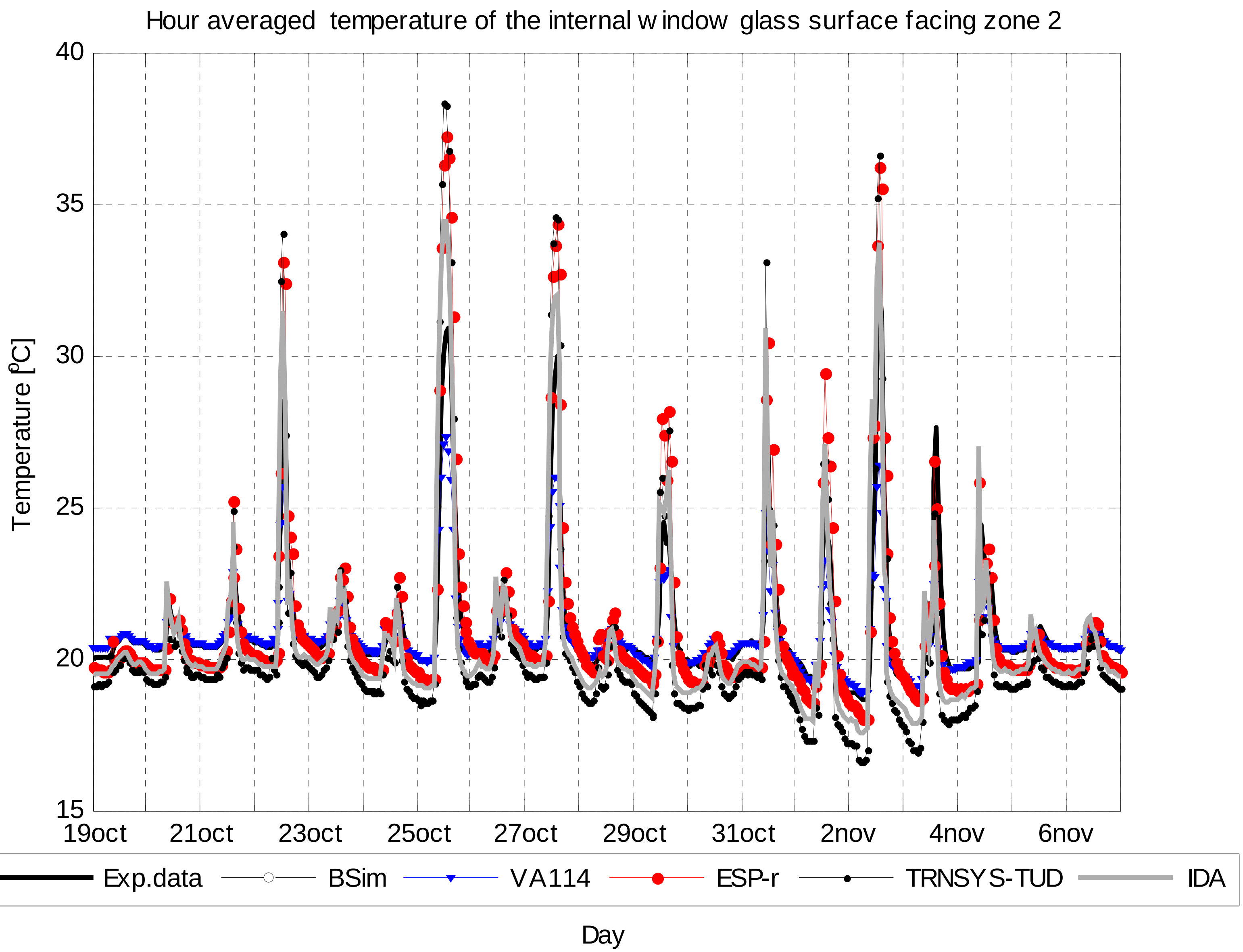

Hour averaged temperature of the internal window glass surface facing zone 2
Temperature [°C]
40
35
30
25
20
15
19oct
21oct
23oct
25oct
27oct
29oct
31oct
2nov
4nov
6nov
Exp.data
BSim
VA114
ESP-r
TRNSYS-TUD
IDA
Day

Floor and ceiling surface temperature

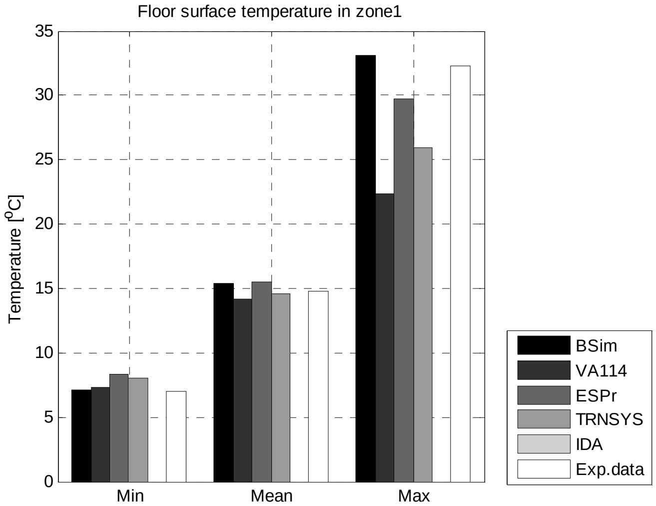

Floor surface temperature in zone 1	BSim	VA114	ESP-r	TRNSYS-TUD	IDA	Exp.
MIN, °C	7.1	7.3	8.3	8.0		7.0
MAX, °C	33.1	22.4	29.7	25.9		32.3
MEAN, °C	15.4	14.2	15.5	14.6		14.8
DT95, °C	-0.6	-4.5	-0.6	-3.1		
DT5, °C	2.6	0.9	2.3	1.9		
MEANDT, °C	0.6	-0.6	0.7	-0.2		
ABMEANDT, °C	0.9	1.0	0.9	1.1		
RSQMEANDT, °C	1.3	1.9	1.2	1.6		
STDERR, °C	1.1	1.8	1.0	1.6		

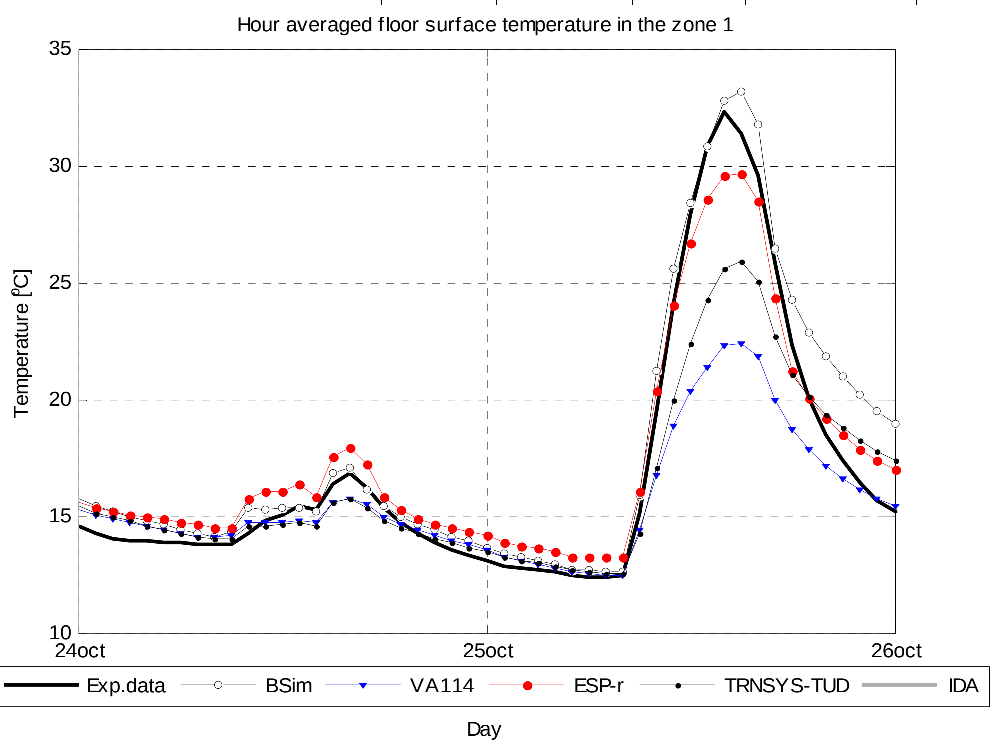

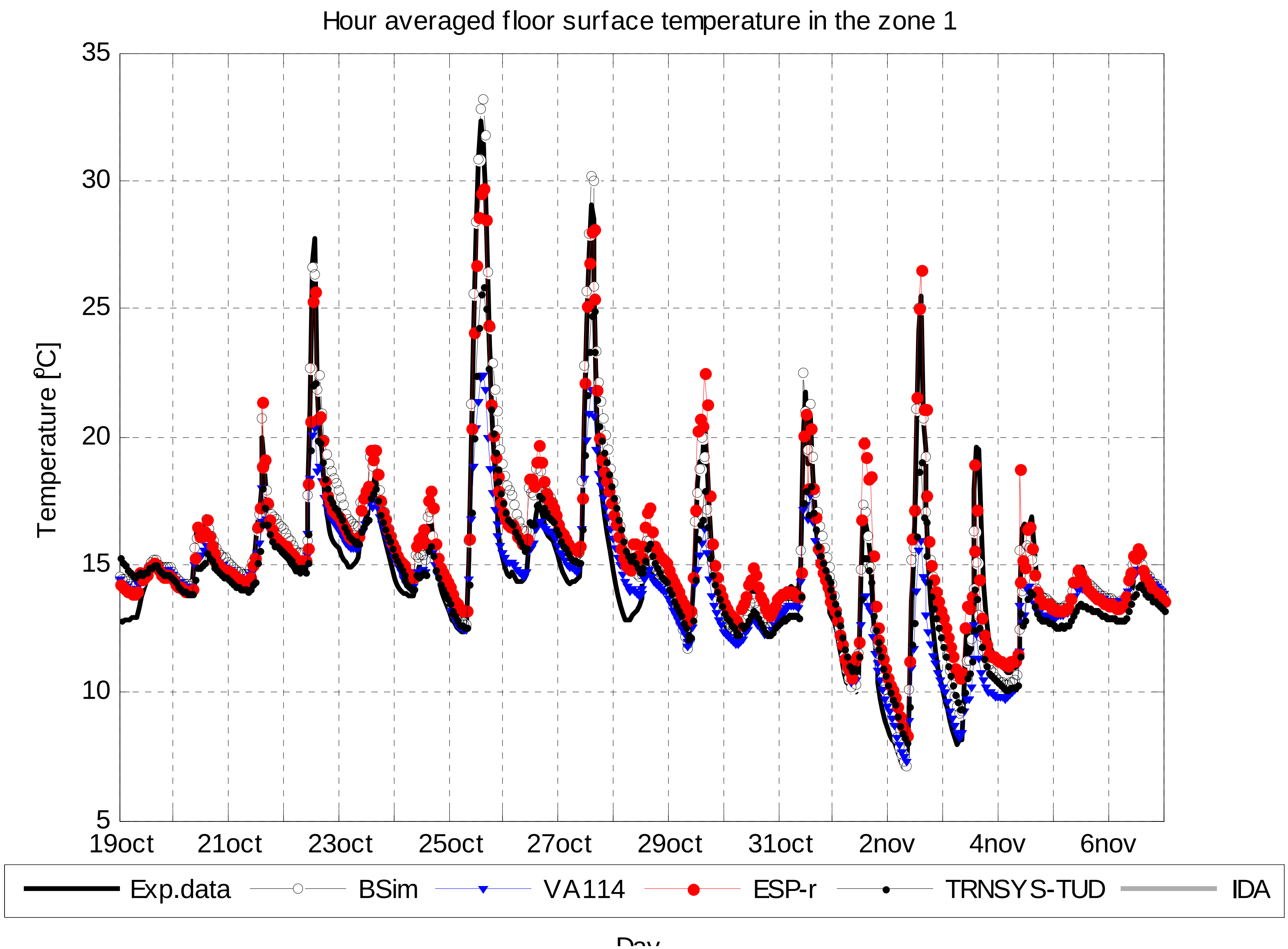
Hour averaged floor surface temperature in the zone 1
Temperature [ºC]
35
30
25
20
15
10
5
19oct
21oct
23oct
25oct
27oct
29oct
31oct
2nov
4nov
6nov
Exp.data
BSim
VA114
ESP-r
TRNSYS-TUD
IDA
Day

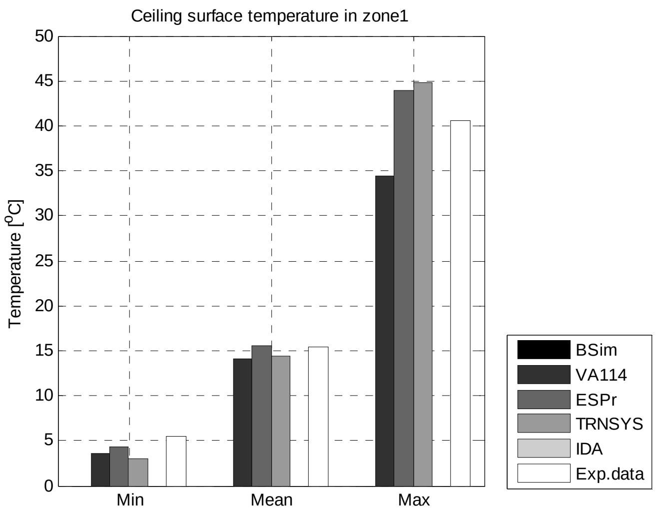

Ceiling surface temperature in zone 1	BSim	VA114	ESP-r	TRNSYS-TUD	IDA	Exp.
MIN, °C	3.7	3.6	4.2	3.0		5.4
MAX, °C	85.7	34.5	43.9	44.8		40.5
MEAN, °C	18.2	14.2	15.6	14.4		15.4
DT95, °C		-7.2	-1.6	-6.3		
DT5, °C		2.2	4.6	5.0		
MEANDT, °C		-1.3	0.2	-1.1		
ABMEANDT, °C		1.9	1.4	2.5		
RSQMEANDT, °C		3.1	2.1	3.5		
STDERR, °C		2.8	2.1	3.4		

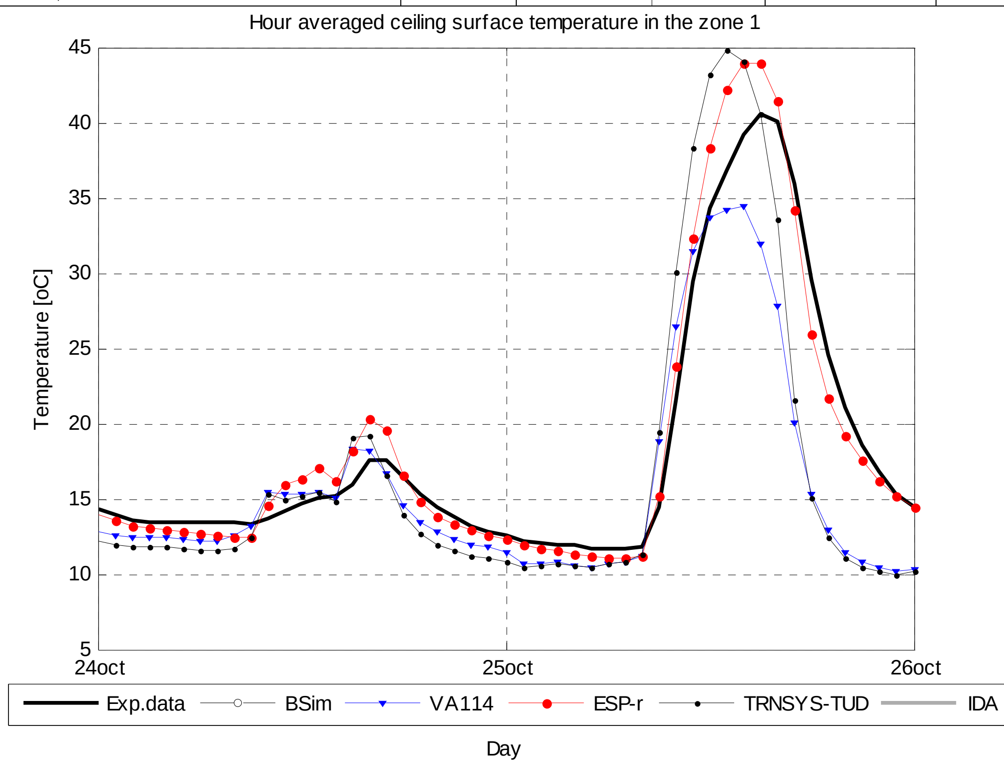

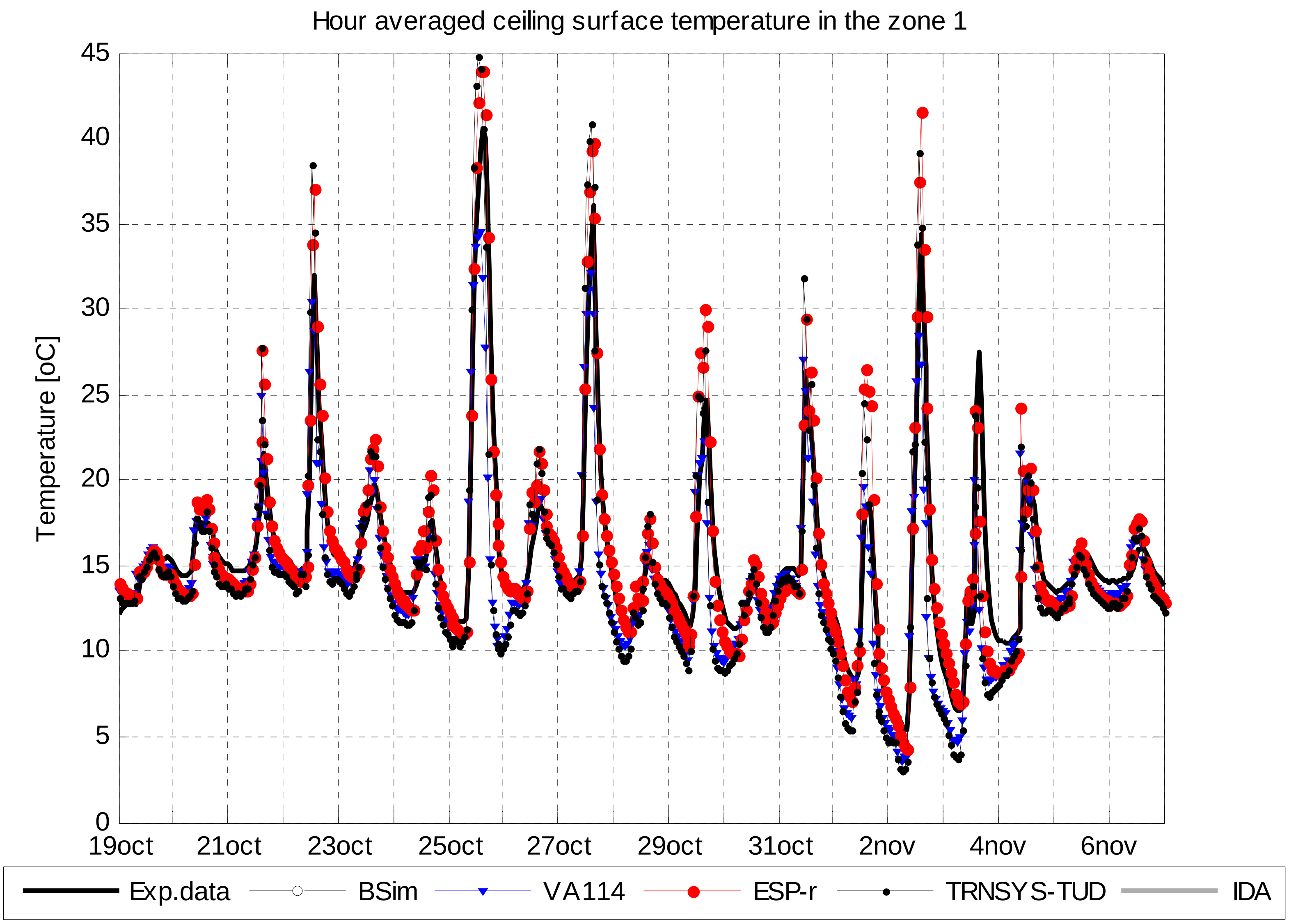

Hour averaged ceiling surface temperature in the zone 1
Temperature [oC]
0
5
10
15
20
25
30
35
40
45
19oct
21oct
23oct
25oct
27oct
29oct
31oct
2nov
4nov
6nov
Exp.data
BSim
VA114
ESP-r
TRNSYS-TUD
IDA

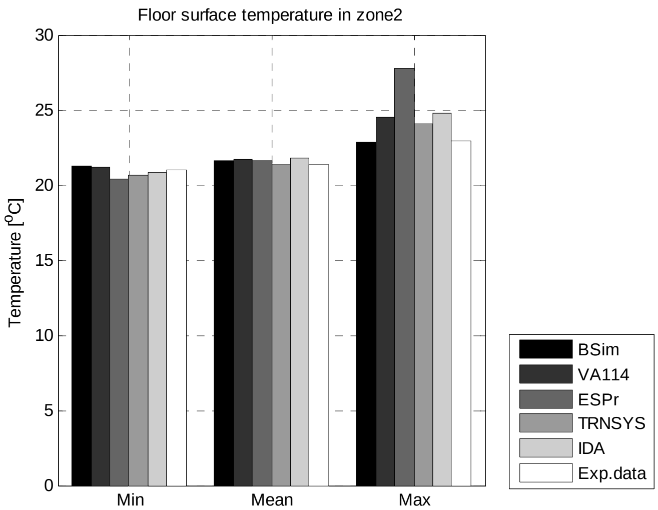

Floor surface temperature in zone 2	BSim	VA114	ESP-r	TRNSYS-TUD	IDA	Exp.
MIN, °C	21.3	21.2	20.4	20.6	20.8	21.0
MAX, °C	22.9	24.5	27.7	24.1	24.8	22.9
MEAN, °C	21.7	21.7	21.7	21.3	21.8	21.3
DT95, °C	0.0	0.1	-0.6	-0.4	-0.2	
DT5, °C	0.5	1.0	2.2	0.8	1.7	
MEANDT, °C	0.3	0.4	0.3	0.0	0.5	
ABMEANDT, °C	0.3	0.4	0.6	0.3	0.5	
RSQMEANDT, °C	0.3	0.5	1.0	0.4	0.7	
STDERR, °C	0.1	0.3	0.9	0.4	0.6	

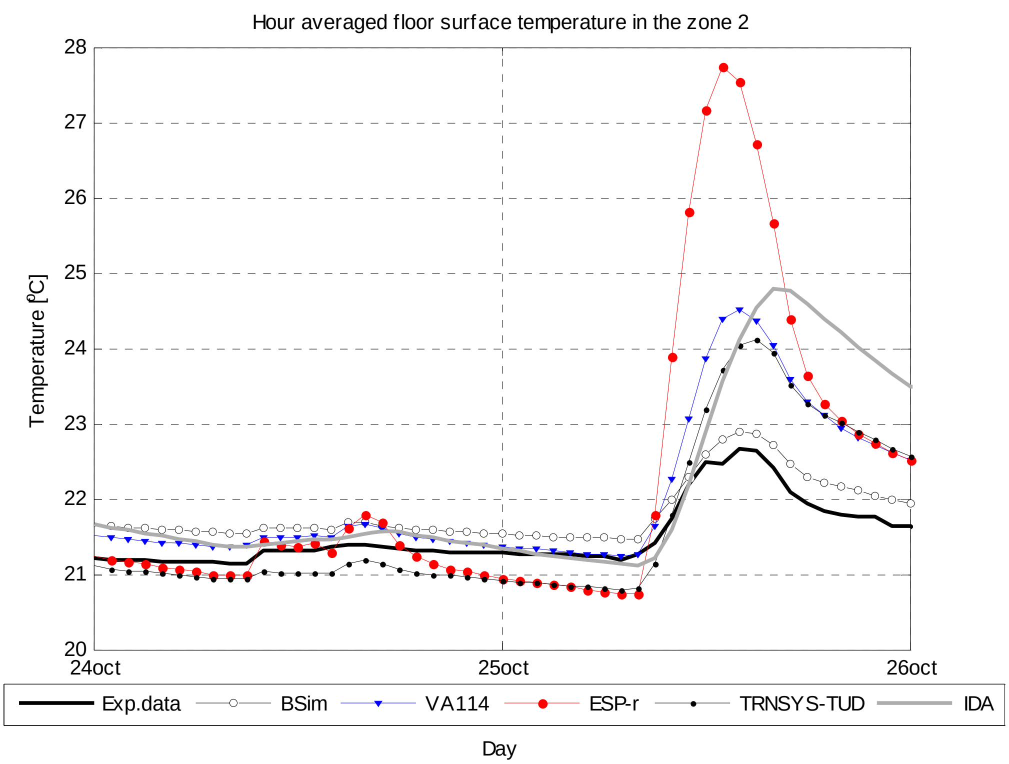

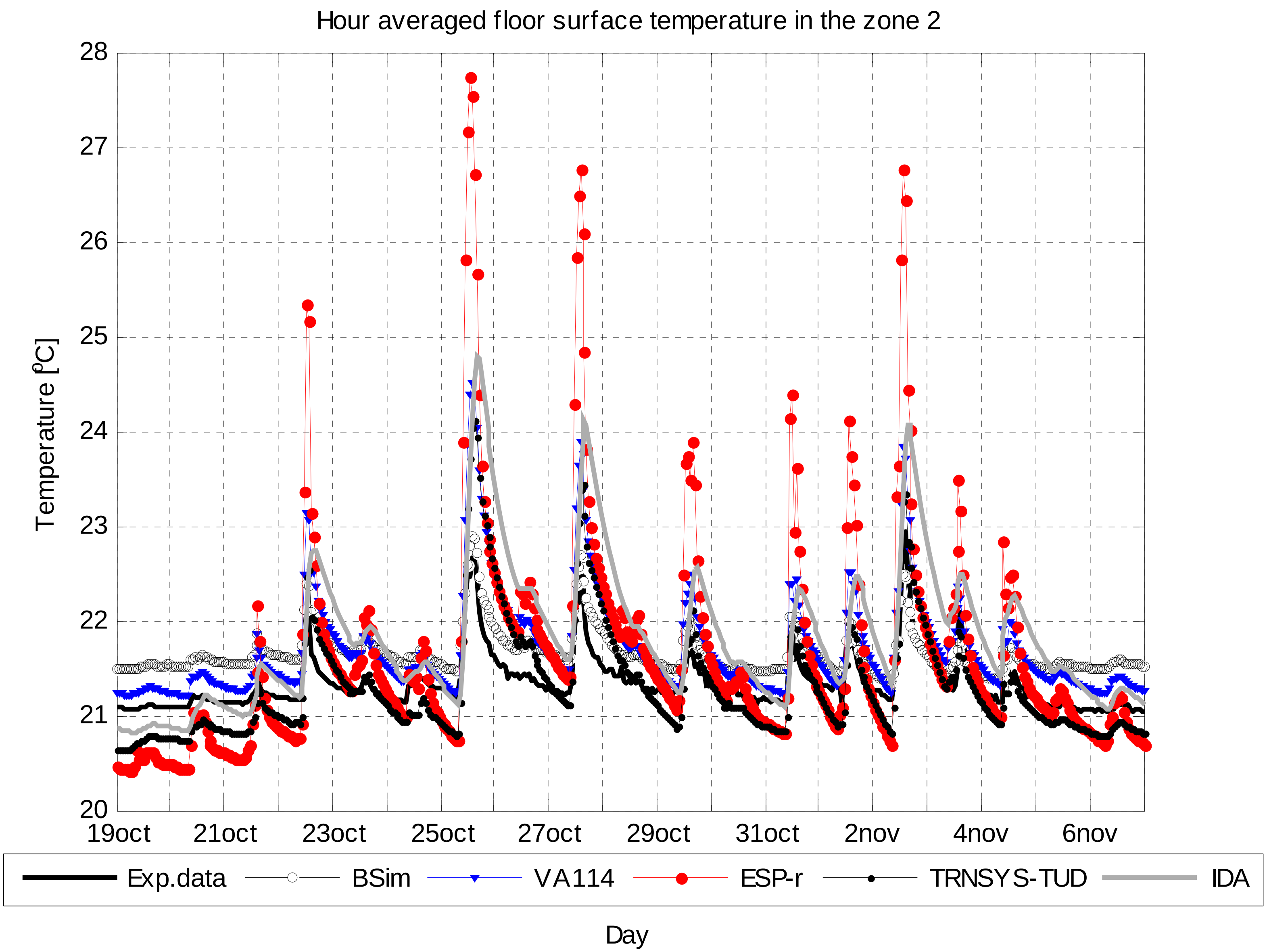

Hour averaged floor surface temperature in the zone 2
Temperature [ºC]
28
27
26
25
24
23
22
21
20
19oct
21oct
23oct
25oct
27oct
29oct
31oct
2nov
4nov
6nov
Day
Exp.data
BSim
VA114
ESP-r
TRNSYS-TUD
IDA

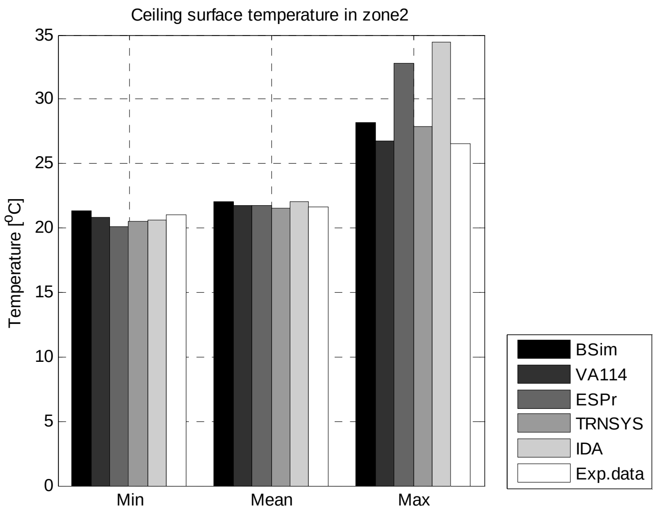

Ceiling surface temperature in zone 2	BSim	VA114	ESP-r	TRNSYS-TUD	IDA	Exp.
MIN, °C	21.4	20.8	20.1	20.5	20.6	21.0
MAX, °C	28.2	26.8	32.8	27.9	34.5	26.6
MEAN, °C	22.0	21.7	21.8	21.5	22.1	21.6
DT95, °C	-0.1	-0.2	-0.7	-0.5	-0.4	
DT5, °C	1.8	1.1	3.4	0.8	4.8	
MEANDT, °C	0.4	0.1	0.2	-0.1	0.5	
ABMEANDT, °C	0.5	0.2	0.8	0.3	0.8	
RSQMEANDT, °C	0.7	0.4	1.4	0.5	1.8	
STDERR, °C	0.6	0.4	1.4	0.5	1.7	

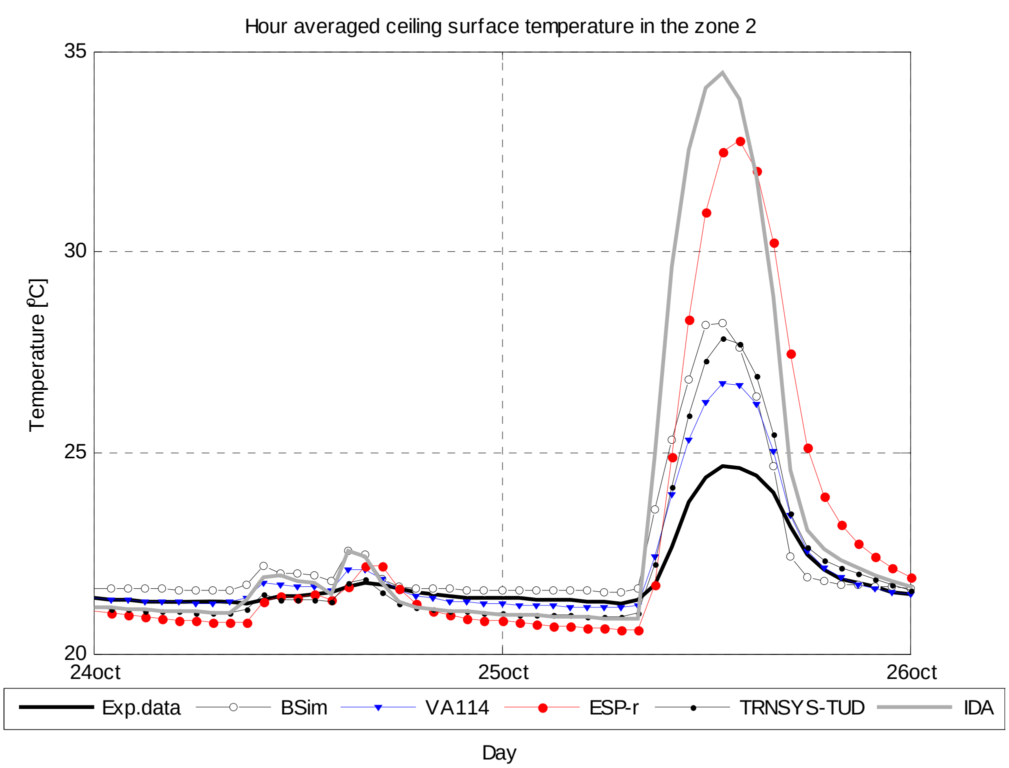

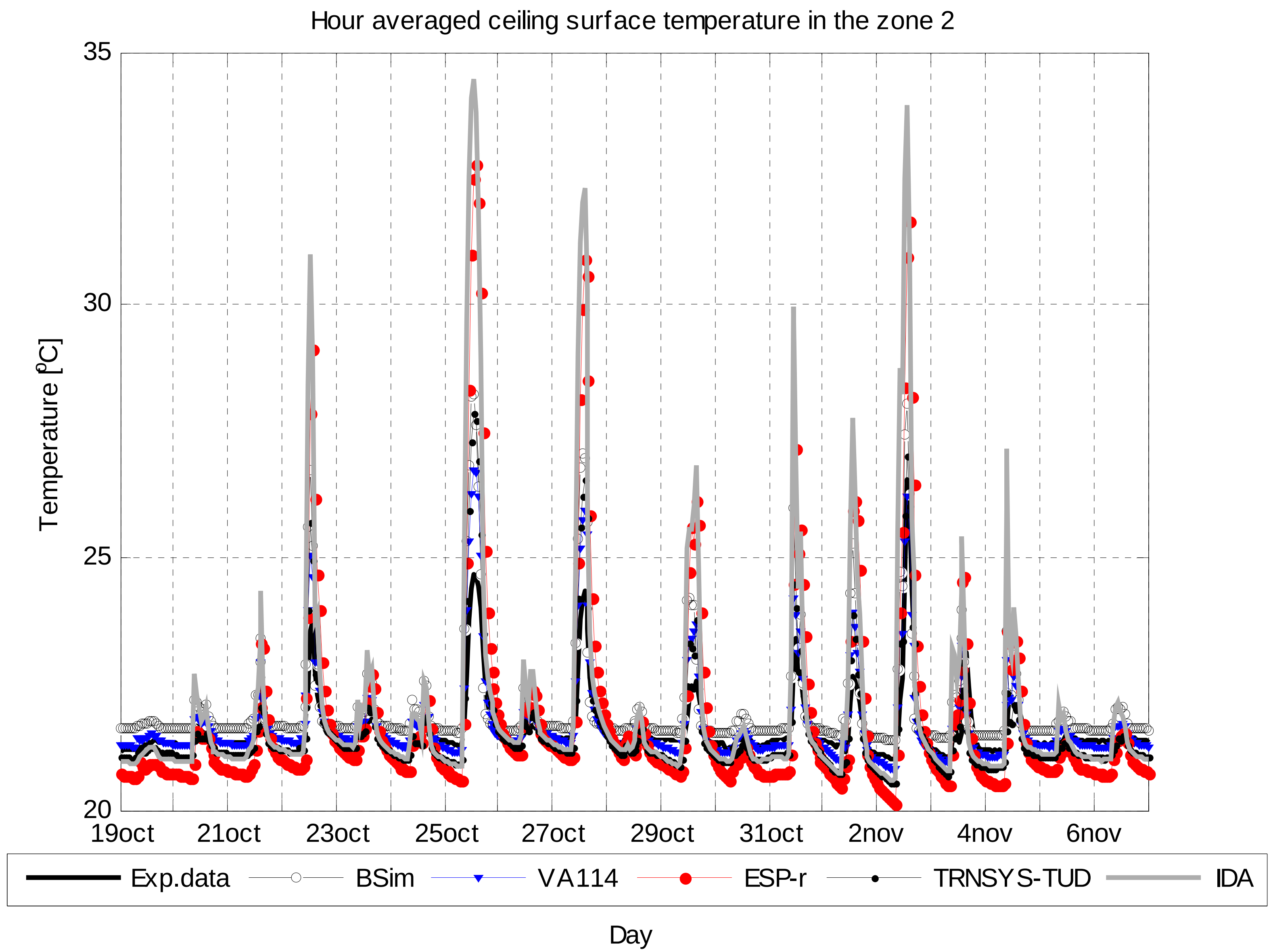

Hour averaged ceiling surface temperature in the zone 2
35
30
25
20
Temperature [ºC]
19oct
21oct
23oct
25oct
27oct
29oct
31oct
2nov
4nov
6nov
Exp.data
BSim
VA114
ESP-r
TRNSYS-TUD
IDA
Day

Test case DSF200_e

Surface temperature of the glazing

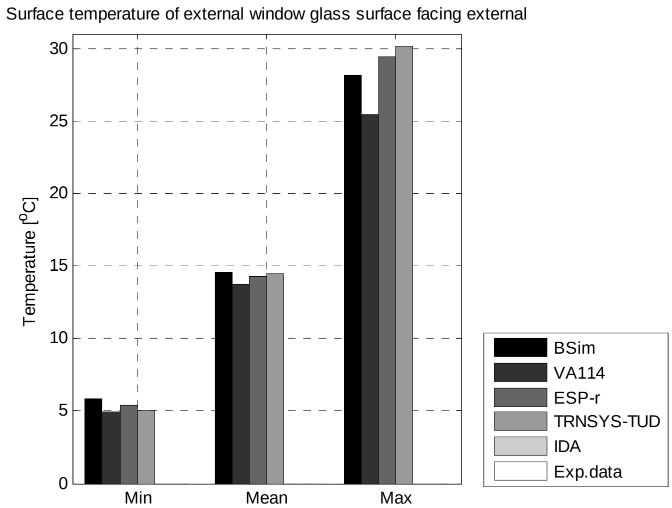

Temperature of external widow glass surface facing external	BSim	VA114	ESP-r	TRNSYS-TUD	IDA	Exp.
MIN, °C	5.8	4.9	5.4	5.0		5.8
MAX, °C	28.2	25.5	29.4	30.1		28.2
MEAN, °C	14.6	13.8	14.3	14.5		14.6

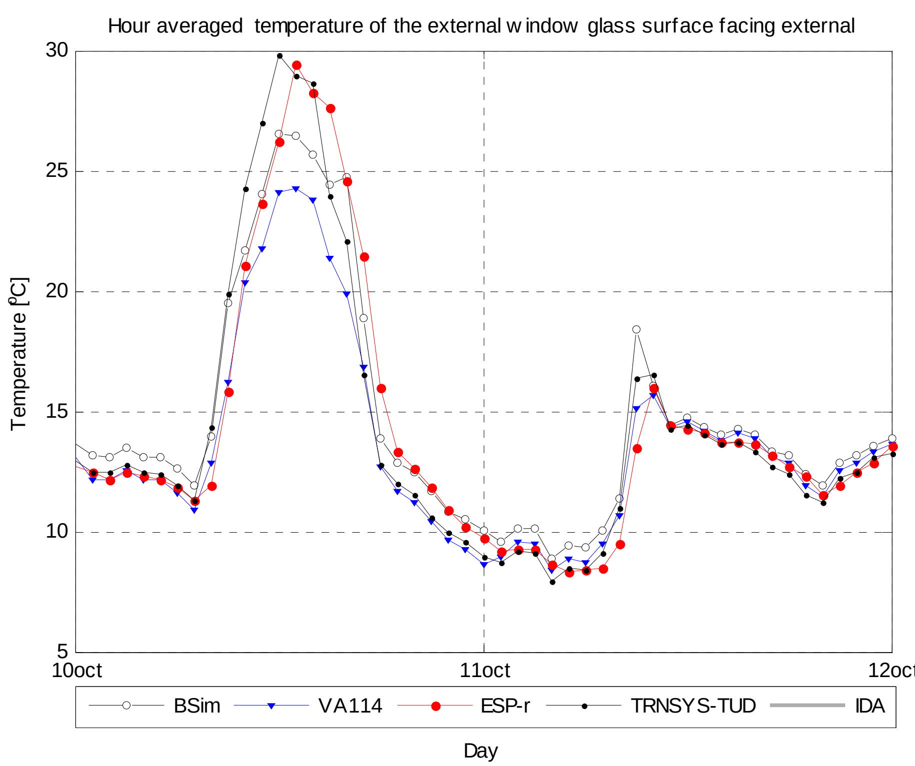

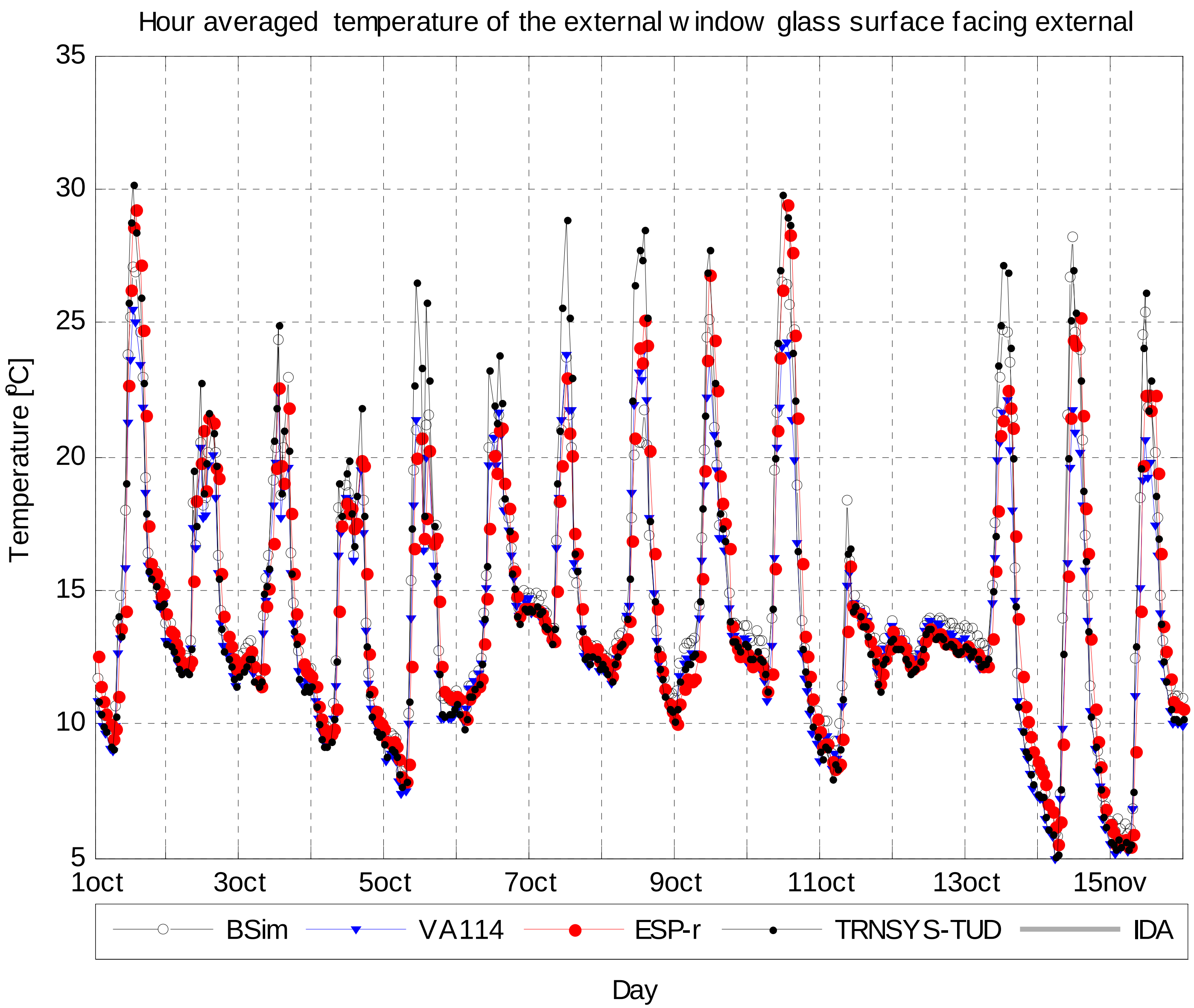

Hour averaged temperature of the external w indow glass surface facing external
35
30
25
20
15
10
5
Temperature [ºC]
1oct
3oct
5oct
7oct
9oct
11oct
13oct
15nov
BSim
VA114
ESP-r
TRNSYS-TUD
IDA
Day

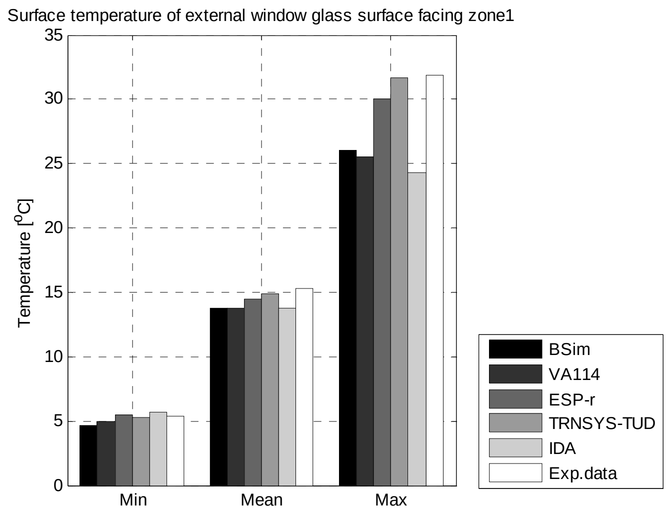

Temperature of external widow glass surface facing zone1	BSim	VA114	ESP-r	TRNSYS-TUD	IDA	Exp.
MIN, °C	4.6	4.9	5.5	5.2	5.7	5.3
MAX, °C	26.0	25.5	30.0	31.7	24.3	31.9
MEAN, °C	13.8	13.8	14.5	14.9	13.8	15.3
DT95, °C	-5.7	-5.9	-3.5	-2.8	-6.6	
DT5, °C	0.0	0.0	0.7	2.7	0.3	
MEANDT, °C	-1.5	-1.5	-0.8	-0.4	-1.5	
ABMEANDT, °C	1.6	1.5	1.0	1.1	1.6	
RSQMEANDT, °C	2.3	2.3	1.4	1.6	2.5	
STDERR, °C	1.8	1.8	1.2	1.6	2.0	

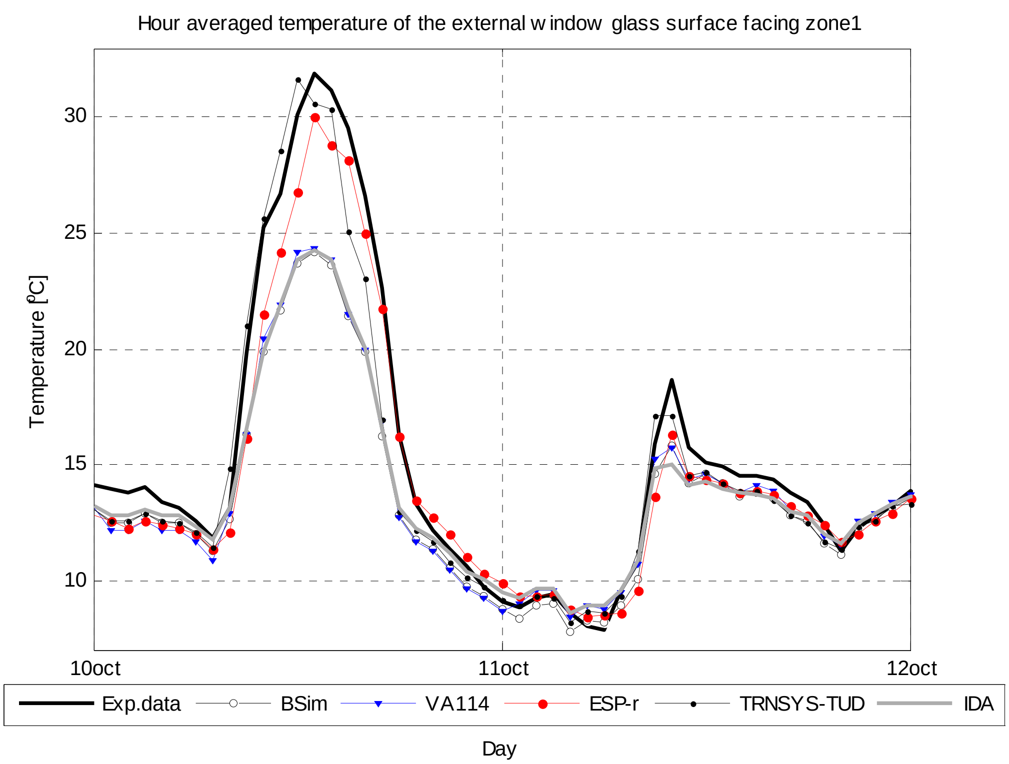

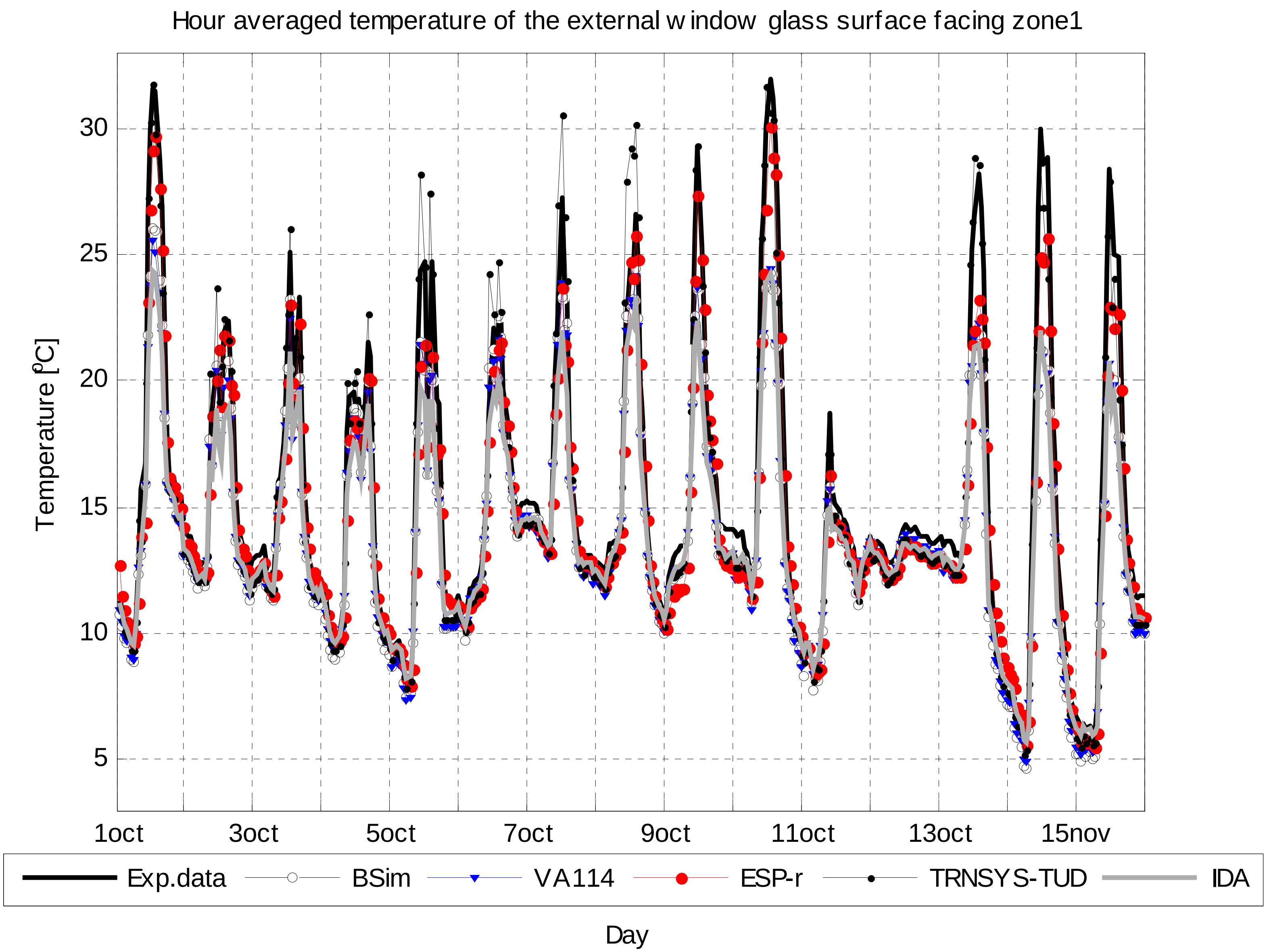

Hour averaged temperature of the external w indow glass surface facing zone1
Temperature [ºC]
30
25
20
15
10
5
1oct
3oct
5oct
7oct
9oct
11oct
13oct
15nov
Exp.data
BSim
VA114
ESP-r
TRNSYS-TUD
IDA
Day

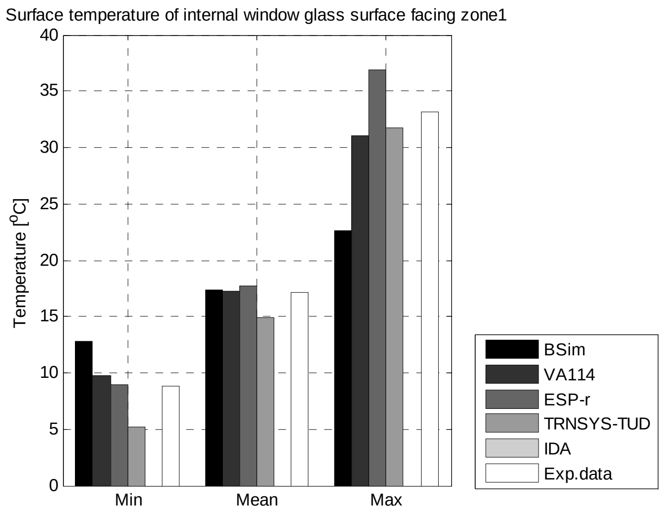

Temperature of internal widow glass surface facing zone1	BSim	VA114	ESP-r	TRNSYS-TUD	IDA	Exp.
MIN, °C	12.8	9.7	8.9	5.2		8.9
MAX, °C	22.7	31.1	36.9	31.7		33.2
MEAN, °C	17.4	17.3	17.7	14.9		17.1
DT95, °C	-7.8	-2.1	-0.5	-4.5		
DT5, °C	3.3	2.3	3.1	1.8		
MEANDT, °C	0.3	0.2	0.6	-2.2		
ABMEANDT, °C	2.7	0.9	0.8	2.6		
RSQMEANDT, °C	3.4	1.3	1.3	2.9		
STDERR, °C	3.4	1.3	1.1	1.8		

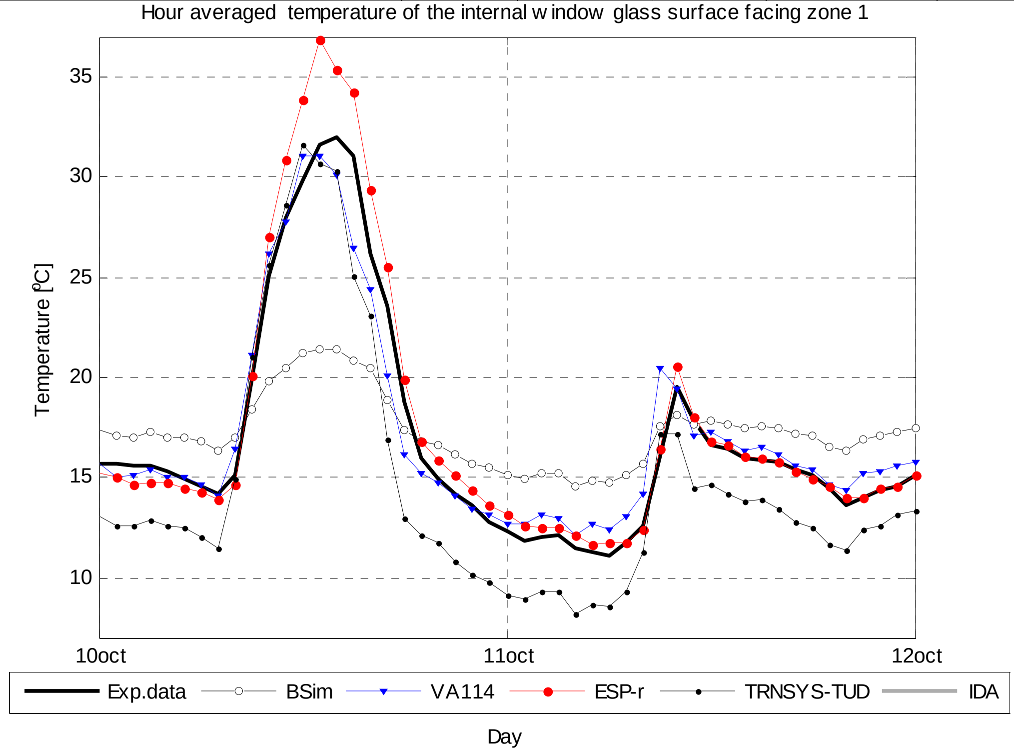

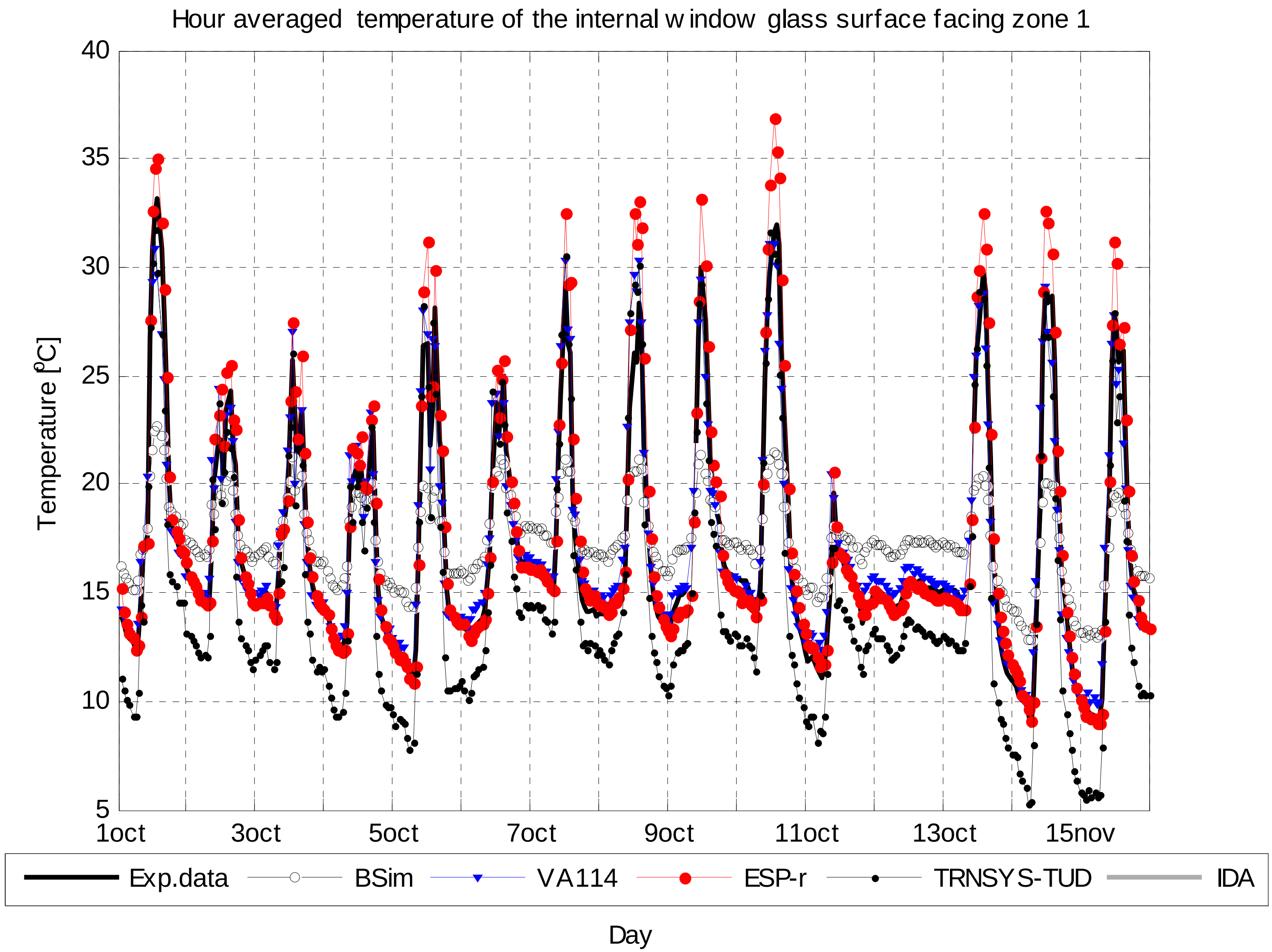

Hour averaged temperature of the internal window glass surface facing zone 1
40
35
30
25
20
15
10
5
Temperature [^{o}C]
1oct
3oct
5oct
7oct
9oct
11oct
13oct
15nov
Exp.data
BSim
VA114
ESP-r
TRNSYS-TUD
IDA
Day

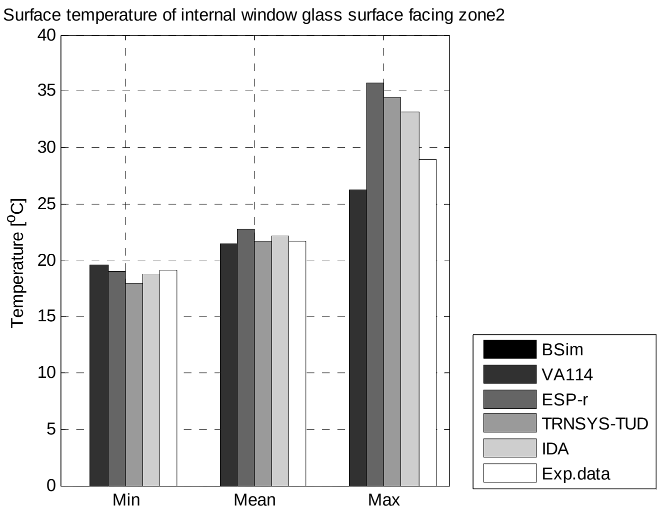

Temperature of internal widow glass surface facing internal	BSim	VA114	ESP-r	TRNSYS-TUD	IDA	Exp.
MIN, °C	15.8	19.6	19.0	17.9	18.8	19.1
MAX, °C	22.3	26.3	35.8	34.5	33.2	29.0
MEAN, °C	18.8	21.5	22.8	21.7	22.2	21.7
DT95, °C		-2.6	-0.3	-1.2	-0.5	
DT5, °C		0.5	5.0	4.1	3.6	
MEANDT, °C		-0.2	1.1	0.0	0.5	
ABMEANDT, °C		0.6	1.2	1.2	0.8	
RSQMEANDT, °C		1.0	2.0	1.7	1.4	
STDERR, °C		0.9	1.7	1.7	1.3	

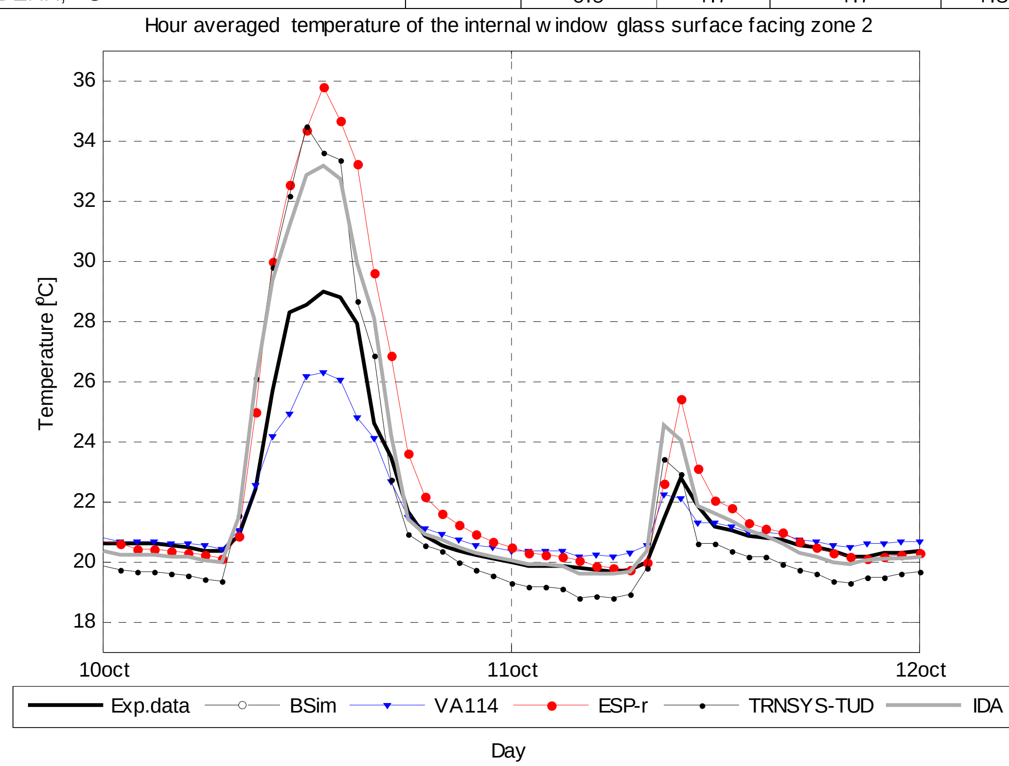

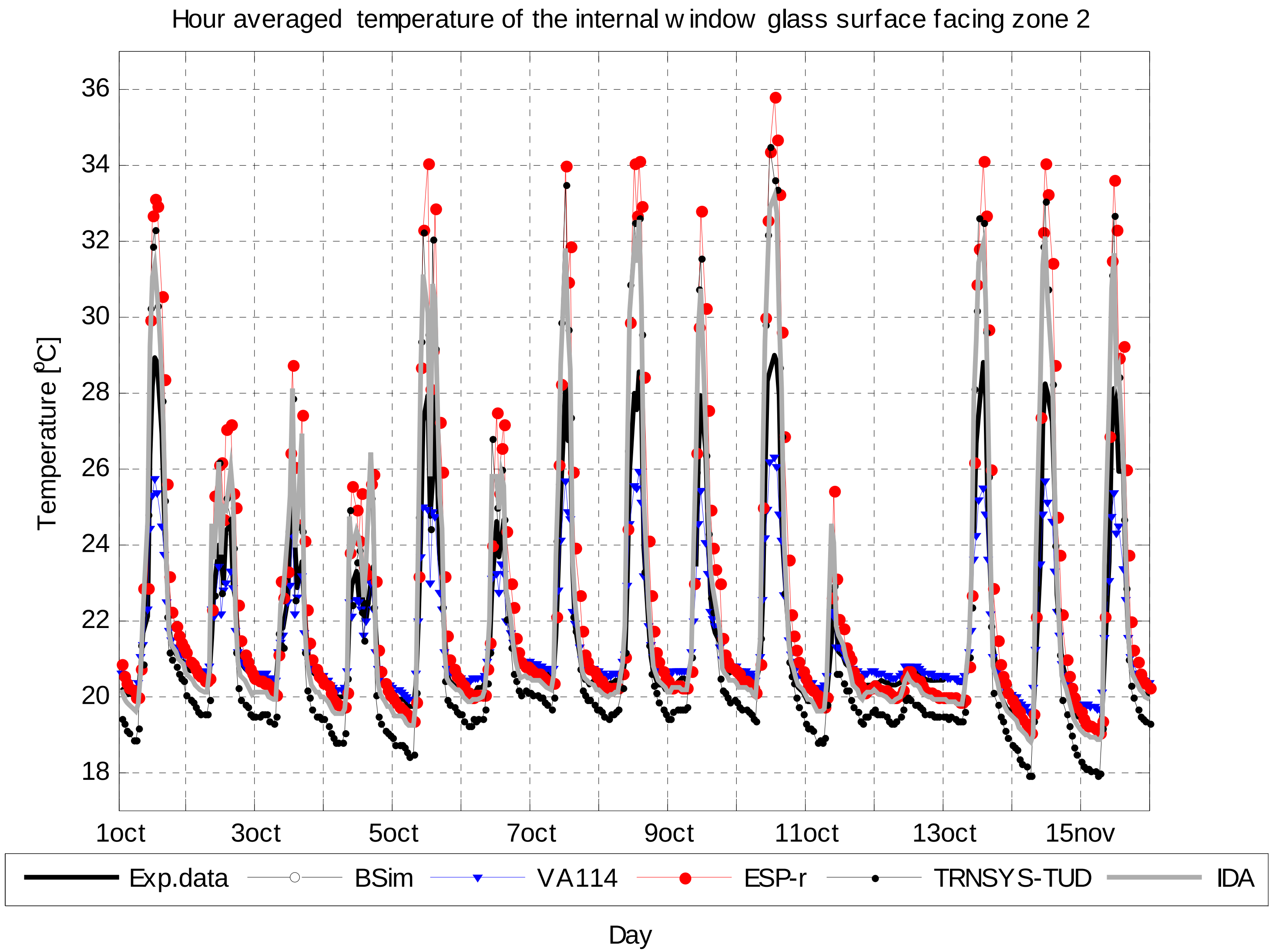

Hour averaged temperature of the internal w indow glass surface facing zone 2
Temperature [°C]
36
34
32
30
28
26
24
22
20
18
1oct
3oct
5oct
7oct
9oct
11oct
13oct
15nov
Exp.data
BSim
VA114
ESP-r
TRNSYS-TUD
IDA
Day

Floor and ceiling surface temperature

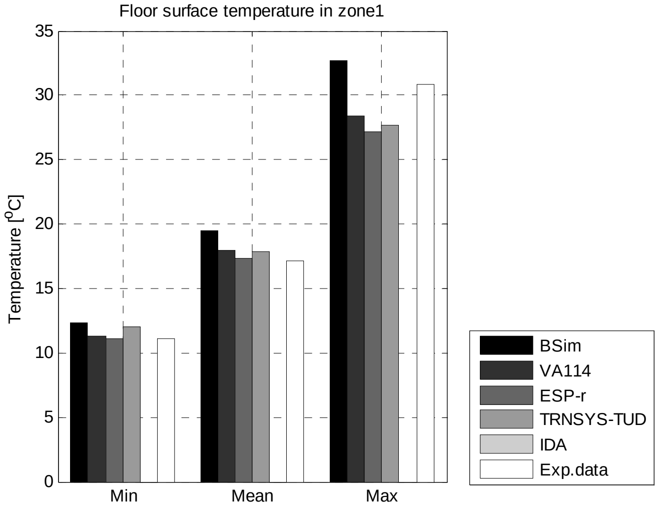

Floor surface temperature in zone 1	BSim	VA114	ESP-r	TRNSYS-TUD	IDA	Exp.
MIN, °C	12.3	11.4	11.1	12.0		11.1
MAX, °C	32.7	28.4	27.2	27.7		30.9
MEAN, °C	19.5	18.0	17.4	17.8		17.2
DT95, °C	-0.1	-2.9	-2.4	-3.0		
DT5, °C	4.9	3.6	1.4	3.4		
MEANDT, °C	2.3	0.8	0.2	0.6		
ABMEANDT, °C	2.3	1.7	0.8	1.6		
RSQMEANDT, °C	2.8	2.2	1.1	1.9		
STDERR, °C	1.5	2.0	1.1	1.8		

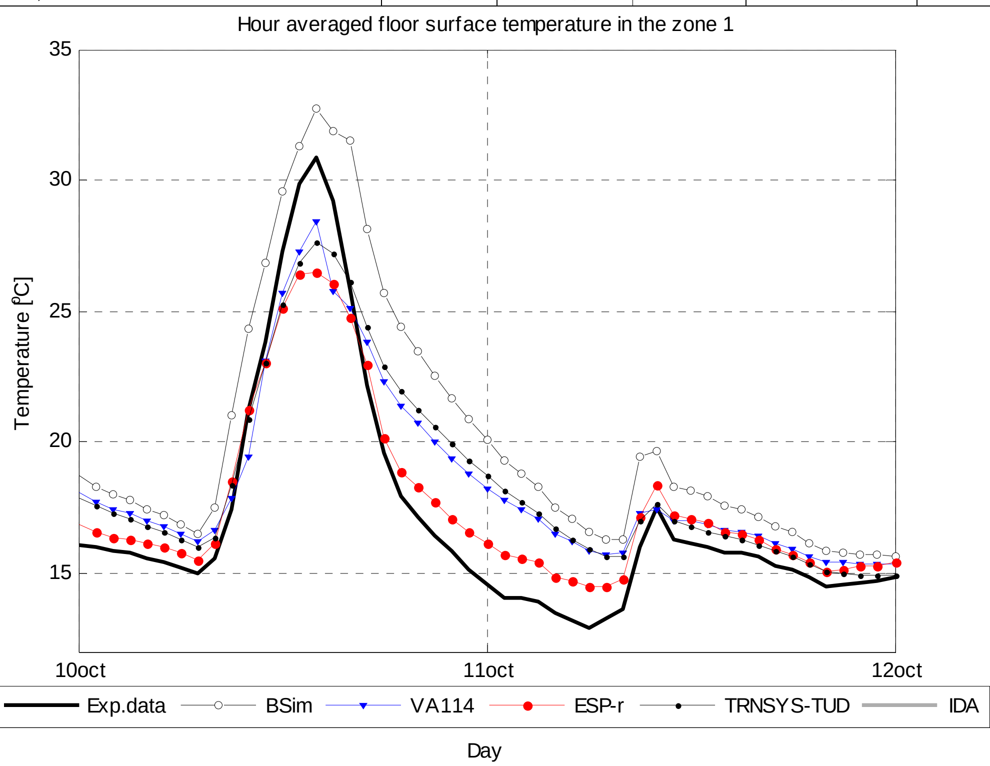

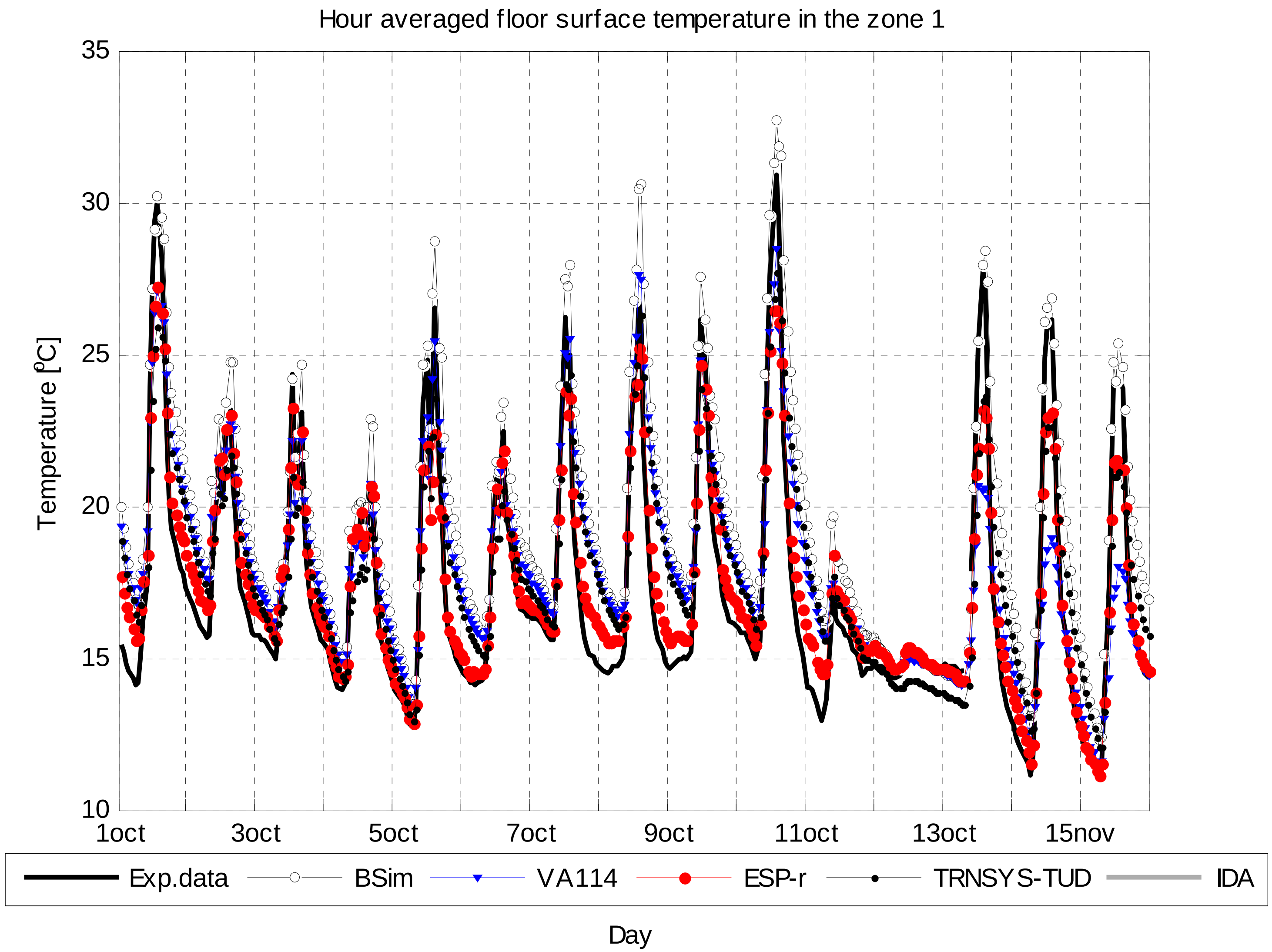
Hour averaged floor surface temperature in the zone 1
Temperature [^{0}C]
35
30
25
20
15
10
1oct
3oct
5oct
7oct
9oct
11oct
13oct
15nov
Exp.data
BSim
VA114
ESP-r
TRNSYS-TUD
IDA
Day

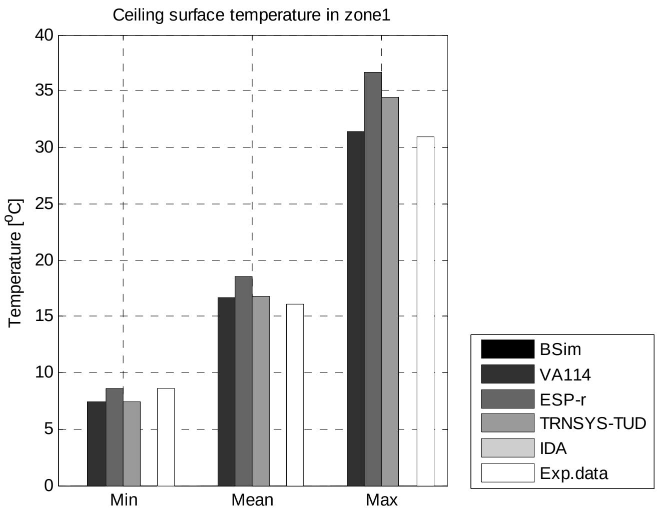

Ceiling surface temperature in zone 1	BSim	VA114	ESP-r	TRNSYS-TUD	IDA	Exp.
MIN, °C	7.5	7.4	8.6	7.4		8.6
MAX, °C	81.5	31.4	36.7	34.4		30.9
MEAN, °C	25.2	16.6	18.5	16.8		16.1
DT95, °C		-2.7	0.0	-2.8		
DT5, °C		5.3	8.0	6.6		
MEANDT, °C		0.5	2.4	0.6		
ABMEANDT, °C		1.7	2.4	1.9		
RSQMEANDT, °C		2.4	3.4	2.9		
STDERR, °C		2.3	2.4	2.8		

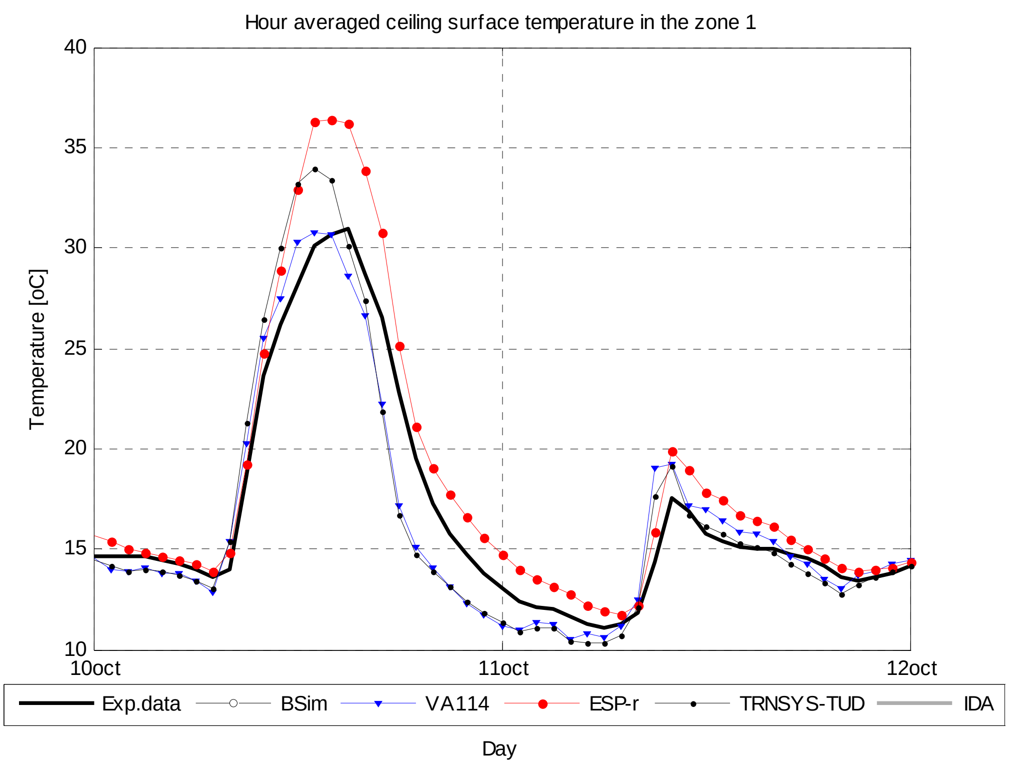

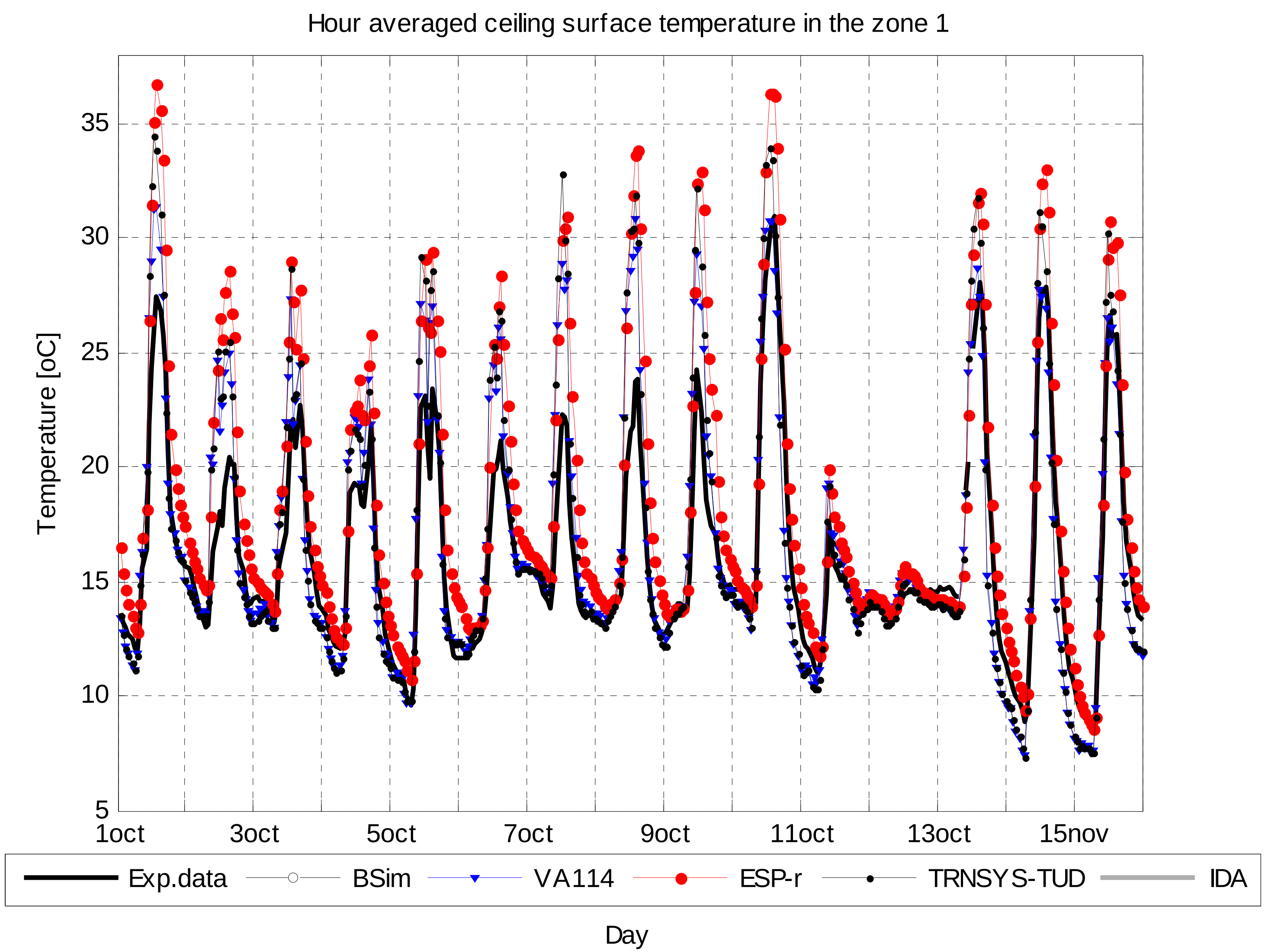
Hour averaged ceiling surface temperature in the zone 1
Temperature [oC]
35
30
25
20
15
10
5
1oct
3oct
5oct
7oct
9oct
11oct
13oct
15nov
Exp.data
BSim
VA114
ESP-r
TRNSYS-TUD
IDA
Day

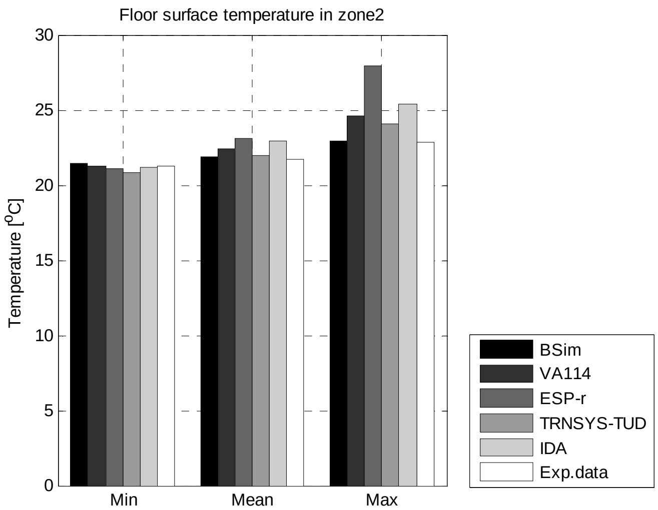

Floor surface temperature in zone 2	BSim	VA114	ESP-r	TRNSYS-TUD	IDA	Exp.
MIN, °C	21.5	21.3	21.1	20.9	21.2	21.3
MAX, °C	22.9	24.6	27.9	24.1	25.4	22.8
MEAN, °C	21.9	22.4	23.1	22.0	23.0	21.7
DT95, °C	0.0	0.1	0.2	-0.3	0.2	
DT5, °C	0.4	1.5	3.9	1.0	2.4	
MEANDT, °C	0.2	0.7	1.4	0.3	1.3	
ABMEANDT, °C	0.2	0.7	1.4	0.4	1.3	
RSQMEANDT, °C	0.2	0.8	1.8	0.5	1.4	
STDERR, °C	0.1	0.4	1.1	0.4	0.7	

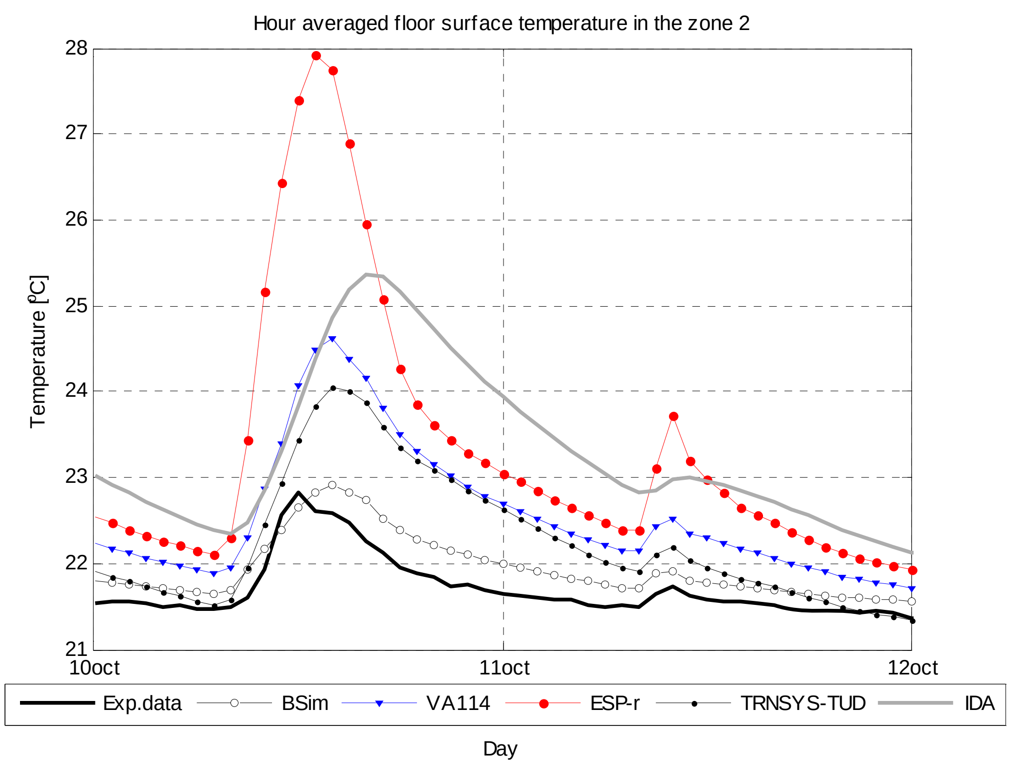

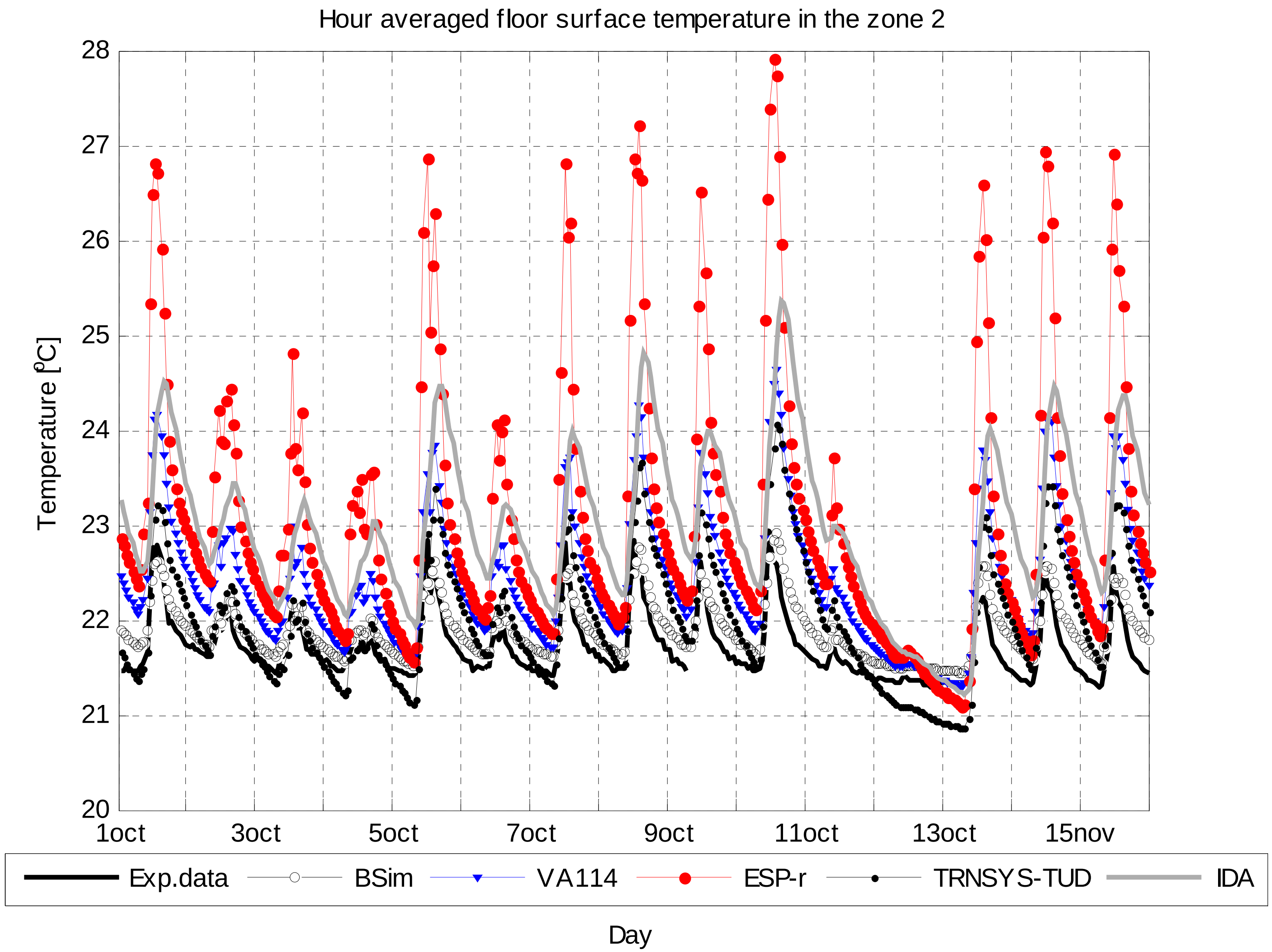

Hour averaged floor surface temperature in the zone 2
Temperature [ºC]
28
27
26
25
24
23
22
21
20
1oct
3oct
5oct
7oct
9oct
11oct
13oct
15nov
Exp.data
BSim
VA114
ESP-r
TRNSYS-TUD
IDA
Day

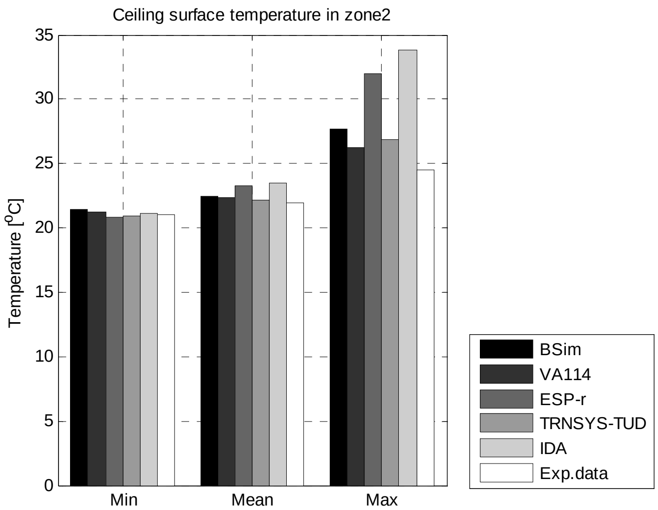

Ceiling surface temperature in zone 2	BSim	VA114	ESP-r	TRNSYS-TUD	IDA	Exp.
MIN, °C	21.5	21.2	20.8	21.0	21.1	21.1
MAX, °C	27.7	26.3	32.0	26.8	33.8	24.5
MEAN, °C	22.5	22.3	23.2	22.2	23.5	21.9
DT95, °C	-0.1	-0.1	-0.4	-0.3	-0.2	
DT5, °C	2.7	1.6	6.0	1.8	7.5	
MEANDT, °C	0.5	0.4	1.3	0.2	1.6	
ABMEANDT, °C	0.6	0.4	1.5	0.4	1.6	
RSQMEANDT, °C	1.0	0.7	2.4	0.7	2.9	
STDERR, °C	0.9	0.5	2.0	0.6	2.4	

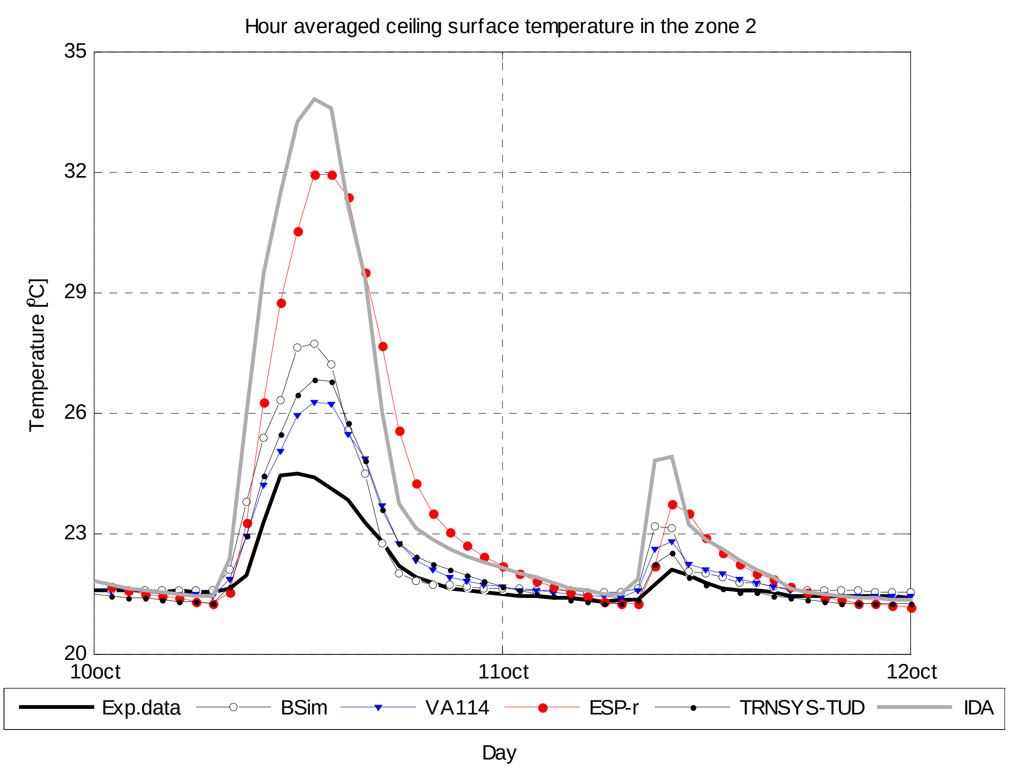

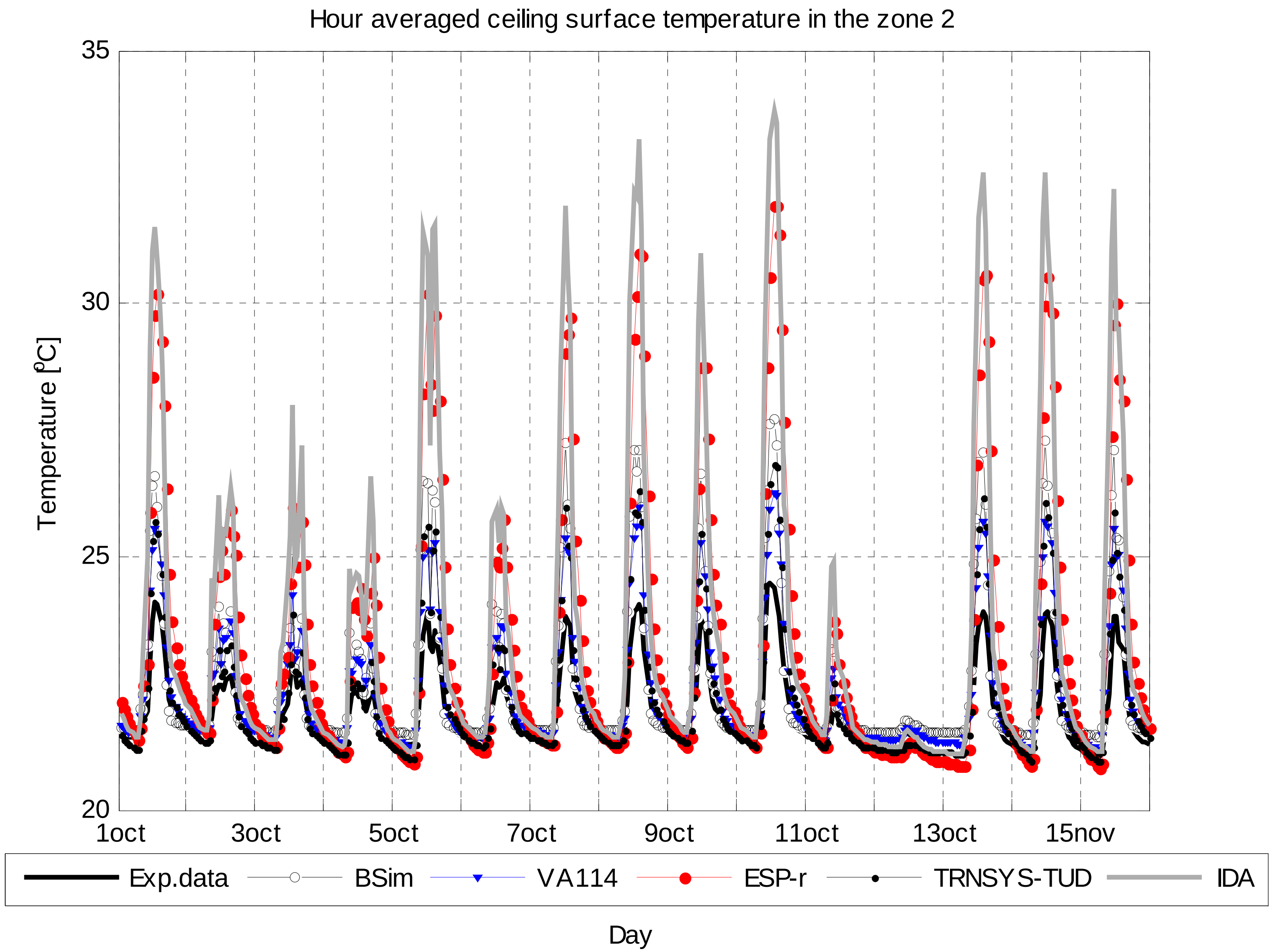

Hour averaged ceiling surface temperature in the zone 2
35
30
25
20
Temperature [ºC]
1oct
3oct
5oct
7oct
9oct
11oct
13oct
15nov
Exp.data
BSim
VA114
ESP-r
TRNSYS-TUD
IDA
Day

APPENDIX: Questionnaires

GENERAL

Empirical

1	**Program name and version number**	**BSim 4.7.1.18**
2	**Name of organization performed the simulations**	**Aalborg University**
3	**Name of person performed simulations and contact information**	**Olena Kalyanova Ph.D. student, Aalborg University Sohngaardsholmsvej 57 DK-9000 tel. +45 9635 8587 ok@civil.aau.dk**

4 Program status

☐ Freeware
☒ Commercial
☐ Other, please specify

5 Time convention for weather data: first interval in the weather input lasts 00:00-01:00, climate is assumed constant over the sampling interval

☒ Yes
☐ No, please specify

CALCULATION OF BOUNDARY CONDITIONS

6 Please specify the solar model for calculation of incident solar radiation

Perez

7 Transmission of the direct solar radiation into zone 1

☐ Calculated with the constant solar heat gain coefficient (g-value)
☐ Calculated with the g-value as a function of incidence (function of incidence is fixed within code)
☒ Calculated with the g-value as a function of incidence (function of incidence is user defined)
☐ Other, please specify

8 Transmission of the direct solar radiation into zone 2

☐ Treated as diffuse solar radiation and calculated with the constant g-value
☐ Calculated with the g-value as a function of incidence (function of incidence is fixed within code)
☒ Calculated with the g-value as a function of incidence (function of incidence is user defined)
☐ Other, please specify

9 Transmission of the diffuse solar radiation into zone 1

☒ Calculated with the solar heat gain coefficient at the solar incidence 60^{o}
☐ Other, please specify

10 Distribution of solar radiation to the surfaces in the zone 1

☐ Distributed equally to all surfaces
☐ Calculated according surface area weighting
☐ Calculated according to solar path and view factors
☐ Other, please specify: direct solar radiation is distributed according to the solar path, the diffuse solar radiation is area weighted

11 Distribution of solar radiation to the surfaces in the zone 2

☐ Distributed equally to all surfaces
☐ Calculated according surface area weighting
☐ Calculated according to solar path and view factors
☐ Other, please specify: direct solar radiation is distributed according to the solar path, the diffuse solar radiation is area weighted

MODEL DEFINITIONS

12 Air temperature in the zone 1 is calculated as:

☒ One node temperature
☐ Few zones are stacked on the top of each other and the air temperature in each of zones is calculated, please specify number of stacked zones
☐ Other, please specify

13 Air temperature in the zone 2 is calculated as:

☒ One node temperature
☐ Few zones are stacked on the top of each other and the air temperature in each of zones is calculated, please specify number of stacked zones
☐ Other, please specify

HEAT EXCHANGE WITH EXTERIOR

14 External heat transfer coefficients

☒ Split radiative/convective
☐ Combined radiative/ convective
☐ Other, please specify

15 External heat transfer coefficients are calculated with identical assumptions for all surfaces (window frame, window glazing, walls etc.)

☒ Yes
☐ No, please specify

16 External convection

☐ Constant coefficients fixed within code
☐ User-specified constant coefficients
☐ Calculated within code as a function of orientation
☒ Calculated within code as a function of wind speed
☐ Calculated within code as a function of wind speed and direction
☐ Other, please specify

17 External radiative heat exchange
☐ Assumed to be ambient temperature
☒ Assumed to be sky temperature
☐ Other, please specify

HEAT TRANSFER WITHIN ZONES

18 Internal heat transfer coefficients

☒ Split radiative/convection
☐ Combined radiative/ convective
☐ Other, please specify

19 Internal heat transfer coefficients are calculated with identical assumptions in all zones and for all surfaces (window frame, window glazing, walls etc.)

☒ Yes
☐ No, please specify

20 Internal convection

☐ Constant coefficients fixed within code
☐ User-specified constant coefficients
☒ Calculated within code as a function of orientation (vertical/horizontal)
☒ Calculated within code as a function of temperature difference
☐ Calculated within code as a function of air velocity in the zone
☐ Calculated within code as a function of surface finishes
☐ Other, please specify

21 Longwave radiation exchange within zone

☐ Constant linearized coefficients
☒ Linearized coefficients based on view factors
☐ Linearized coefficients based on surface emissivities
☐ Nonlinear treatment of radiation heat exchange
☐ Other, please specify

WINDOW

22 Window

☐ Window frame and glazing are modeled as separate elements of construction
☐ Window frame and glazing are modeled as separate elements of construction, but the total U-value is calculated within the code
☐ Window frame and glazing are modeled as separate elements of construction, but the total U-value and g-value are calculated within the code
☒ Other, please specify : Window frame and glazing are modelled as separate elements of construction, but the total U-value is calculated within the code, but the g-value is calculated in the code on the basis of user defined solar transmission

23 Glazing temperature

☐ Calculated for 1 nodal point on the basis of fixed resistance
☐ Calculated dynamically, using the same scheme as for opaque elements
☒ Other, please specify: Calculated as a thermal ballance for the surface, depending on ammount of absorbed/reflected solar radiation and air temperature in the neighbouring zones

AIRFLOW MODEL

24 Discharge coefficient

☒ Fixed within the code
☐ User-specified fixed value
☐ Calculated by code, please specify what are the parameters involved in code calculations
☐ Other, please specify

25 Pressure difference coefficients

☒ Fixed within the code, identical for all openings sharing the same surface
☐ User-specified, identical for all openings sharing the same surface
☐ User-specified for every opening
☐ Other, please specify

26 Calculated mass flow rate in the model is a function of

☒ Buoyancy force
☒ Wind pressure
☐ Wind turbulence
☐ Other, please specify

GENERAL

Empirical

1	**Program name and version number**	**VA114 – version 2.25**
2	**Name of organization performed the simulations**	**VABI Software bv**
3	**Name of person performed simulations and contact information**	**A. Wijsman** **Email: a.wijsman@vabi.nl**

4 Program status

☐ Freeware
X Commercial
☐ Other, please specify

5 Time convention for weather data: first interval in the weather input lasts 00:00-01:00, climate is assumed constant over the sampling interval

X Yes
☐ No, please specify

CALCULATION OF BOUNDARY CONDITIONS

6 Please specify the solar model for calculation of incident solar radiation
See appendix D to this Modeler report

7 Transmission of the direct solar radiation into zone 1

☐ Calculated with the constant solar heat gain coefficient (g-value)
☐ Calculated with the g-value as a function of incidence (function of incidence is fixed within code)
☐ Calculated with the g-value as a function of incidence (function of incidence is user defined)
X Other, please specify: Calculated with Transmission (as a function of incidence – user defined) and Absorption in the pane;

8 Transmission of the direct solar radiation into zone 2

☐ Treated as diffuse solar radiation and calculated with the constant g-value
☐ Calculated with the g-value as a function of incidence (function of incidence is fixed within code)
☐ Calculated with the g-value as a function of incidence (function of incidence is user defined)
X Other, please specify: Calculated with Transmission and Absorption in the panes; properties at angle of incidence of 45 degree

9 Transmission of the diffuse solar radiation into zone 1

☐ Calculated with the solar heat gain coefficient at the solar incidence 60^o
X Other, please specify: Calculated with Transmission (at solar incidence of $58\ ^o$) and Absorption in the pane.

10 Distribution of solar radiation to the surfaces in the zone 1

☐ Distributed equally to all surfaces
☐ Calculated according surface area weighting
☐ Calculated according to solar path and view factors
X Other, please specify: Different treatment for Direct and Diffuse solar radiation. Distribution of Direct solar is calculated by solar path; partly absorbed and partly diffuse reflected at surfaces that are hit. Distribution of Diffuse solar and Diffuse reflected Direct solar is calculated by absorption factors (based on view factors and absorption coefficients of the surfaces that are hit)

11 Distribution of solar radiation to the surfaces in the zone 2

☐ Distributed equally to all surfaces
☐ Calculated according surface area weighting
☐ Calculated according to solar path and view factors
X Other, please specify: same as distribution in zone 1

MODEL DEFINITIONS

12 Air temperature in the zone 1 is calculated as:

X One node temperature
☐ Few zones are stacked on the top of each other and the air temperature in each of zones is calculated, please specify number of stacked zones
☐ Other, please specify

13 Air temperature in the zone 2 is calculated as:

X One node temperature
☐ Few zones are stacked on the top of each other and the air temperature in each of zones is calculated, please specify number of stacked zones
☐ Other, please specify

HEAT EXCHANGE WITH EXTERIOR

14 External heat transfer coefficients

X Split radiative/convective
☐ Combined radiative/ convective
☐ Other, please specify

15 External heat transfer coefficients are calculated with identical assumptions for all surfaces (window frame, window glazing, walls etc.)

☐ Yes
X No, please specify : External heat transfer coefficients are not calculated (see external convection and external radiative heat exchange)

16 External convection

☐ Constant coefficients fixed within code
X User-specified constant coefficients
☐ Calculated within code as a function of orientation
☐ Calculated within code as a function of wind speed
☐ Calculated within code as a function of wind speed and direction
☐ Other, please specify

17 External radiative heat exchange

☐ Assumed to be ambient temperature
X Assumed to be sky temperature
☐ Other, please specify

HEAT TRANSFER WITHIN ZONES

18 Internal heat transfer coefficients

X Split radiative/convection
☐ Combined radiative/ convective
☐ Other, please specify

19 Internal heat transfer coefficients are calculated with identical assumptions in all zones and for all surfaces (window frame, window glazing, walls etc.)

☐ Yes
☐ No, please specify : Ixternal heat transfer coefficients are not calculated (see internal convection and internal radiative heat exchange)

20 Internal convection

☐ Constant coefficients fixed within code
X User-specified constant coefficients
☐ Calculated within code as a function of orientation (vertical/horizontal)
☐ Calculated within code as a function of temperature difference
☐ Calculated within code as a function of air velocity in the zone
☐ Calculated within code as a function of surface finishes
☐ Other, please specify

21 Longwave radiation exchange within zone

☐ Constant linearized coefficients
☐ Linearized coefficients based on view factors
X Linearized coefficients based on view factors and surface emissivities
☐ Nonlinear treatment of radiation heat exchange
☐ Other, please specify

WINDOW

22 Window

X Window frame and glazing are modeled as separate elements of construction; properties are user defined
☐ Window frame and glazing are modeled as separate elements of construction, but the total U-value is calculated within the code
☐ Window frame and glazing are modeled as separate elements of construction, but the total U-value and g-value are calculated within the code
☐ Other, please specify

23 Glazing temperature

☐ Calculated for 1 nodal point on the basis of fixed resistance
X Calculated dynamically, using the same scheme as for opaque elements
☐ Other, please specify

AIRFLOW MODEL

24 Discharge coefficient

X Fixed within the code
☐ User-specified fixed value
☐ Calculated by code, please specify what are the parameters involved in code calculations
☐ Other, please specify

25 Pressure difference coefficients

☐ Fixed within the code, identical for all openings sharing the same surface
X User-specified, identical for all openings sharing the same surface
☐ User-specified for every opening
☐ Other, please specify

26 Calculated mass flow rate in the model is a function of

X Buoyancy force
X Wind pressure
X Wind fluctuations
☐ Other, please specify

GENERAL

empirical

1 Program name and version number — **ESP-r 11.3**

2 Name of organization performed the simulations — **ESRU, University of Strathclyde**

3 Name of person performed simulations and contact information — **Paul Strachan**
paul@esru.strath.ac.uk
tel: +44 141 548 2041

4 Program status

☒ Freeware (Open Source)
☐ Commercial
☐ Other, please specify

5 Time convention for weather data: first interval in the weather input lasts 00:00-01:00, climate is assumed constant over the sampling interval

☐ Yes
☒ No, please specify: Solar data is hour centred (i.e. covers period 00:00-01:00) in these simulations. Linear interpolation is carried out for sub-hourly simulations

CALCULATION OF BOUNDARY CONDITIONS

6 Please specify the solar model for calculation of incident solar radiation
See report. Perez 1990 is used for the anisotropic diffuse sky model.

7 Transmission of the direct solar radiation into zone 1

☐ Calculated with the constant solar heat gain coefficient (g-value)
☐ Calculated with the g-value as a function of incidence (function of incidence is fixed within code)
☐ Calculated with the g-value as a function of incidence (function of incidence is user defined)
☒ Other, please specify See report - transmittance is an input optical property as are layer absorptances. The convection and radiation are calculated explicitly at the glazing system boundaries. g-values are not used.

8 Transmission of the direct solar radiation into zone 2

☐ Treated as diffuse solar radiation and calculated with the constant g-value
☐ Calculated with the g-value as a function of incidence (function of incidence is fixed within code)
☐ Calculated with the g-value as a function of incidence (function of incidence is user defined)
☒ Other, please specify As above

9 Transmission of the diffuse solar radiation into zone 1

☐ Calculated with the solar heat gain coefficient at the solar incidence 60°
☒ Other, please specify As above; incident angle assumed to be 51 degrees

10 Distribution of solar radiation to the surfaces in the zone 1

☐ Distributed equally to all surfaces
☐ Calculated according surface area weighting
☒ Calculated according to solar path and view factors
☐ Other, please specify

11 Distribution of solar radiation to the surfaces in the zone 2

☐ Distributed equally to all surfaces
☐ Calculated according surface area weighting
☒ Calculated according to solar path and view factors
☐ Other, please specify

MODEL DEFINITIONS

12 Air temperature in the zone 1 is calculated as:

☒ One node temperature (for DSF100 case only)
☒ Few zones are stacked on the top of each other and the air temperature in each of zones is calculated, please specify number of stacked zones 3
☐ Other, please specify

13 Air temperature in the zone 2 is calculated as:

☒ One node temperature
☐ Few zones are stacked on the top of each other and the air temperature in each of zones is calculated, please specify number of stacked zones
☐ Other, please specify

HEAT EXCHANGE WITH EXTERIOR

14 External heat transfer coefficients

☒ Split radiative/convective
☐ Combined radiative/ convective
☐ Other, please specify

15 External heat transfer coefficients are calculated with identical assumptions for all surfaces (window frame, window glazing, walls etc.)

☒ Yes
☐ No, please specify

16 External convection

☐ Constant coefficients fixed within code
☐ User-specified constant coefficients
☐ Calculated within code as a function of orientation
☐ Calculated within code as a function of wind speed
☒ Calculated within code as a function of wind speed and direction
☐ Other, please specify

17 External radiative heat exchange

☐ Assumed to be ambient temperature
☐ Assumed to be sky temperature
☒ Other, please specify Sky and ground surface temperatures, depending on viewfactors

HEAT TRANSFER WITHIN ZONES

18 Internal heat transfer coefficients

☒ Split radiative/convection
☐ Combined radiative/ convective
☐ Other, please specify

19 Internal heat transfer coefficients are calculated with identical assumptions in all zones and for all surfaces (window frame, window glazing, walls etc.)

☒ Yes (with exception of mechanically ventilated case – see report)
☐ No, please specify

20 Internal convection

☐ Constant coefficients fixed within code
☐ User-specified constant coefficients
☐ Calculated within code as a function of orientation (vertical/horizontal)
☒ Calculated within code as a function of temperature difference
☐ Calculated within code as a function of air velocity in the zone
☐ Calculated within code as a function of surface finishes
☐ Other, please specify

21 Longwave radiation exchange within zone

☐ Constant linearized coefficients
☒ Linearized coefficients based on view factors
☒ Linearized coefficients based on surface emissivities
☐ Nonlinear treatment of radiation heat exchange
☐ Other, please specify

WINDOW

22 Window

☒ Window frame and glazing are modeled as separate elements of construction
☐ Window frame and glazing are modeled as separate elements of construction, but the total U-value is calculated within the code
☐ Window frame and glazing are modeled as separate elements of construction, but the total U-value and g-value are calculated within the code
☐ Other, please specify

23 Glazing temperature

☐ Calculated for 1 nodal point on the basis of fixed resistance
☒ Calculated dynamically, using the same scheme as for opaque elements
☐ Other, please specify

AIRFLOW MODEL

24 Discharge coefficient

- ☐ Fixed within the code
- ☒ User-specified fixed value
- ☐ Calculated by code, please specify what are the parameters involved in code calculations
- ☐ Other, please specify

25 Pressure difference coefficients

- ☐ Fixed within the code, identical for all openings sharing the same surface
- ☐ User-specified, identical for all openings sharing the same surface
- ☒ User-specified for every opening
- ☐ Other, please specify

26 Calculated mass flow rate in the model is a function of

- ☒ Buoyancy force
- ☒ Wind pressure
- ☐ Wind turbulence
- ☐ Other, please specify

GENERAL

Empirical

1 Program name and version number — **TRNSYS-TUD**

2 Name of organization performed the simulations — **Technical University of Dresden**

3 Name of person performed simulations and contact information

Clemens Felsmann
felsmann@itg-dresden.de

Program status

☐ Freeware
☐ Commercial
☒ Other: The code was developed based on commercial TRNSYS for research purposes

5 Time convention for weather data: first interval in the weather input lasts 00:00-01:00, climate is assumed constant over the sampling interval

☐ Yes
☒ No: normally inputs change linearly but solar radiation is calculated using a special smoothing function..

CALCULATION OF BOUNDARY CONDITIONS

6 Please specify the solar model for calculation of incident solar radiation
Perez model

7 Transmission of the direct solar radiation into zone 1

☐ Calculated with the constant solar heat gain coefficient (g-value)
☐ Calculated with the g-value as a function of incidence (function of incidence is fixed within code)
☐ Calculated with the g-value as a function of incidence (function of incidence is user defined)
☒ Other: Calculated with the g-value as a function of incidence (function of incidence was calculated by WINFOW5 Software)

8 Transmission of the direct solar radiation into zone 2

☒ Treated as diffuse solar radiation and calculated with the constant g-value
☐ Calculated with the g-value as a function of incidence (function of incidence is fixed within code)
☐ Calculated with the g-value as a function of incidence (function of incidence is user defined)
☐ Other, please specify

9 Transmission of the diffuse solar radiation into zone 1

☐ Calculated with the solar heat gain coefficient at the solar incidence 60°
☒ Other: Calculated with the solar heat gain coefficient was calculated by WINFOW5 Software

10 Distribution of solar radiation to the surfaces in the zone 1

☒ Distributed equally to all surfaces: diffuse radiation
☐ Calculated according surface area weighting
☒ Calculated according to solar path and view factors: direct radiation
☐ Other, please specify

11 Distribution of solar radiation to the surfaces in the zone 2

☒ Distributed equally to all surfaces because all radiation was treated as diffuse radiation
☐ Calculated according surface area weighting
☐ Calculated according to solar path and view factors
☐ Other, please specify

MODEL DEFINITIONS

12 Air temperature in the zone 1 is calculated as:

☒ One node temperature was reported but…
☒ Few zones are stacked on the top of each other and the air temperature in each of zones is calculated, please specify number of stacked zones 4
☐ Other, please specify

13 Air temperature in the zone 2 is calculated as:

☒ One node temperature was reported but …
☒ Few zones are stacked on the top of each other and the air temperature in each of zones is calculated, please specify number of stacked zones 4
☐ Other, please specify

HEAT EXCHANGE WITH EXTERIOR

14 External heat transfer coefficients

☒ Split radiative/convective
☐ Combined radiative/ convective
☐ Other, please specify

15 External heat transfer coefficients are calculated with identical assumptions for all surfaces (window frame, window glazing, walls etc.)

☒ Yes
☐ No, please specify

16 External convection

☐ Constant coefficients fixed within code
☒ User-specified constant coefficients
☐ Calculated within code as a function of orientation
☐ Calculated within code as a function of wind speed
☐ Calculated within code as a function of wind speed and direction
☐ Other, please specify

17 External radiative heat exchange

☐ Assumed to be ambient temperature
☐ Assumed to be sky temperature
☒ Other: it depends on the orientation whether ambient or sky temperature will be used

HEAT TRANSFER WITHIN ZONES

18 Internal heat transfer coefficients

☒ Split radiative/convection
☐ Combined radiative/ convective
☐ Other, please specify

19 Internal heat transfer coefficients are calculated with identical assumptions in all zones and for all surfaces (window frame, window glazing, walls etc.)

☒ Yes
☐ No, please specify

20 Internal convection

☐ Constant coefficients fixed within code
☒ User-specified constant coefficients
☐ Calculated within code as a function of orientation (vertical/horizontal)
☐ Calculated within code as a function of temperature difference
☐ Calculated within code as a function of air velocity in the zone
☐ Calculated within code as a function of surface finishes
☐ Other, please specify

21 Longwave radiation exchange within zone

☐ Constant linearized coefficients
☐ Linearized coefficients based on view factors
☐ Linearized coefficients based on surface emissivities
☒ Nonlinear treatment of radiation heat exchange
☐ Other, please specify

WINDOW

22 Window

☐ Window frame and glazing are modeled as separate elements of construction
☐ Window frame and glazing are modeled as separate elements of construction, but the total U-value is calculated within the code
☒ Window frame and glazing are modeled as separate elements of construction, but the total U-value and g-value are calculated within the code
☐ Other, please specify

23 Glazing temperature

☒ Calculated for 1 nodal point on the basis of fixed resistance
☐ Calculated dynamically, using the same scheme as for opaque elements
☐ Other, please specify

AIRFLOW MODEL

24 Discharge coefficient

☐ Fixed within the code
☒ User-specified fixed value
☐ Calculated by code, please specify what are the parameters involved in code calculations
☐ Other, please specify

25 Pressure difference coefficients

☐ Fixed within the code, identical for all openings sharing the same surface
☐ User-specified, identical for all openings sharing the same surface
☒ User-specified for every opening
☐ Other, please specify

26 Calculated mass flow rate in the model is a function of

☒ Buoyancy force
☒ Wind pressure
☐ Wind turbulence
☐ Other, please specify

GENERAL

EMPIRICAL

1	**Program name and version number**	**IDA ICE 3.0**
2	**Name of organization performed the simulations**	**EBD, LTH, Sweden**
3	**Name of person performed simulations and contact information**	Harris Poirazis Lund University harris.poirazis@ebd.lth.se

4 Program status

☐ Freeware
☒ Commercial
☐ Other, please specify

5 Time convention for weather data: first interval in the weather input lasts 00:00-01:00, climate is assumed constant over the sampling interval

☒ Yes
☐ No, please specify

CALCULATION OF BOUNDARY CONDITIONS

6 Please specify the solar model for calculation of incident solar radiation
Model by Perez (1990)

7 Transmission of the direct solar radiation into zone 1

☐ Calculated with the constant solar heat gain coefficient (g-value)
☒ Calculated with the g-value as a function of incidence (function of incidence is fixed within code)
☐ Calculated with the g-value as a function of incidence (function of incidence is user defined)
☐ Other, please specify

8 Transmission of the direct solar radiation into zone 2

☐ Treated as diffuse solar radiation and calculated with the constant g-value
☒ Calculated with the g-value as a function of incidence (function of incidence is fixed within code)
☐ Calculated with the g-value as a function of incidence (function of incidence is user defined)
☐ Other, please specify

9 Transmission of the diffuse solar radiation into zone 1

☐ Calculated with the solar heat gain coefficient at the solar incidence 60^o
☒ Other, please specify Calculated as 0.77/0.87*T-normal

10 Distribution of solar radiation to the surfaces in the zone 1

☐ Distributed equally to all surfaces
☐ Calculated according surface area weighting
☒ Calculated according to solar path and view factors
☐ Other, please specify

11 Distribution of solar radiation to the surfaces in the zone 2

☐ Distributed equally to all surfaces
☐ Calculated according surface area weighting
☐ Calculated according to solar path and view factors
☒ Other, please specify Calculated according to view factors and surface reflectance values

<u>MODEL DEFINITIONS</u>

12 Air temperature in the zone 1 is calculated as:

☒ One node temperature
☐ Few zones are stacked on the top of each other and the air temperature in each of zones is calculated, please specify number of stacked zones
☐ Other, please specify

13 Air temperature in the zone 2 is calculated as:

☒ One node temperature
☐ Few zones are stacked on the top of each other and the air temperature in each of zones is calculated, please specify number of stacked zones
☐ Other, please specify

<u>HEAT EXCHANGE WITH EXTERIOR</u>

14 External heat transfer coefficients

☒ Split radiative/convective
☐ Combined radiative/ convective
☐ Other, please specify

15 External heat transfer coefficients are calculated with identical assumptions for all surfaces (window frame, window glazing, walls etc.)

☒ Yes
☐ No, please specify

16 External convection

☐ Constant coefficients fixed within code
☐ User-specified constant coefficients
☐ Calculated within code as a function of orientation
☐ Calculated within code as a function of wind speed
☒ Calculated within code as a function of wind speed and direction
☐ Other, please specify

17 External radiative heat exchange

☐ Assumed to be ambient temperature
☐ Assumed to be sky temperature
☒ Other, please specify Sky/ambient temperatures according to view factors for sky/ground. Sky temperature is calculated as ambient temperature minus 5°C

HEAT TRANSFER WITHIN ZONES

18 Internal heat transfer coefficients

☒ Split radiative/convection
☐ Combined radiative/ convective
☐ Other, please specify

19 Internal heat transfer coefficients are calculated with identical assumptions in all zones and for all surfaces (window frame, window glazing, walls etc.)

☒ Yes
☐ No, please specify

20 Internal convection

☐ Constant coefficients fixed within code
☐ User-specified constant coefficients
☒ Calculated within code as a function of orientation (vertical/horizontal)
☒ Calculated within code as a function of temperature difference
☐ Calculated within code as a function of air velocity in the zone
☐ Calculated within code as a function of surface finishes
☐ Other, please specify

21 Longwave radiation exchange within zone

☐ Constant linearized coefficients
☒ Linearized coefficients based on view factors
☒ Linearized coefficients based on surface emissivities
☐ Nonlinear treatment of radiation heat exchange
☐ Other, please specify

WINDOW

22 Window

☒ Window frame and glazing are modeled as separate elements of construction
☐ Window frame and glazing are modeled as separate elements of construction, but the total U-value is calculated within the code
☐ Window frame and glazing are modeled as separate elements of construction, but the total U-value and g-value are calculated within the code
☐ Other, please specify

23 Glazing temperature

☒ Calculated for 1 nodal point on the basis of fixed resistance
☐ Calculated dynamically, using the same scheme as for opaque elements
☐ Other, please specify

AIRFLOW MODEL

24 Discharge coefficient

☐ Fixed within the code
☒ User-specified fixed value
☐ Calculated by code, please specify what are the parameters involved in code calculations
☐ Other, please specify

25 Pressure difference coefficients

☐ Fixed within the code, identical for all openings sharing the same surface
☒ User-specified, identical for all openings sharing the same surface
☐ User-specified for every opening
☐ Other, please specify

26 Calculated mass flow rate in the model is a function of

☒ Buoyancy force
☒ Wind pressure
☐ Wind turbulence
☐ Other, please specify

APPENDIX: Modeler reports

ISSN 1901-726X
DCE Technical Report No. 030